Age of the Lospe Formation (Early Miocene) and Origin of the Santa Maria Basin, California

Petroleum Source Potential and Thermal Maturity of the Lospe Formation (Lower Miocene) near Point Sal, Onshore Santa Maria Basin, California

Obispo Formation, California: Remobilized Pyroclastic Material

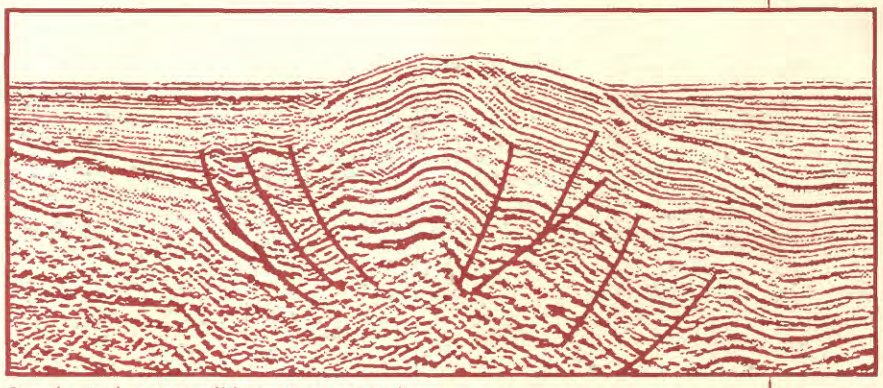

Geophysical section offshore Santa Maria basin

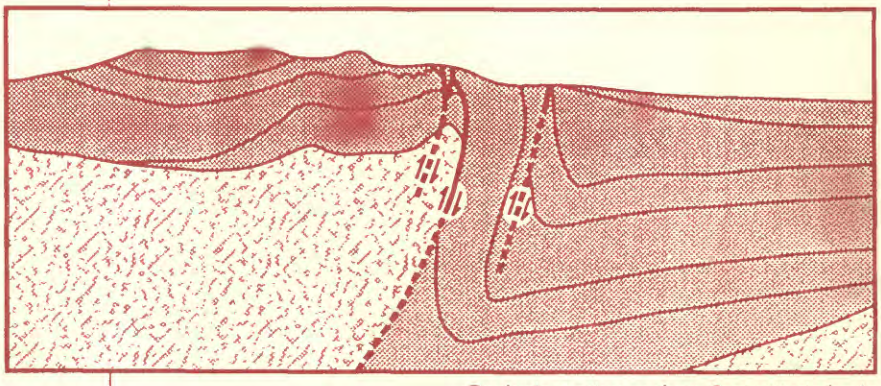

Geologic section onshore Santa Maria basin

U.S. GEOLOGICAL SURVEY BULLETIN 1995–M, N, O

AVAILABILITY OF BOOKS AND MAPS OF THE U.S. GEOLOGICAL SURVEY

Instructions on ordering publications of the U.S. Geological Survey, along with prices of the last offerings, are given in the current-year issues of the monthly catalog "New Publications of the U.S. Geological Survey." Prices of available U.S. Geological Survey publications released prior to the current year are listed in the most recent annual "Price and Availability List." Publications that may be listed in various U.S. Geological Survey catalogs (**see back inside cover**) but not listed in the most recent annual "Price and Availability List" may no longer be available.

Reports released through the NTIS may be obtained by writing to the National Technical Information Service, U.S. Department of Commerce, Springfield, VA 22161; please include NTIS report number with inquiry.

Order U.S. Geological Survey publications **by mail** or **over the counter** from the offices listed below.

BY MAIL

Books

Professional Papers, Bulletins, Water-Supply Papers, Techniques of Water-Resources Investigations, Circulars, publications of general interest (such as leaflets, pamphlets, booklets), single copies of Earthquakes & Volcanoes, Preliminary Determination of Epicenters, and some miscellaneous reports, including some of the foregoing series that have gone out of print at the Superintendent of Documents, are obtainable by mail from

U.S. Geological Survey, Information Services
Box 25286, Federal Center
Denver, CO 80225

Subscriptions to periodicals (Earthquakes & Volcanoes and Preliminary Determination of Epicenters) can be obtained ONLY from the

Superintendent of Documents
Government Printing Office
Washington, DC 20402

(Check or money order must be payable to Superintendent of Documents.)

Maps

For maps, address mail orders to

U.S. Geological Survey, Information Services
Box 25286, Federal Center
Denver, CO 80225

Residents of Alaska may order maps from

U.S. Geological Survey, Earth Science Information Center
101 Twelfth Ave., Box 12
Fairbanks, AK 99701

OVER THE COUNTER

Books and Maps

Books and maps of the U.S. Geological Survey are available over the counter at the following U.S. Geological Survey offices, all of which are authorized agents of the Superintendent of Documents.

- **ANCHORAGE, Alaska**–Rm. 101, 4230 University Dr.
- **LAKEWOOD, Colorado**–Federal Center, Bldg. 810
- **MENLO PARK, California**–Bldg. 3, Rm. 3128, 345 Middlefield Rd.
- **RESTON, Virginia**–USGS National Center, Rm. 1C402, 12201 Sunrise Valley Dr.
- **SALT LAKE CITY, Utah**–Federal Bldg., Rm. 8105, 125 South State St.
- **SPOKANE, Washington**–U.S. Post Office Bldg., Rm. 135, West 904 Riverside Ave.
- **WASHINGTON, D.C.**–Main Interior Bldg., Rm. 2650, 18th and C Sts., NW.

Maps Only

Maps may be purchased over the counter at the following U.S. Geological Survey offices:

- **FAIRBANKS, Alaska**–New Federal Bldg, 101 Twelfth Ave.
- **ROLLA, Missouri**–1400 Independence Rd.
- **STENNIS SPACE CENTER, Mississippi**–Bldg. 3101

Age of the Lospe Formation (Early Miocene) and Origin of the Santa Maria Basin, California

By RICHARD G. STANLEY, SAMUEL Y. JOHNSON, CARL C. SWISHER, III, MARK A. MASON, JOHN D. OBRADOVICH, MARY LOU COTTON, MARK V. FILEWICZ, and DAVID R. VORK

Petroleum Source Potential and Thermal Maturity of the Lospe Formation (Lower Miocene) near Point Sal, Onshore Santa Maria Basin, California

By RICHARD G. STANLEY, MARK J. PAWLEWICZ, DAVID R. VORK, SAMUEL Y. JOHNSON, and ZENON VALIN

Obispo Formation, California: Remobiled Pyroclastic Material

By JEAN-LUC SCHNEIDER and RICHARD V. FISHER

Chapters M, N, and O are issued as a single volume
and are not available separately

U.S. GEOLOGICAL SURVEY BULLETIN 1995

EVOLUTION OF SEDIMENTARY BASINS/ONSHORE OIL AND GAS INVESTIGATIONS—
SANTA MARIA PROVINCE

Edited by Margaret A. Keller

U.S. DEPARTMENT OF THE INTERIOR

BRUCE BABBITT, Secretary

U.S. GEOLOGICAL SURVEY

Gordon P. Eaton, Director

UNITED STATES GOVERNMENT PRINTING OFFICE, WASHINGTON : 1996

For sale by
U.S. Geological Survey
Information Services
Box 25286, Federal Center
Denver, CO 80225

Chapter M

Age of the Lospe Formation (Early Miocene) and Origin of the Santa Maria Basin, California

By RICHARD G. STANLEY, SAMUEL Y. JOHNSON, CARL C. SWISHER, III, MARK A. MASON, JOHN D. OBRADOVICH, MARY LOU COTTON, MARK V. FILEWICZ, and DAVID R. VORK

U.S. GEOLOGICAL SURVEY BULLETIN 1995–M

EVOLUTION OF SEDIMENTARY BASINS/ONSHORE OIL AND GAS INVESTIGATIONS—SANTA MARIA PROVINCE

Edited by Margaret A. Keller

CONTENTS

FIGURES

TABLES

Age of the Lospe Formation (Early Miocene) and Origin of the Santa Maria Basin, California

By Richard G. Stanley, Samuel Y. Johnson, Carl C. Swisher, III[1], Mark A. Mason[2], John D. Obradovich, Mary Lou Cotton[3], Mark V. Filewicz[4], *and* David R. Vork[5]

Abstract

The Lospe Formation is an 830-m-thick sequence of nonmarine and shallow-marine sedimentary rocks and interbedded rhyolitic tuffs at the base of the oil-bearing Neogene Santa Maria basin of south-central coastal California. New isotopic and biostratigraphic data demonstrate that the Lospe in its type area in the northwestern Casmalia Hills was deposited about 18–17 Ma during the late early Miocene. Samples of water-laid rhyolitic tuffs from 30 m and 210 m above the base of the Lospe gave single crystal laser fusion $^{40}Ar/^{39}Ar$ ages of 17.70±0.02 Ma (mean of seven determinations on sanidine) and 17.39±0.06 Ma (mean of six determinations on plagioclase), respectively. Samples of tuffs from 30 m and 40 m above the base of the Lospe analyzed by the $^{40}Ar/^{39}Ar$ incremental-heating method showed saddle-shaped spectra indicating maximum ages on sanidine of 18.46±0.06 Ma and 18.10±0.06 Ma, respectively. The exact location of the eruptive source of the Lospe tuffs is unknown, but it may have been in the vicinity of Tranquillon Mountain, about 30 km south of the Lospe outcrops. Currently available data are consistent with the hypothesis that tuffs in the Lospe were derived from the same eruptive source as (1) a sample of welded rhyolitic tuff from the Tranquillon Volcanics on Tranquillon Mountain, which yielded a single crystal laser fusion $^{40}Ar/^{39}Ar$ age of 17.80±0.05 Ma (mean of five determinations on sanidine); and (2) a sample of altered tuff from near the base of the Monterey Formation near Naples, about 60 km east of Tranquillon Mountain, which yielded a single crystal laser fusion $^{40}Ar/^{39}Ar$ age of 18.42±0.06 Ma (mean of four determinations on sanidine).

Alluvial fan and fan-delta conglomerates, sandstones, and mudstones in the lower member of the Lospe Formation are unfossiliferous, but lacustrine and shallow-marine mudstones in the upper member of the Lospe contain palynomorphs of early to middle Miocene age and benthic foraminifers of probable Saucesian age. The Lospe is conformably and abruptly overlain by bathyal marine shale and sandstone of the Miocene Point Sal Formation. Samples from the lower 15 m of the Point Sal Formation yielded palynomorphs of early and (or) middle Miocene age, benthic foraminifers of Saucesian and Relizian age, planktic foraminifers of early Miocene zones N4–N6, and calcareous nannofossils of early and early middle Miocene zone CN3. The boundary between the Saucesian and Relizian Stages occurs about 1–2 m stratigraphically above the base of the Point Sal Formation, and about 205 m above the tuff within the Lospe Formation dated at about 17.4 Ma.

The type Lospe Formation is younger than the middle Eocene to lower Miocene Sespe Formation of southern California, with which the Lospe has been previously correlated. The Sespe is a regionally extensive fluvial and deltaic unit that was deposited in a subduction-related forearc basin by river systems flowing from Arizona and the Mojave Desert to the Santa Barbara–Ventura coastal area. In contrast, the Lospe is restricted to the central Santa Maria basin and records bathymetric deepening, volcanism, active faulting, and rapid tectonic subsidence that began about 18 Ma in concert with regional transtension and initial clockwise rotation of the western Transverse Ranges.

INTRODUCTION

The Lospe Formation consists of nonmarine and shallow-marine sedimentary rocks and subordinate rhyolitic tuffs that record initial subsidence of the oil-bearing Neogene Santa Maria basin of south-central coastal California (fig. 1). The Lospe also is present in the subsurface of the Santa Maria basin, where it has been penetrated by numerous exploratory wells and has yielded modest amounts of petroleum from sandstone reservoirs (Woodring and Bramlette, 1950; Dibblee, 1950; Hall, 1978a, 1982; McLean, 1991; California Division of Oil and Gas, 1991).

[1]Berkeley Geochronology Center, 2455 Ridge Road, Berkeley, CA 94709.

[2]Geologist, 1215 Roosevelt Ave., Richmond, CA 94801.

[3]Consultant, 244 Hermosa Drive, Bakersfield, CA 93305.

[4]Unocal Frontier Exploration, Far East Group, P.O. Box 4570, Houston, TX 77210.

[5]Unocal Corporation, P.O. Box 4551, Houston, TX 77210.

Until recently, the age of the Lospe Formation was uncertain because no datable fossils or isotopic ages on volcanic rocks had been recovered from it. Because the Lospe includes red conglomerate and sandstone of continental origin, it was correlated by many geologists with the middle Eocene to lower Miocene nonmarine Sespe Formation of the Santa Barbara-Ventura area (for example, see Wissler and Dreyer, 1943, p. 237-238; Woodring and Bramlette, 1950, p. 13; Hall, 1975, 1978a, 1981a, 1982; Bartow, 1978, p. 77; Anderson, 1980). However, Woodring and Bramlette (1950, p. 99-100) and Dibblee (1950, p. 33) assigned an early Miocene(?) age to the Lospe on the basis of its conformable upper contact with the lower Miocene Point Sal Formation, and the resemblance of tuffs in the Lospe to tuffs near San Luis Obispo that subsequently were assigned to the Obispo Formation by Hall and others (1966).

This report presents new isotopic ($^{40}Ar/^{39}Ar$) and biostratigraphic data that demonstrate that the type Lospe Formation in the northwestern Casmalia Hills (figs. 1, 2) is entirely of late early Miocene age. The new data strongly imply that rapid tectonic subsidence of the Santa Maria basin began about 18 Ma. Furthermore, the new data show that the lowest part of the Point Sal Formation is of Saucesian age, rather than early Relizian as previously thought; that the boundary between the Relizian and Saucesian Stages is younger than 17.4 Ma in the Santa Maria area; and that tuffs in the Lospe Formation are about the same age and may have been derived from the same eruptive center as volcanic rocks on and near Tranquillon Mountain in the western Transverse Ranges (fig. 1).

ACKNOWLEDGMENTS

We thank the United States Air Force for permission to work on Vandenberg Air Force Base, and the Unocal Corporation for providing biostratigraphic support. We also thank our colleagues J.A. Barron, K.J. Bird, G.H. Blake, David Bukry, R.B. Cole, J.C. Ingle, Jr., P.A. McCrory, Hugh McLean, C.C. Sorlien, M.E. Tennyson, E.C. Thomas, M.L. Tuttle, J.G. Vedder, and T.J. Wiley for many stimulating discussions. Comments by R.B. Cole, J.C. Ingle, Jr., and S.W. Starratt were helpful in revising early drafts of this report.

TYPE AREA AND ORIGIN OF NAME

The type area of the Lospe Formation was designated by Wissler and Dreyer (1943, p. 237) as a 2,600-ft section of unfossiliferous, continental beds underlying the Point Sal Formation "***on the southwest slope of Mount Lospe, near the western end of the Casmalia Hills, approximately 2 miles south of Point Sal Landing and half a mile north of Lions Head Beach (Guadalupe quadrangle)." No type section was designated, but Wissler and Dreyer (1943, p. 237) note that "The best exposures are in Chute Creek which has eroded a narrow channel down the southern slope of Mount Lospe." The name "Chute Creek" does not appear on modern U.S. Geological Survey topographic maps but probably is the same creek that Woodring and Bramlette (1950, p. 13) had in mind when they discussed a thick section of Lospe "***in the first canyon northwest of Lions Head and its middle upper tributary." The mouth of this creek is about 600 m southwest of a place known locally as "The Chute" and shown on the geologic map of Fairbanks (1896, pl. 1).

The term "Lospe" was used as an informal stratigraphic name in the Santa Maria basin for many years before it first appeared in print in a stratigraphic column by Tolman (1927, p. 459). According to Gudde (1960, p.174), the name is from the Chumash word "ospe," meaning "flower field."

STRATIGRAPHIC AND SEDIMENTOLOGIC SETTING

In the Casmalia Hills, the Lospe Formation rests nonconformably on igneous rocks of the Jurassic Point Sal ophiolite (Hopson and Frano, 1977), and in angular unconformity on conglomerate, sandstone, shale, and chert of the Jurassic and Cretaceous Great Valley sequence (fig. 3; stratigraphic names used as in McLean, 1991). The Lospe is conformably overlain by the Point Sal Formation. Generally this contact is covered, but in exposures at North Beach (figs. 4, 5) and Chute Creek (figs. 6, 7) the transition from greenish-gray mudstone and sandstone of the Lospe Formation to dark-brown and black shale of the Point Sal Formation is concordant and abrupt. This transition occurs about 3.5–4.5 m above the top of the informally named "cannonball sandstone unit," a laterally persistent bed about 4–6 m thick of resistant, plane-laminated sandstone with abundant spheroidal calcareous concretions. About 1 km north of Point Sal (fig. 8), the cannonball sandstone unit is present but the contact between the Lospe and Point Sal Formations is complicated by folds and faults.

The type Lospe Formation is as thick as 830 m and was divided by Woodring and Bramlette (1950) into two mappable members. The lower member is as much as 210 m thick and consists mainly of reddish-brown and greenish-gray conglomerate and sandstone that were derived from nearby fault-bounded uplifts of Mesozoic sedimentary and igneous rocks and deposited in alluvial fan and fan-delta environments (Stanley and others, 1990, 1991; Johnson and Stanley, 1994; McLean and Stanley, 1994). At North Beach, the lower and upper members are in fault contact. Along Chute Creek, the coarse-grained deposits grade upward into the upper member, which consists mainly of interbedded mudstone and turbidite sandstone that may have accumulated in a lake with possible intermittent connections to the ocean (Stanley and others, 1991). Primary and secondary gypsum occur locally in the

lake deposits; studies of stable isotopes suggest that the sulfur in the gypsum was derived from hydrothermal springs on the floor of the lake (M.L. Tuttle, U.S. Geological Survey, oral commun., 1991; Stanley and others, 1992a). Both the lower and upper members of the Lospe include interbedded lenses of nonwelded, water-laid rhyolitic tuff ranging from a few centimeters to more than 20 m thick (Cole and others, 1991a, b; Cole and Stanley, 1994).

The uppermost 30 m of the Lospe Formation consists of storm-deposited, plane-laminated to bioturbated sandstone and bioturbated mudstone containing shallow-marine microfossils (Stanley and others, 1990). These shallow-marine deposits are abruptly overlain by the Point Sal Formation, which in this area is more than 450 m thick and consists mainly of dark-gray to black silty shale with interbeds of turbidite sandstone. Generally, the shale is hard, fissile, and calcareous, with laminations and calcareous microfossils that suggest deposition in oxygen-poor environments at bathyal water depths (Stanley and others, 1991). In places, the Point Sal Formation is intruded by sills of diabase (Woodring and Bramlette, 1950;

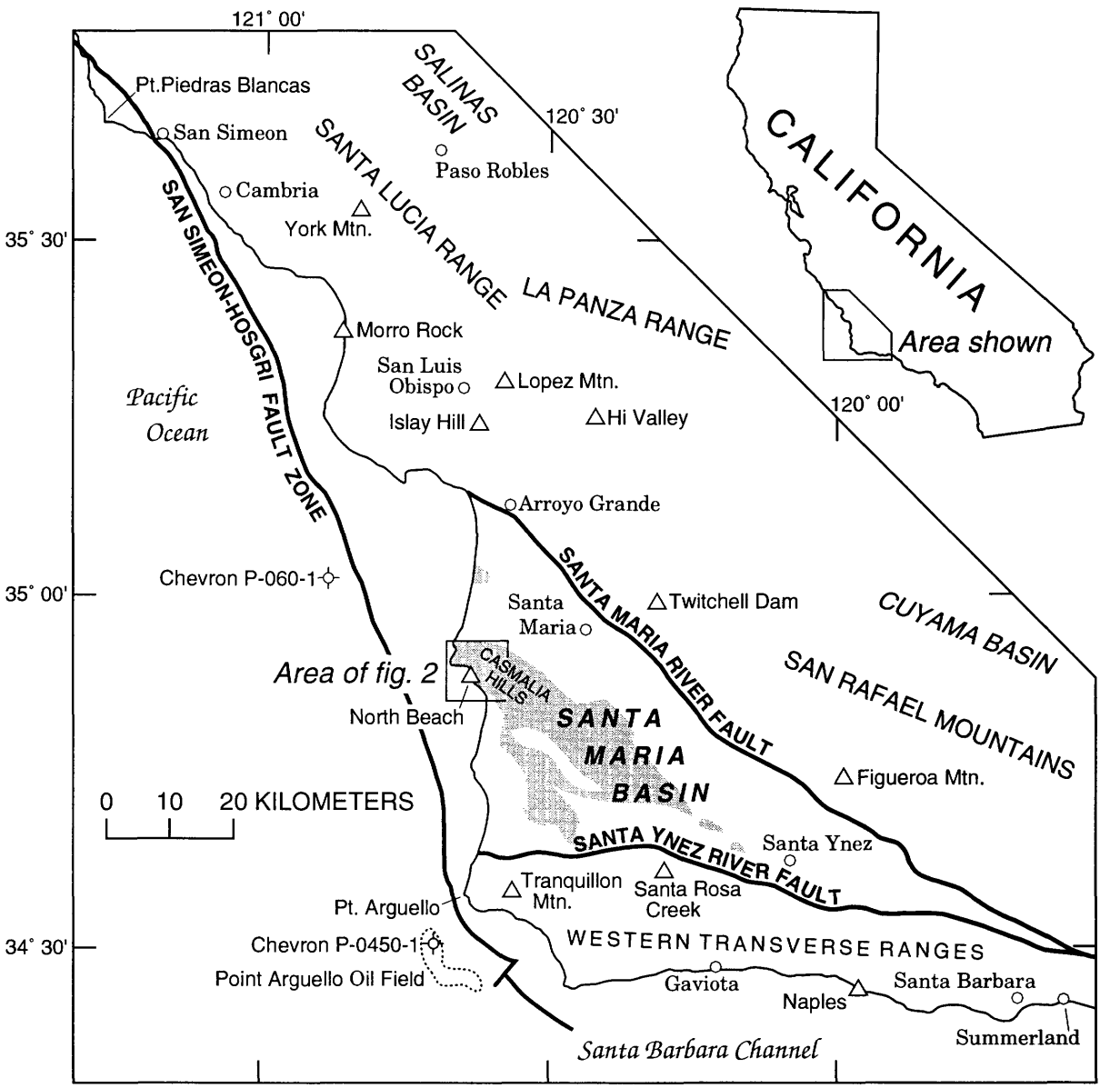

Figure 1. Regional location map showing towns (circles), outcrop localities (triangles), Point Arguello oil field (dotted outline), and offshore wells (bracketed circles) mentioned in text. Shaded areas show the onshore surface and subsurface distribution of the Lospe Formation according to Hall (1982) with modifications from McLean (1991). Generally, the onshore Santa Maria basin is the triangular area bounded by the Santa Maria River fault (Hall, 1978a), the Santa Ynez River fault (Sylvester and Darrow, 1979), and the present shoreline. Location of the San Simeon-Hosgri fault compiled and simplified from Hall (1975) and Steritz (1986).

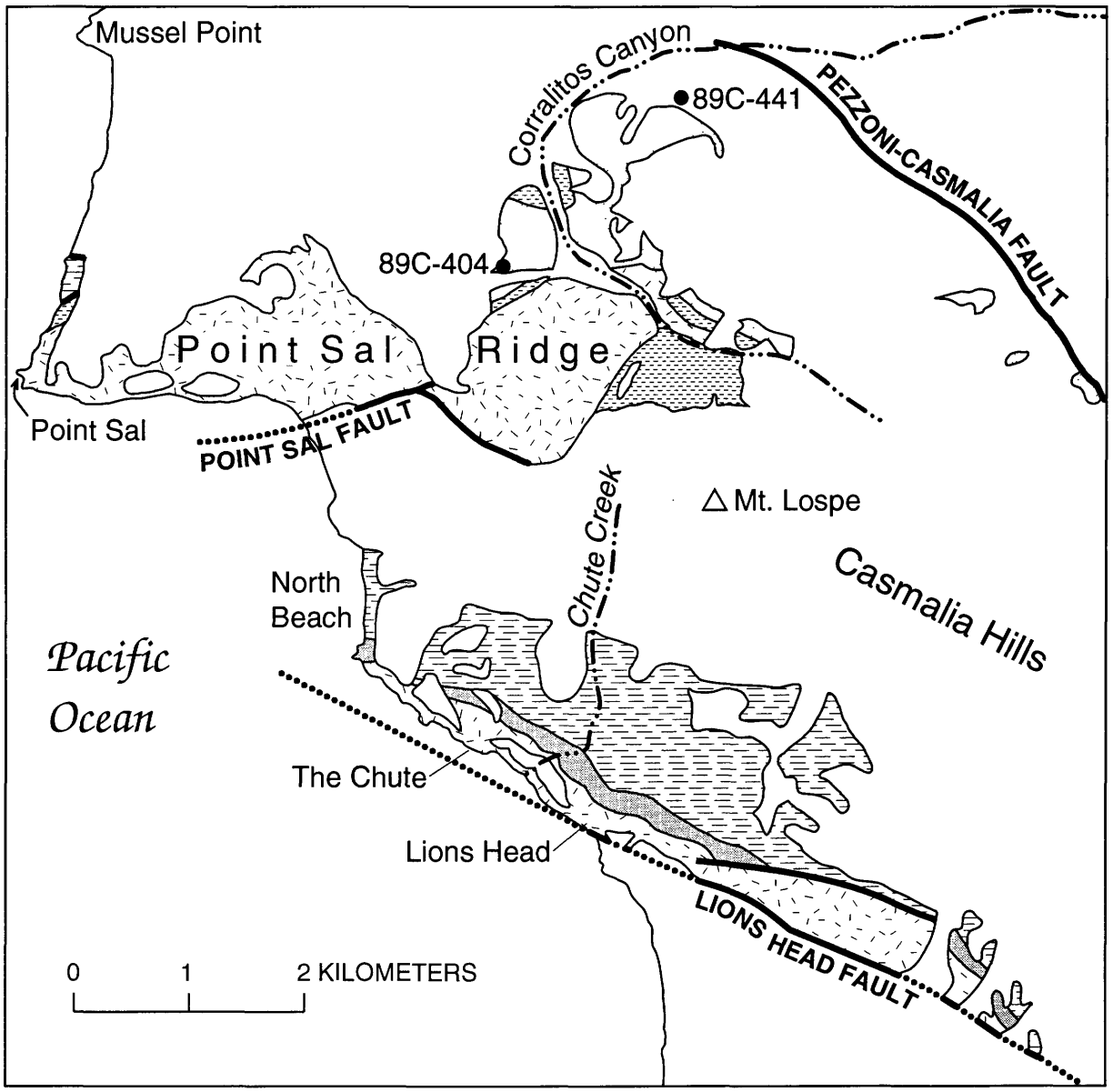

EXPLANATION

- Lospe Formation, upper member
- Lospe Formation, lower member
- Lospe Formation, undivided
- Espada Formation of Dibblee (1950, 1989b)
- Point Sal ophiolite of Hopson and Frano (1977)
- Geologic contact
- Fault--Dotted where concealed or inferred

Figure 2. Location map of the Point Sal area showing sampling sites (filled circles) and other localities mentioned in text, important faults, and distribution of the Point Sal ophiolite, Espada Formation, and Lospe Formation (modified from mapping by Dibblee, 1989a, b). Blank areas are underlain by unconsolidated deposits and by non-Lospe rocks of Cenozoic age.

Dibblee, 1989b). No $^{40}Ar/^{39}Ar$ or other isotopic ages have been obtained from these intrusions, but field relations and regional correlations suggest that they are probably of late early Miocene or middle Miocene age (Stanley and others, 1995).

ISOTOPIC ($^{40}Ar/^{39}Ar$) AGE DETERMINATIONS

Samples for $^{40}Ar/^{39}Ar$ dating were obtained from three horizons of rhyolitic tuff in the Lospe Formation at North Beach; from a welded rhyolitic tuff within the Tranquillon Volcanics of Dibblee (1950) near the top of Tranquillon Mountain, about 34 km south of North Beach; and from a tuff near the base of the Monterey Formation near Naples, about 60 km east of Tranquillon Mountain (fig. 1). Samples 88C-100 and 88C-113 from the Lospe Formation and sample 89C-57 from the Tranquillon Volcanics were dated in the laboratories of the Berkeley Geochronology Center (Berkeley, Calif.) using the single crystal laser fusion $^{40}Ar/^{39}Ar$ method; the analytical procedures employed are described by Swisher and others (1993). Samples 88C-100 and 88C-101 from the Lospe were dated in the laboratories of the U.S. Geological Survey (Denver, Colo.) using the incremental heating $^{40}Ar/^{39}Ar$ method; the analytical procedures employed are described by Tysdal and others (1990). Sample 122734 from the Monterey Formation was dated in the laboratories of the U.S. Geological Survey (Menlo Park, Calif.) using the single crystal laser fusion $^{40}Ar/^{39}Ar$ method; the analytical procedures employed are described by Obradovich (1993).

Sample 88C-100 was taken from a 20-cm-thick tuff bed about 30 m above the base of the Lospe Formation (figs. 4, 9). Sanidine from this tuff yielded a single crystal laser fusion $^{40}Ar/^{39}Ar$ age of 17.70±0.02 Ma (table 1) and an incremental heating age of 18.46±0.06 Ma (fig. 10). The bed strikes east-west and dips about 40°N. The tuff has a greenish-gray color on freshly broken surfaces, weathers white, and is less resistant than the darker colored, red alluvial fan conglomerates above and below. The lower boundary of the tuff bed is sharp

AGE (Ma)	PERIOD	EPOCH	SUBEPOCH	STAGE[1]	STRATIGRAPHY		THICKNESS, IN METERS
16	TERTIARY	Miocene	Middle	Luisian	Monterey Formation		490
17			Early	Relizian	Point Sal Formation		460
17.4				Saucesian	Lospe Formation	Upper member	620
17.7						Lower member	210
	Hiatus (unconformity)						
96	CRETACEOUS	Late			Great Valley sequence	Upper petrofacies[2]	Unknown
		Early				Lower petrofacies[2] (Espada Formation[3])	380
138	JURASSIC				Point Sal ophiolite[4]		Unknown
170	Inferred tectonic contact (Coast Range thrust of Page, 1981)						
	TERTIARY(?) TO JURASSIC				Franciscan Complex		Unknown

[1]Modified from Kleinpell (1938, 1980).
[2]Modified from McLean (1991).
[3]Espada Formation of Dibblee (1950, 1989b).
[4]Point Sal ophiolite of Hopson and Frano (1977).

Figure 3. Stratigraphic chart showing the Lospe Formation and bounding rock units in the onshore Santa Maria basin.

and flat to slightly scoured, but in places the tuff is draped over large clasts in the underlying conglomerate. The upper boundary of the tuff bed is abrupt and erosionally truncated (fig. 9). The lower half of the bed is hard and platy, whereas the upper half is soft and fibrous. In thin section, the tuff consists of about 5–10 percent crystals (mainly quartz and sanidine, with minor plagioclase and biotite) and rock fragments (including siltstone, sandstone, and altered ophiolitic rocks) in a fibrous, translucent brown, clayey matrix of altered glass shards and pumice.

The age inferred from the incremental heating results for sample 88C-100 is nearly 0.8 million years older than the age obtained for the same sample by single crystal laser fusion. This discrepancy can be explained by the use of different stan-

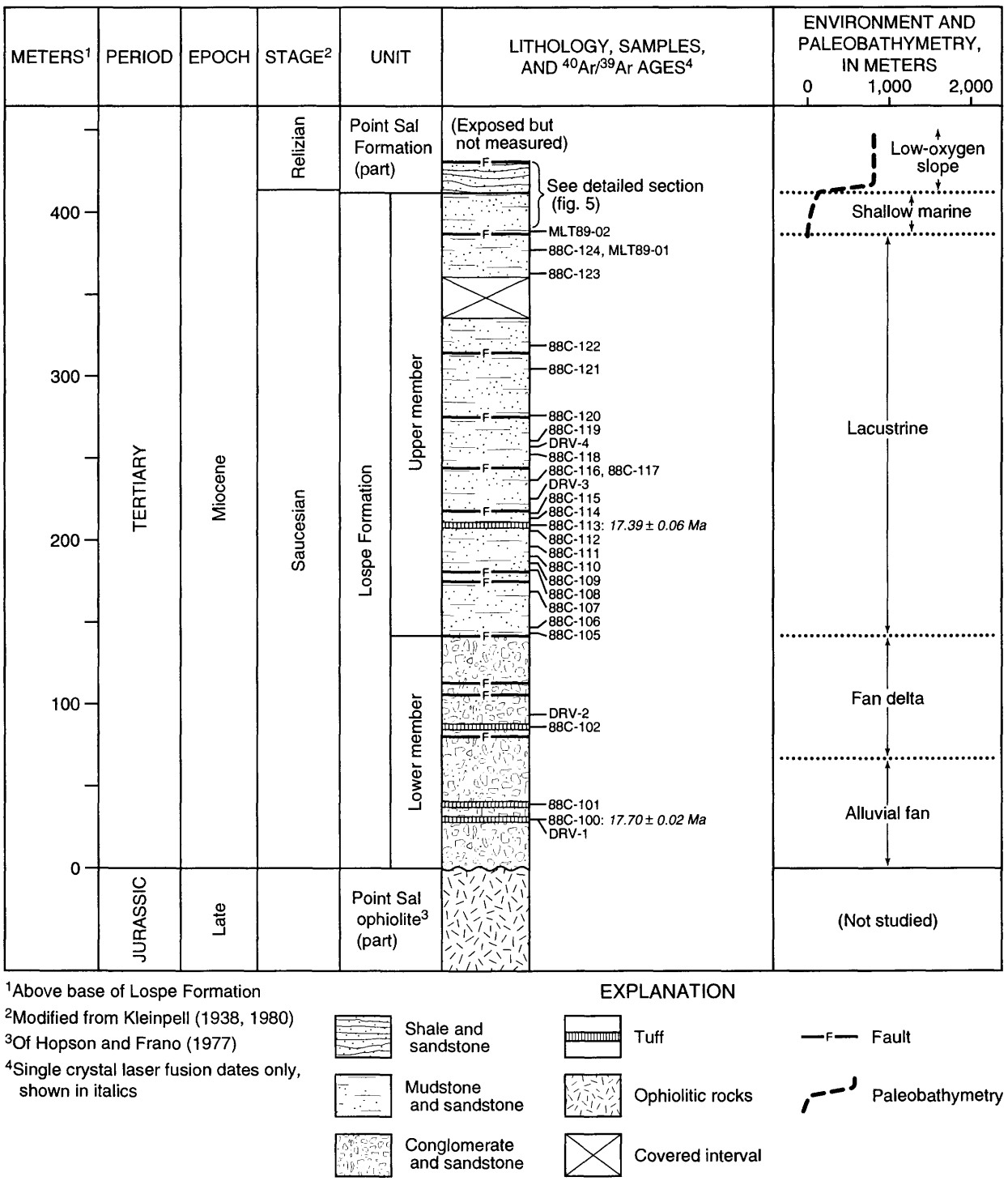

Figure 4. Schematic stratigraphic section of the Lospe Formation at North Beach.

dards, equipment, and analytical techniques by the laboratories involved, and also by differences in sample preparation prior to dating. The crystals dated by the single-crystal method were carefully hand-picked under a microscope to include only the freshest volcanogenic crystals of sanidine; the age obtained from these crystals is herein interpreted as representing the actual cooling time of the mineral grains and the time of eruption of the tuff. In contrast, the crystals dated by the incremental heating method were obtained by heavy-liquid separation and may include, in addition to volcanogenic sanidine, crystals of sanidine derived from an older volcanic edifice, as well as detrital or accidental grains of potassium feldspar that were recycled from Paleogene or older quartzofeldspathic sandstone and ultimately from Mesozoic or older granitoids. Thus, the somewhat older age given by the incremental heating method probably results from dating a mixture of Miocene

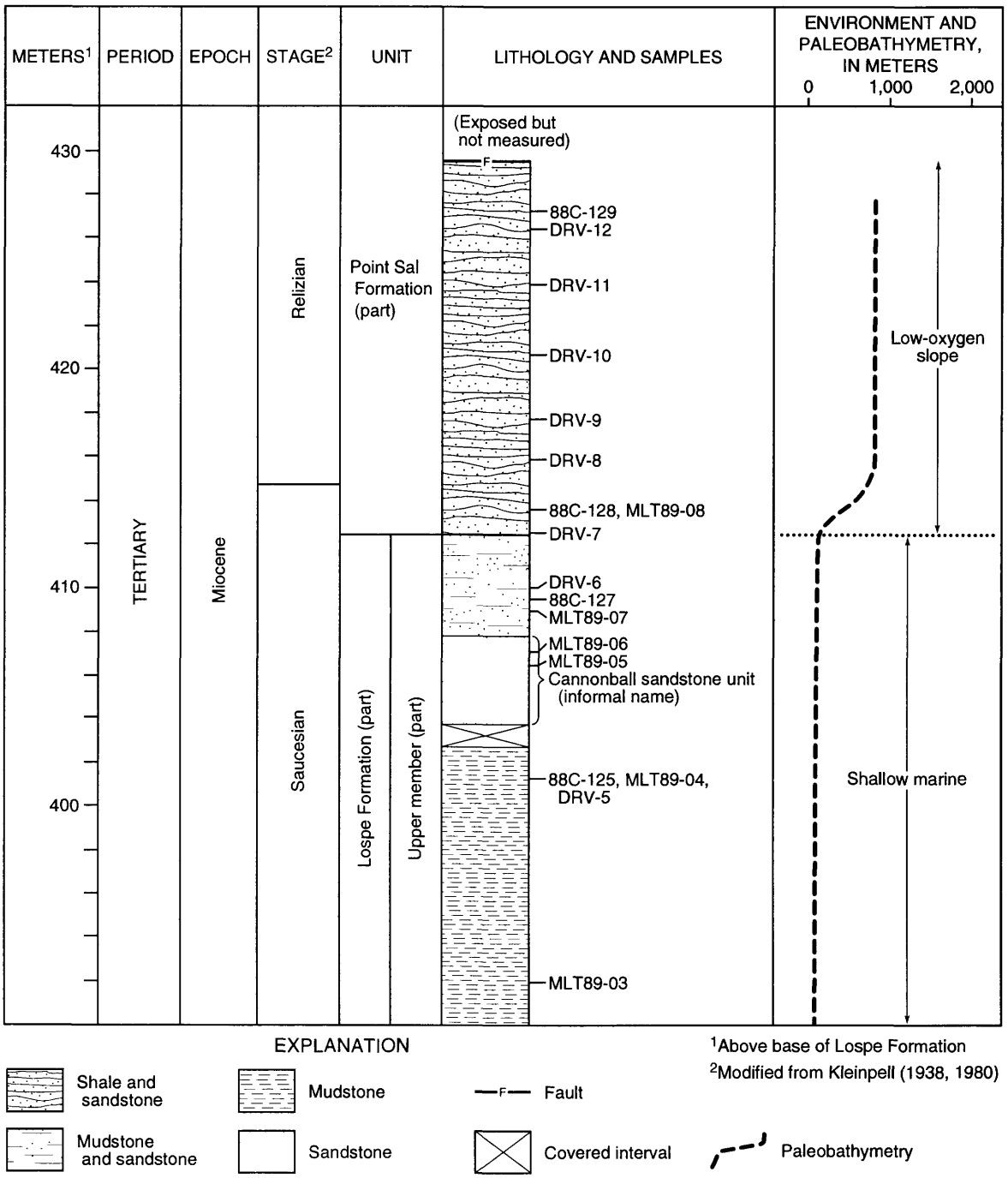

Figure 5. Schematic stratigraphic section across the contact between the Lospe and Point Sal Formations at North Beach.

volcanogenic crystals and older grains. The minimum of the saddle-shaped spectra (fig. 10) is inferred to represent a maximum age for the sample.

Sample 88C-101 was collected from a lenticular, 20-cm-thick tuff bed about 40 m above the base of the Lospe Formation (figs. 4, 11). Sanidine from this tuff gave an incremental heating $^{40}Ar/^{39}Ar$ age of 18.10±0.06 Ma (fig. 10). The tuff bed strikes east-west and dips about 47°N, and it is similar in lithology to sample 88C-100 (described above) except that it is harder and has a greater proportion of granule-sized and larger accidental clasts. The accidental clasts are generally well rounded and consist mainly of sandstone and ophiolitic debris (including greenstone and red silica-carbonate rock). The accidental clasts range in size from sand to as large as 5

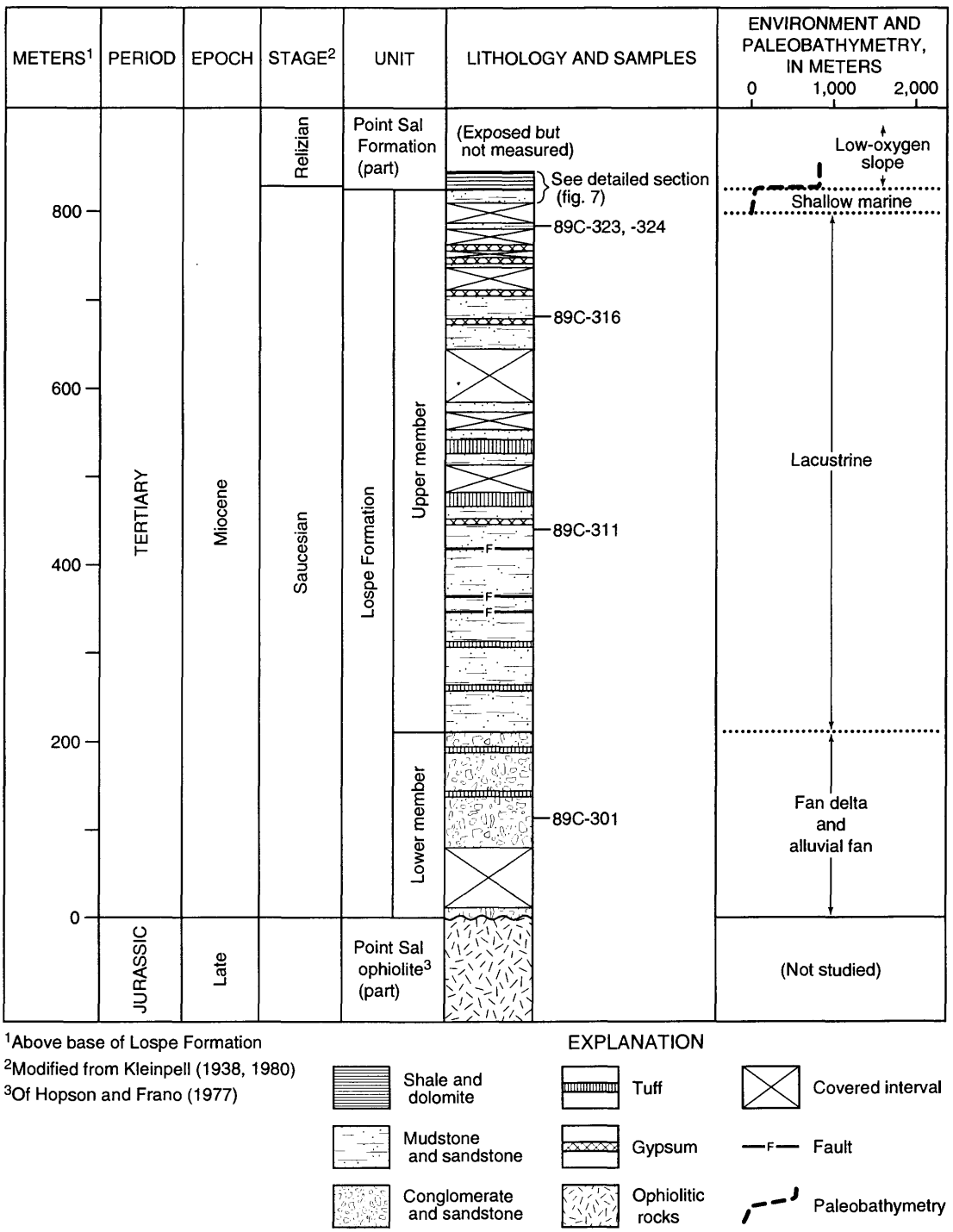

Figure 6. Schematic stratigraphic section of the Lospe Formation along Chute Creek.

cm (fig. 12) and decrease in size upward in the bed (normal grading). The lower part of the tuff bed fills scoured erosional depressions that penetrate as deep as 40 cm into the underlying red sandstone and conglomerate. The upper bed boundary is abrupt and erosionally truncated. The volcanic material in samples 88C-100 and 88C-101 may have been transported to the North Beach area as airfall or a pyroclastic flow from some distant eruptive center, but it probably was reworked and deposited by flowing streams. The latter conclusion is supported by the following observations: (1) the tuffs are interbedded with stream-dominated alluvial fan deposits (Johnson and Stanley, 1994); (2) the tuffs exhibit erosional lower bed boundaries, lenticular bed geometry, and normal grading consistent with deposition by streams; and (3) the tuffs consist of a mixture of fine-grained volcanic material and coarser, rounded accidental clasts that are identical to clasts within the enclosing alluvial fan deposits.

Sample 88C-113 was obtained from a prominent, white-weathering, 65-cm-thick tuff bed in the upper member of the Lospe, about 210 m above the base of the Lospe at North Beach (figs. 4, 13). Plagioclase from this tuff yielded a single crystal laser fusion $^{40}Ar/^{39}Ar$ age of 17.39±0.06 Ma (table 1). The bed strikes about N. 45°W. and dips about 19°N. The tuff rests abruptly on hard, darker colored, gray-green mudstone; slight irregularities about 1–2 cm deep along the lower bed boundary may represent load casts or filled scours. The tuff is abruptly overlain by hard gray-green to red-brown mudstone. The lower 25 cm of the tuff is soft, recessive weathering, and

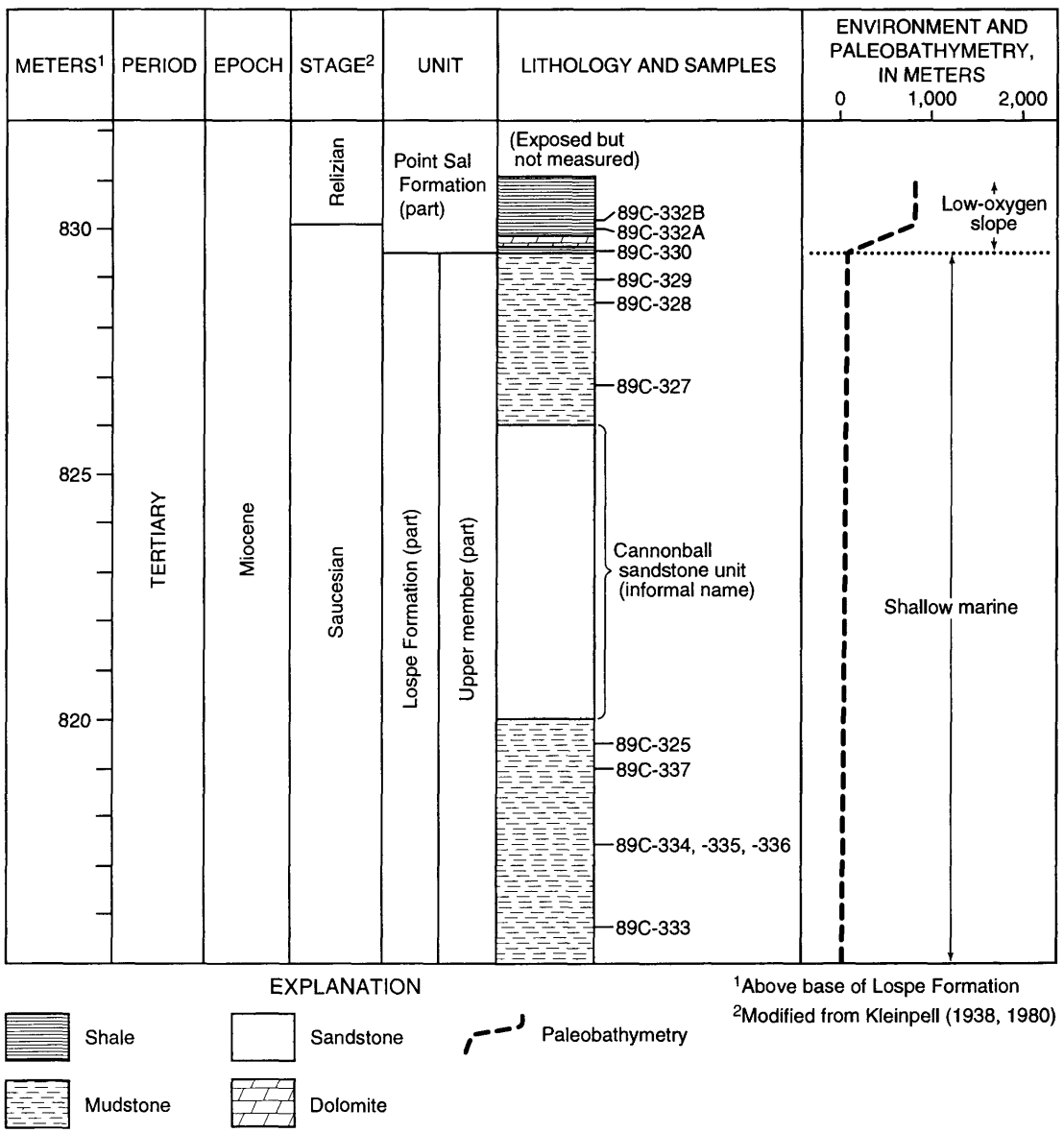

Figure 7. Schematic stratigraphic section across the contact between the Lospe and Point Sal Formations at Chute Creek.

apparently vitric rich and crystal poor. The upper 40 cm of the tuff is hard, has a slight pinkish color on freshly broken surfaces, grades upward from crystal rich to crystal poor (apparent normal grading), and is flat laminated in its lower part and cross-laminated in its upper part (fig. 13). The cross-laminations suggest paleoflow to the northeast. In thin section, the tuff consists of crystals of plagioclase and minor quartz and biotite in a slightly altered matrix of bubble-wall glass shards and pumice grains. The tuff is enclosed within lacustrine mudstone and therefore was probably deposited on the floor of a lake (Stanley and others, 1990, 1991). Deposition from a waning flow, possibly a turbidity current, is suggested by normal grading and by the upward change from plane lamination to cross-lamination.

For comparison with tuffs in the Lospe, sample 89C-57 was taken from extremely hard welded tuff exposed in a roadcut about 230 m (750 ft) northeast of the peak of Tranquillon Mountain (fig. 1), and roughly 50–90 m

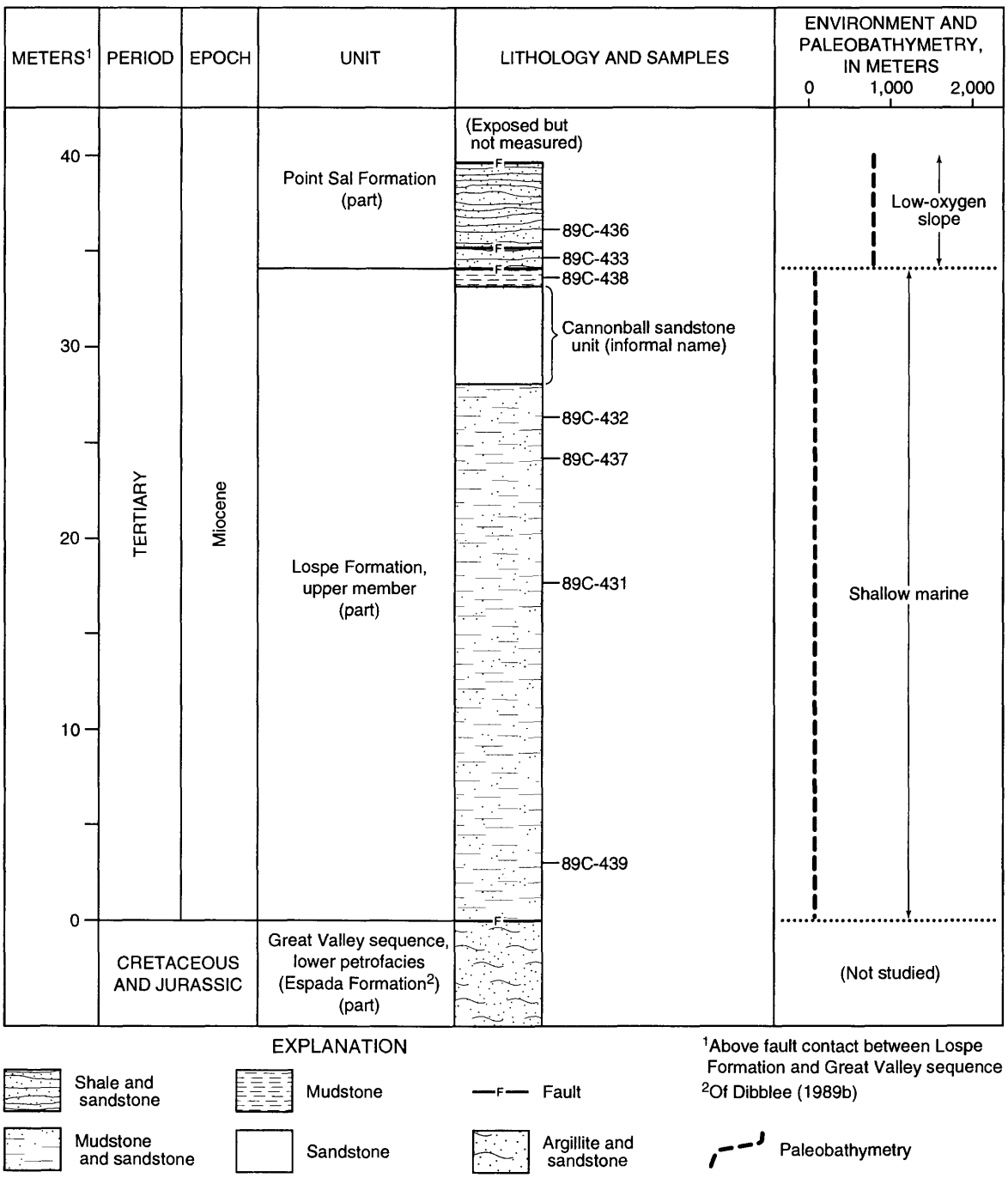

Figure 8. Schematic stratigraphic section of the Lospe Formation about 1 km north of Point Sal.

stratigraphically above the contact between the Tranquillon Volcanics and the underlying Rincon Shale. Sanidine from this tuff gave a single crystal laser fusion $^{40}Ar/^{39}Ar$ age of 17.80±0.05 Ma (table 1). A thin section from the tuff shows about 5-10 percent euhedral to subhedral crystals of quartz, sanidine, and minor plagioclase in an altered glassy matrix with eutaxitic texture, in which pumice and other glassy grains are elongate and aligned parallel to stratification.

Sample 122734 was collected in 1974 by John Van Couvering from white clayey tuff near the base of the Monterey Formation, stratigraphically just above the covered contact with the underlying Rincon Shale, in a sea cliff exposure near the mouth of Las Varas Canyon near Naples (fig. 1). Sanidine from this tuff gave a single crystal laser fusion $^{40}Ar/^{39}Ar$ age of 18.42±0.06 Ma (table 2).

BIOSTRATIGRAPHY

Biostratigraphic correlations based on assemblages of microfossils—including benthic and planktic foraminifers, calcareous nannofossils, and palynomorphs—are consistent with the isotopic ages discussed above and confirm that the Lospe Formation in the Casmalia Hills is of late early Miocene age. Samples were collected from the Lospe and Point Sal Formations in measured sections at North Beach, Chute Creek, and about 1 km north of Point Sal, and at two localities near Corralitos Canyon (figs. 1, 2). Samples were prepared and examined in the laboratories of Unocal Oil and Gas Division, Ventura, California. Of a total of 69 samples, 48 were processed and analyzed for benthic and planktic foraminifers, 40 for calcareous nannofossils,and 69 for palynomorphs. The following biostratigraphic zonations were used (fig. 14): for benthic foraminifers, Kleinpell (1938, 1980) as modified by Unocal Corporation; for planktic foraminifers, Bolli and Saunders (1985); for calcareous nannofossils, Bukry (1973, 1975) and Okada and Bukry (1980); for palynomorphs, a proprietary zonation developed by Unocal Corporation. Estimates of water depth were made by comparing the benthic foraminiferal assemblages in our samples with the paleobathymetric biofacies of Ingle (1980). Biostratigraphic results are summarized in table 3 and discussed below.

No fossil remains of vertebrates or plant leaves, and only fragments of probable molluscan shells, have been found in the Lospe Formation in the Casmalia Hills. A single occurrence of unidentifiable bird tracks was discovered in fine-grained sandstone of the upper member of the Lospe by M.A. Mason (unpub. data, 1988).

Figure 9. Field photograph of white-weathering 20-cm-thick tuff bed overlain and underlain by red (dark colored in this black-and-white photograph) alluvial fan conglomerate and sandstone, about 30 m above the base of the Lospe Formation at North Beach. Sample 88C-100 from this tuff was dated at 17.70±0.02 Ma by the $^{40}Ar/^{39}Ar$ single crystal laser fusion method (mean of seven determinations on sanidine), and at 18.46±0.06 Ma by the $^{40}Ar/^{39}Ar$ incremental heating method on sanidine. S.Y. Johnson for scale.

Benthic Foraminifers

Assemblages of benthic foraminifers in four samples from the Point Sal Formation (88C-128 and DRV-7 at North Beach; 89C-332A and 89C-330 at Chute Creek; see table 3) were assigned a Saucesian age on the basis of the joint occurrence of *Nonion incisum* and *Valvulineria casitasensis*. Assemblages in five samples from the Lospe Formation (MLT89-07, MLT89-06, and DRV-5 at North Beach; 89C-328 and 89C-327 at Chute Creek; see table 3) contain shallow-water species that are not diagnostic of the Saucesian but are considered to be probable Saucesian because of their stratigraphic posi-

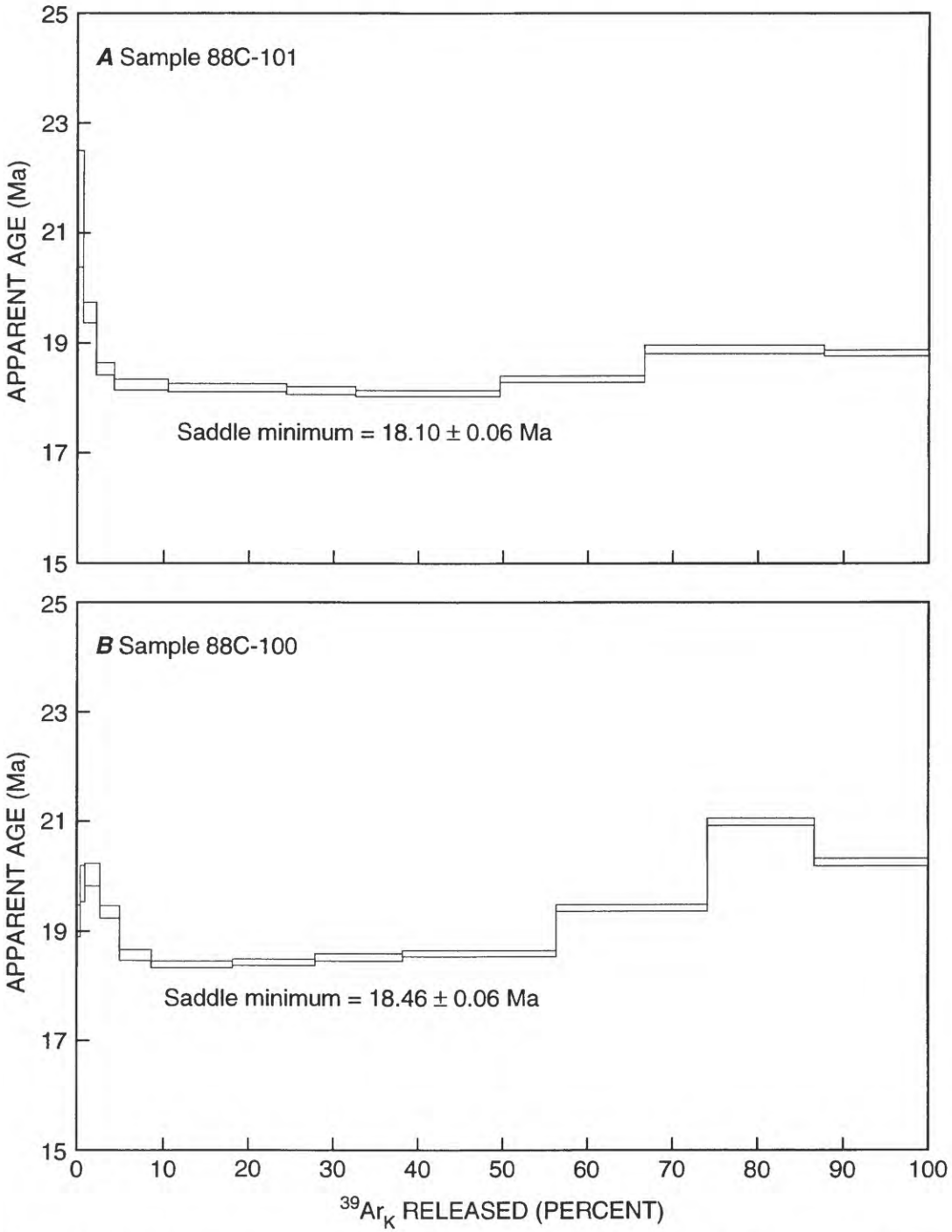

Figure 10. Argon age-spectrum diagrams ($^{40}Ar/^{39}Ar$ incremental heating method) for (*A*) sample 88C-101 and (*B*) sample 88C-100 from the Lospe Formation at North Beach. $^{39}Ar_K$ is the reactor-produced ^{39}Ar from ^{39}K. The saddle minimum for each sample is interpreted as the maximum age for the time of eruption.

Table 1. Total single crystal laser fusion $^{40}Ar/^{39}Ar$ data for the Lospe Formation and Tranquillon Volcanics of Dibblee (1950)

[All analyses were made on single mineral crystals. Procedures and methods employed for the $^{40}Ar/^{39}Ar$ analyses follow Swisher and others (1993) and references therein. L, laboratory sample number; SD, one standard deviation; $^{40}Ar^*$, radiogenic ^{40}Ar]

L Number	$^{37}Ar/^{39}Ar$	$^{36}Ar/^{39}Ar$	$^{40}Ar^*/^{39}Ar$	$^{40}Ar^*$ (percent)	Age (Ma)	SD (1σ)
LOSPE FORMATION						
88C-113 (plagioclase)						
2586-01[1]	1.630	0.00147	0.544	64.1	17.30	0.25
2586-02[1]	1.750	.00319	.542	40.5	17.40	.31
2586-03[1]	1.614	.00076	.542	84.9	17.25	.23
2586-04[1]	1.618	.00073	.545	86.2	17.34	.17
2586-05[1]	1.708	.00088	.552	81.9	17.54	.17
2586-06[1]	1.696	.00156	.551	62.9	17.53	.31
Weighted mean age					**17.39**	**.06**
88C-100 (sanidine)						
1744-01[2]	0.008	0.00030	1.786	95.2	17.69	0.11
1744-02[2]	.010	.00010	1.787	98.3	17.71	.10
1744-04[2]	.007	.00053	1.791	91.9	17.74	.10
1744-05[2]	.012	.00019	1.784	97.0	17.67	.10
1744-07[2]	.008	.00030	1.779	95.2	17.63	.10
2588-01[1]	.009	.00002	0.557	98.6	17.72	.06
2588-03[1]	.008	.00040	0.556	82.5	17.69	.07
Weighted mean age					**17.70**	**.02**
TRANQUILLON VOLCANICS						
89C-57 (sanidine)						
2590-01[1]	0.040	0.00009	0.563	95.6	17.89	0.07
2590-02[1]	.040	.00016	.563	92.5	17.90	.08
2590-03[1]	.021	.00008	.556	95.9	17.68	.09
2590-04[1]	.037	.00041	.558	82.3	17.75	.08
2590-06[1]	.040	.00015	.558	92.7	17.73	.09
Weighted mean age					**17.80**	**.05**
Contaminant or altered grain						
2590-05	0.033	0.00057	0.570	77.2	18.11	0.08

[1]Irradiation # 27E J = 0.017708 ± 0.00004.
[2]Irradiation # 19A J = 0.0055196 ± 0.00001.

tion in a conformable sequence immediately beneath Saucesian strata of the Point Sal Formation. Assemblages in seven samples from the Point Sal Formation (89C-129, DRV-12, DRV-11, DRV-10, DRV-9 and DRV-8 at North Beach; 89C-332B at Chute Creek; see table 3) were assigned a Relizian age on the basis of the joint occurrence of *Valvulineria ornata* and *Bolivina advena*, which are considered typical of the Relizian, and *Bolivina imbricata*, which has its stratigraphically lowest occurrence in the Relizian (Kleinpell, 1938, 1980). Sample 89C-441 from the Point Sal Formation in the Corralitos Canyon area includes *Bolivina advena* and is considered to be of Relizian age or older. Thirty-one additional samples from the Lospe and Point Sal Formations were processed for foraminifers and were barren or yielded sparse assemblages of indeterminate age.

Paleobathymetric analysis of benthic foraminiferal biofacies shows that the upper part of the upper member of the Lospe Formation was deposited generally at neritic depths, or about 0–150 m (according to the scheme of Ingle, 1980). Assemblages from the Point Sal Formation suggest deposition at upper bathyal to middle bathyal depths, or about 150–1,500 m. An abrupt deepening associated with the contact between the Lospe and Point Sal Formations is apparent in the North Beach and Chute Creek sections (figs. 4, 5, 6, 7).

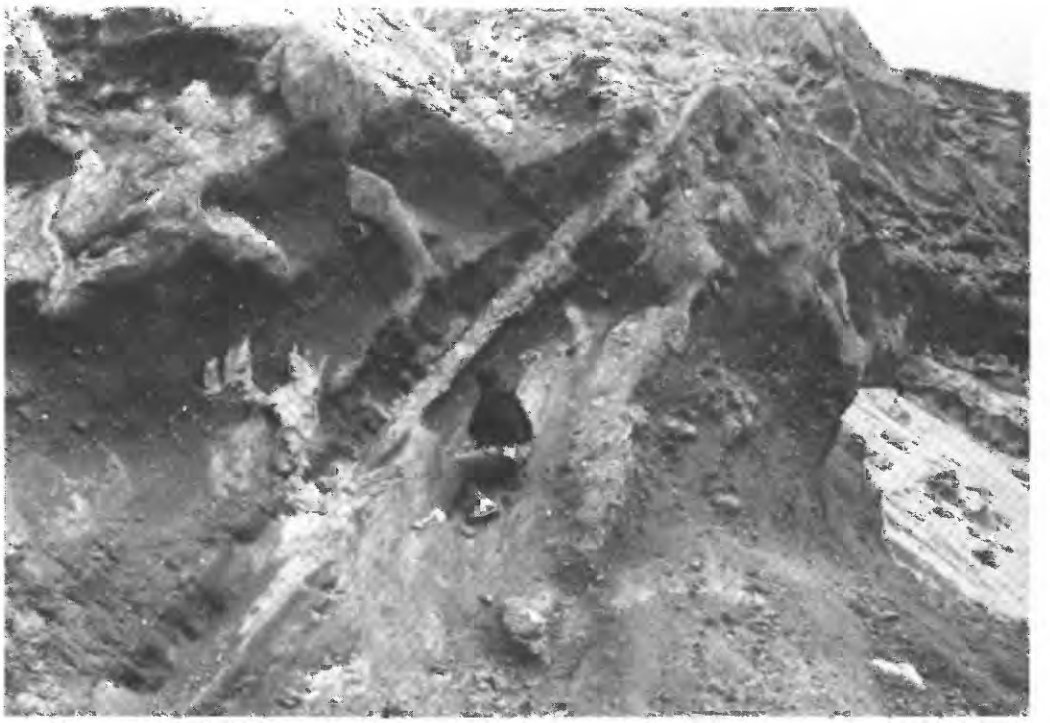

Figure 11. Field photograph of white-weathering 20-cm-thick tuff bed overlain and underlain by dark-colored alluvial fan conglomerate and sandstone, about 40 m above the base of the Lospe Formation at North Beach. Sanidine from sample 88C-101 from this tuff was dated at 18.10±0.06 Ma by the $^{40}Ar/^{39}Ar$ incremental heating method. R.B. Cole for scale.

Figure 12. Detail of part of the tuff bed in figure 11, showing a rounded, dark-colored accidental clast of altered serpentinite about 5 cm in diameter in the lower part of the bed (above pen).

Some of the benthic foraminiferal assemblages in the Point Sal Formation (for example, sample 88C-128 at North Beach) include displaced outer neritic taxa in association with upper to middle bathyal taxa, indicating downslope transport. Additionally, several Point Sal assemblages (for example, samples DRV-11, DRV-10, DRV-9, and DRV-8 at North Beach) contain species thought to be indicative of low-oxygen conditions, including *Bolivina advena*, *Bolivina imbricata*, *Buliminella curta*, and *Virgulina californiensis* (but the role of oxygen content in controlling the distribution of foraminiferal taxa is debated; see, for example, Bernhard, 1992; Gooday, 1994; Rathburn and Corliss, 1994). Deposition under low-oxygen conditions is further suggested by sedimentological evidence including high organic content, abundant pyrite, absence of megafossils, and the presence of phosphatic laminae and nodules (Stanley and others, 1990, 1995). Such features are common in low-oxygen muds in modern marine environments and in other shales of inferred low-oxygen origin in the geologic record (Garrison, 1981; Pisciotto and Garrison, 1981; Soutar and others, 1981).

Planktic Foraminifers

The only planktic foraminifers found in samples from the Lospe Formation (89C-325, 89C-336, and 89C-333 at Chute Creek; see table 3) consist of rare specimens of *Globigerina* spp. that are not age diagnostic. However, several samples from the Point Sal Formation (MLT89-08 at North Beach; 89C-332A and 89C-330 at Chute Creek; 89C-441 near Corralitos Canyon; see table 3) yielded assemblages of planktic foraminifers including *Catapsydrax dissimilis*, whose last occurrence coincides with the top of zone N6 (Bolli and Saunders, 1985, p. 165; see fig. 14). Other species found in samples from the Point Sal Formation include *Globorotaloides suteri*, which last appears in zone N8 (Bolli and Saunders, 1985, p. 172), and *Globigerina concinna*, a long-ranging Miocene form (Bandy and Ingle, 1970, p. 141).

The assemblage in sample 88C-128 from the Point Sal Formation at North Beach was assigned to zones N4-N6 because it contains *Catapsydrax dissimilis* along with a form tentatively identified as *Globorotalia kugleri*, whose last occurrence coincides with the top of zone N4 (Bolli and Saunders, 1985, p. 165). This assemblage occurs about 206 m stratigraphically above a tuff (sample 88C-113; see fig. 4) dated isotopically at about 17.4 Ma, indicating that the top of zone N4 must be younger than 17.4 Ma. However, this presents a dilemma because the top of zone N4 in coastal southern California is thought to be close to 20 Ma (fig. 14; Bartow, 1992; Mayer and others, 1992). If our identification of *G. kugleri* is correct, then the range of this species spans a longer stratigraphic interval in coastal southern California than previously

Figure 13. Field photograph of white-weathering 65-cm-thick tuff bed overlain and underlain by darker-colored lacustrine mudstone, about 210 m above the base of the Lospe Formation at North Beach. Sample 88C-113 from this tuff was dated at 17.39±0.06 Ma by the $^{40}Ar/^{39}Ar$ single crystal laser fusion method (mean of six determinations on plagioclase). The mudstone and tuff are overlain in angular unconformity by boulder conglomerate of Quaternary age. Helen Gibbons for scale.

Table 2. Total single crystal laser fusion $^{40}Ar/^{39}Ar$ data for the Monterey Formation

[All analyses were made on single mineral crystals. Procedures and methods employed for the $^{40}Ar/^{39}Ar$ analyses follow Obradovich (1993) and references therein. L, laboratory sample number; SD, one standard deviation; $^{40}Ar^*$, radiogenic ^{40}Ar]

L Number[2]	$^{40}Ar/^{39}Ar$	$^{37}Ar/^{39}Ar$	$^{36}Ar/^{39}Ar$	$^{40}Ar^*/^{39}Ar$	$^{40}Ar^*$ (percent)	K/Ca	Age (Ma)	SD[1] (1σ)
				122734 (sanidine)				
93Z0580	3.96545	0.03150	0.000084	3.93419	99.21	15.56	18.42	0.13
93Z0581	3.97573	.03400	.000040	3.95756	99.54	14.41	18.53	.09
93Z0583	3.99481	.02797	.000300	3.89931	97.61	17.52	18.26	.13
93Z0584	3.97506	.04280	.000075	3.94724	99.30	11.45	18.48	.09
Unweighted mean age							**18.42**	**.06**
				Contaminant or altered grain				
93Z0582	5.75640	0.03800	0.000105	5.71931	99.35	12.89	26.72	0.10

[1]Error of the mean at the 95 percent confidence level

[2]For all analyses:

$J = 0.002609$

$(^{36}Ar/^{37}Ar)_{Ca} = 2.69 \pm 0.24 \times 10^{-4}$

$(^{39}Ar/^{37}Ar)_{Ca} = 6.79 \pm 0.051 \times 10^{-4}$

$(^{40}Ar/^{39}Ar)_K = 9.1 \pm 5.4 \times 10^{-3}$

$\lambda_\varepsilon + \lambda_{\varepsilon'} = 0.581 \times 10^{-10}\ yr^{-1}$

$\lambda_\beta = 4.962 \times 10^{-10}\ yr^{-1}$

$^{40}K/K = 1.167 \times 10^{-4}$ atom/atom

thought, and zone N4 in this area must be redefined and recalibrated to the geochronometric time scale so that its top is younger than 17.4 Ma. It should be noted that several previous workers have encountered problems in using zonations developed in the tropics to correlate the low-diversity planktic foraminiferal assemblages typical of the cooler, temperate waters of California (for example, see Bandy and Ingle, 1970; Ingle, 1973; Blake, 1991). Such problems arise because tropical and temperate assemblages differ in taxonomic composition, and because the first and last appearances of some species are diachronous, occurring at different times in different latitudes (Srinivasan and Kennett, 1981).

Calcareous Nannofossils

Twenty-five samples from the Lospe Formation were processed for calcareous nannofossils but yielded none. Of 15 samples processed from the Point Sal Formation, 13 yielded poorly preserved, low-diversity assemblages that could not be assigned to particular zones but include long-ranging species indicative of early Miocene or Miocene ages (table 3). Taxa identified in these samples, with generalized age ranges according to Perch-Nielsen (1985a, b) except where noted, include *Braarudosphaera bigelowii* (Cretaceous to Holocene?), *Coccolithus pelagicus* (Paleocene to Holocene), *Coronocyclus nitescens* (Eocene to Miocene), *Cyclicargolithus floridanus* (Eocene to middle Miocene), *Dictyococcites* sp., *Discoaster calculosus* (late Oligocene and early Miocene), *Discoaster deflandrei* (Eocene to middle Miocene), *Helicosphaera carteri* (a first appearance guide to the Miocene: David Bukry, written commun., 1993), *Reticulofenestra gartneri* (Oligocene and early Miocene: M.V. Filewicz, unpub. data), *Reticulofenestra pseudoumbilica* (Miocene and Pliocene), and *Sphenolithus abies* (Miocene). During a previous study of the Chute Creek area, a calcareous nannofossil assemblage indicative of early and early middle Miocene zone CN3 (fig. 14) was recovered from a sample of the Point Sal Formation immediately above the contact with the Lospe Formation (M.V. Filewicz and Unocal Corporation, unpub. data).

Palynomorphs

Pollen assemblages of early and (or) middle Miocene age were recognized in 18 samples from the Lospe and Point Sal Formations at North Beach and Chute Creek (table 3, figs. 4, 5, 6, 7). This age assignment is based in part on high relative abundances of *Carya* sp. pollen, which is known to be present in significant amounts in strata of early and middle Miocene age elsewhere in southern California (Ballog and Malloy, 1981; Srivastava, 1984; Unocal Corporation, unpub. data). A more precise age of early and (or) early middle Miocene was assigned to five samples from the Point Sal Formation (89C-

332B and 89C-332A at Chute Creek; 89C-436 and 89C-433 near Point Sal; 89C-441 near Corralitos Canyon; see table 2) on the basis of high relative abundances of *Carya* sp. and the occurrence of *Hystrichokolpoma rigaudiae*, a marine dinocyst that has been seen in strata no younger than early and early middle Miocene zone CN3 in southern California (D.R. Vork and Unocal Corporation, unpub. data). Reworked palynomorphs of Cretaceous age, including *Proteacidites thalmanni* and *Classopollis* sp., were found in sample 88C-108 from North Beach. Reworked Late Cretaceous pollen was found in sample DRV-4, and reworked Late Cretaceous and (or) Paleogene pollen in sample DRV-5 (both from North Beach). Sample 89C-328 from Chute Creek contained several redeposited specimens of palynomorphs of Jurassic(?) and (or) Cretaceous(?) age. Of the 69 samples processed for palynomorphs, 46 were barren or yielded very sparse assemblages that could not be dated (table 3).

Palynomorphs from our samples of the Lospe and Point Sal Formations show abundant signs of oxidation during outcrop weathering, but they yield evidence of a diverse terrestrial vascular plant flora including *Carya* (hickory), *Quercus* (oaks), *Juglans* (walnuts), *Ulmus* (elms), *Betula* (birch), *Alnus*

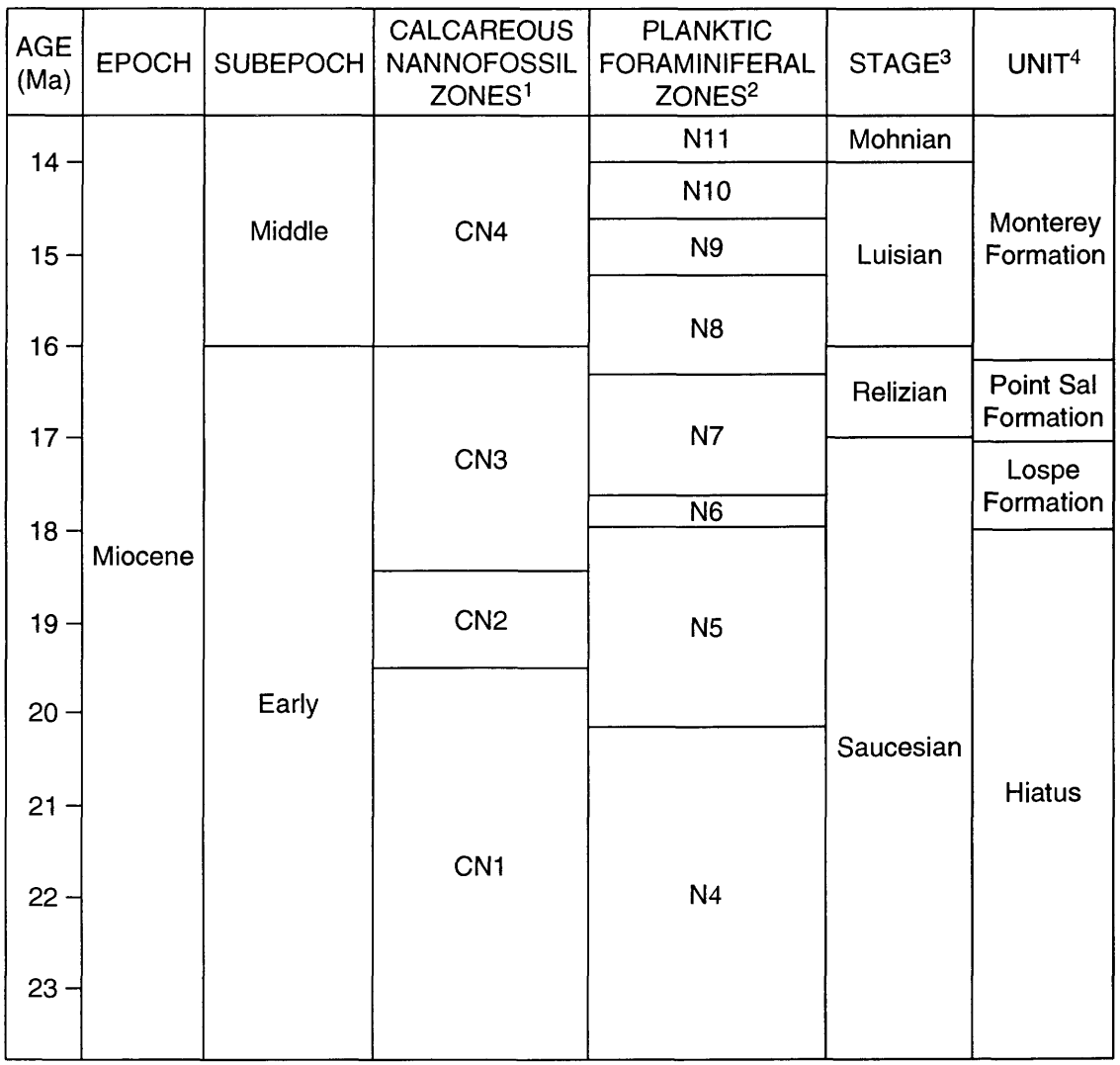

[1]Of Bukry (1973, 1975) and Okada and Bukry (1980).
[2]Of Bolli and Saunders (1985).
[3]Modified from Kleinpell (1938, 1980).
[4]In the Point Sal area and northwestern Casmalia Hills.

Figure 14. Early and middle Miocene time scale used in this report, compiled and somewhat modified from Bartow (1992), Mayer and others (1992), and Cande and Kent (1992, 1995). New data presented and discussed in the text suggest that the top of planktic foraminiferal zone N4 in southern California may be younger than shown.

Table 3. Biostratigraphic results from the Lospe and Point Sal Formations in the Casmalia Hills

[Localities shown on figs. 1 and 2. For each locality, arranged stratigraphically from top to bottom. Identifications and assignments by M.L. Cotton (benthic and planktic foraminifers), M.V. Filewicz (calcareous nannofossils), and D.L. Vork (palynomorphs). Zonations used: benthic foraminifers, Kleinpell (1938, 1980) as modified by Unocal Corporation; planktic foraminifers, Bolli and Saunders (1985); calcareous nannofossils, Bukry (1973, 1975) and Okada and Bukry (1980); palynomorphs, unpublished zonation of Unocal Corporation. Paleobathymetry based on depth-related biofacies of Ingle (1980)]

Sample number	Formation	Age-diagnostic and associated taxa	Age or zone	Paleobathymetry	Remarks
		NORTH BEACH			
88C-129	Point Sal	Benthic foraminifers: *Bolivina advena, Bolivina advena striatella, Valvulineria miocenica, Valvulineria* sp. cf. *V. ornata* Barren of calcareous nannofossils and palynomorphs	Relizian	Upper to middle bathyal	Common pyrite
DRV-12	Point Sal	Benthic and planktic foraminifers: *Bolivina advena, Valvulineria ornata, Globigerina* spp. Calcareous nannofossils: assemblage not zoned, with *Coccolithus pelagicus, Cyclicargolithus floridanus, Helicosphaera carteri, Reticulofenestra gartneri* Barren of palynomorphs	Relizian Early Miocene	Upper to middle bathyal	Rare pyrite
DRV-11, DRV-10, DRV-9, DRV-8	Point Sal	Benthic and planktic foraminifers: *Bolivina advena, Bolivina imbricata, Valvulineria ornata, Globorotaloides suteri, Globigerina concinna* Calcareous nannofossils: assemblage not zoned, with *Coccolithus pelagicus, Cyclicargolithus floridanus, Discoaster calculosus, Discoaster deflandrei, Helicosphaera carteri, Reticulofenestra gartneri* Barren of palynomorphs	Early Relizian Early Miocene	Upper to middle bathyal	Taxa believed to indicate low-oxygen conditions include *Bolivina advena, Bolivina imbricata, Buliminella curta,* and *Virgulina californiensis*. Abundant foraminifers, common to abundant pyrite, and rare fish remains
88C-128	Point Sal	Benthic foraminifers: *Valvulineria casitasensis, Plectofrondicularia miocenica* Planktic foraminifers: *Catapsydrax dissimilis, Globorotalia* sp., cf. *G. kugleri* Calcareous nannofossils: assemblage not zoned Barren of palynomorphs	Saucesian N4-N6 Early Miocene	Upper to middle bathyal	Includes displaced outer neritic indicators, as well as abundant pyrite and rare megafossil fragments
MLT89-08	Point Sal	Benthic foraminifers: assemblage of indeterminate age Planktic foraminifers: *Catapsydrax dissimilis, Globorotaloides suteri* Barren of palynomorphs	N4-N6	Probable upper bathyal	Resample of same locality as 88C-128. Common pyrite
DRV-7	Point Sal	Benthic foraminifers: *Valvulineria casitasensis, Valvulineria ornata, Nonion incisum* Barren of calcareous nannofossils and palynomorphs	Saucesian	Outer neritic to upper bathyal	Stratigraphically lowest sample in Point Sal Formation. Includes rare fish remains

Table 3. Continued

Sample number	Formation	Age-diagnostic and associated taxa	Age or zone	Paleobathymetry	Remarks
DRV-6	Lospe	Barren of foraminifers and calcareous nannofossils			
		Palynomorphs: assemblage with abundant *Carya* sp.	Early and (or) middle Miocene(?)		Marine? Includes one specimen of the marine dinoflagellate cyst *Operculodinium* sp.
88C-127	Lospe	Benthic foraminifers: assemblage of indeterminate age		Outer neritic to upper bathyal	Sparse fauna includes arenaceous and small calcareous foraminifers, rare pyritized radiolarians, and rare pyritized diatoms. Abundant pyrite
		Barren of calcareous nannofossils and palynomorphs			
MLT89-07	Lospe	Benthic foraminifers: assemblage with rare *Nonion costiferum, Nonionella miocenica, Buliminella elegantissima*	Probable Saucesian	Neritic	Abundant pyrite and rare megafossil fragments
		Barren of palynomorphs			
MLT89-06	Lospe	Benthic foraminifers: assemblage with rare *Nonion costiferum, Nonionella miocenica, Buliminella elegantissima*	Probable Saucesian	Neritic	Abundant pyrite and rare megafossil fragments
		Barren of palynomorphs			
MLT89-05	Lospe	Barren of foraminifers and palynomorphs			"Cannonball sandstone unit" (informal name; see text for discussion). Common pyrite and rare fish remains
88C-125	Lospe	Barren of foraminifers, calcareous nannofossils, and palynomorphs		Possible marginal marine	Rare radiolarians and diatoms. Abundant pyrite, common carbonized woody material
MLT89-04	Lospe	Barren of foraminifers			
		Palynomorphs: assemblage with abundant *Carya* sp., *Juglans* sp., *Ulmus* sp., *Quercus* sp., Bombacaceae, Pinaceae, *Betula* sp., Asteraceae, *Alnus* sp., *Ephedra* sp., Chenopodiaceae	Early and (or) middle Miocene		No marine dinoflagellate cysts. Resample of same locality as 88C-125 and DRV-5. Common pyrite
DRV-5	Lospe	Benthic foraminifers: *Cassidulina margareta, Valvulineria ornata, Gyroidina soldanii rotundimargo*	Probable Saucesian	Outer neritic to upper bathyal	Resample of same locality as 88C-125 and MLT89-04
		Barren of calcareous nannofossils			
		Palynomorphs: assemblage with abundant *Carya* and Bombacaceae, and rare to frequent Chenopodiaceae, *Ulmus, Ephedra, Quercus, Salix, Pterocarya, Ilex, Juglans*	Early and (or) middle Miocene		Includes reworked pollen of Late Cretaceous and (or) Paleogene age
MLT89-03	Lospe	Barren of foraminifers and palynomorphs			
MLT89-02	Lospe	Benthic foraminifers: assemblage of indeterminate age		Marginal marine?	Possible marginal marine, on basis of occurrence of *Cibicides* sp.; includes rare fish remains
		Barren of palynomorphs			
88C-124	Lospe	Barren of palynomorphs			
MLT89-01	Lospe	Barren of foraminifers and palynomorphs			Resample of same locality as 88C-124

Table 3. Continued

Sample number	Formation	Age-diagnostic and associated taxa	Age or zone	Paleobathymetry	Remarks
88C-123	Lospe	Palynomorphs: assemblage with abundant *Carya* sp.	Early and (or) middle Miocene(?)		
88C-122	Lospe	Barren of foraminifers Palynomorphs: assemblage with abundant *Carya* sp.	Early and (or) middle Miocene(?)		Marine? Includes one specimen each of the marine dinoflagellate cysts *Spiniferites* sp. (Cretaceous or younger) and *Lejeunecysta* sp. (Eocene or younger), possibly reworked from older strata
88C-121, 88C-120, 88C-119	Lospe	Barren of palynomorphs			
DRV-4	Lospe	Palynomorphs: assemblage, with abundant *Carya* sp.	Early and (or) middle Miocene(?)		Includes reworked pollen of Late Cretaceous age
88C-118	Lospe	Barren of palynomorphs			
88C-117	Lospe	Barren of calcareous nannofossils and palynomorphs			
88C-116	Lospe	Barren of foraminifers Palynomorphs: assemblage of indeterminate age			Marine? Includes two specimens of the marine dinoflagellate cyst *Lingulodinium machaerophorum* (Eocene or younger), possibly reworked from older strata
DRV-3	Lospe	Palynomorphs: assemblage with abundant *Carya* sp.	Early and (or) middle Miocene(?)		
88C-115, 88C-114	Lospe	Barren of palynomorphs			
88C-112	Lospe	Palynomorphs: assemblage with abundant *Carya* sp. and rare Asteraceae pollen; common *Quercus* sp., Malvaceae, *Juglans* sp., and *Ulmus* sp.; frequent Bombacaceae; and Chenopodiaceae(?)	Early and (or) middle Miocene(?)		
88C-111, 88C-110, 88C-109	Lospe	Barren of palynomorphs			
88C-108	Lospe	Palynomorphs: assemblage of indeterminate age			Includes several specimens each of the palynomorphs *Proteacidites thalmanni* and *Classopollis* sp., probably reworked from strata of Cretaceous age

Table 3. Continued

Sample number	Formation	Age-diagnostic and associated taxa	Age or zone	Paleobathymetry	Remarks
88C-107, 88C-106, 88C-105	Lospe	Barren of palynomorphs			
DRV-2	Lospe	Barren of palynomorphs			Reddish-brown mudstone
DRV-1	Lospe	Barren of palynomorphs			Tuff, same horizon as 88C-100
		1 KILOMETER NORTH OF POINT SAL			
89C-436	Point Sal	Benthic and planktic foraminifers: assemblage not zoned, with *Bolivina advena, Bolivina salinasensis, Saracenaria* sp., and *Globigerina concinna*	Early and (or) middle Miocene	Upper to middle bathyal	Includes taxa believed to indicate low-oxygen conditions, and common fish remains
		Calcareous nannofossils: assemblage not zoned, with *Coccolithus pelagicus, Helicosphaera carteri, Dictyococcites* sp., *Reticulofenestra pseudoumbilica*	Miocene		Poorly preserved specimens
		Palynomorphs: assemblage with abundant *Carya* sp.	Early and (or) early middle Miocene		Abundant marine dinoflagellate cysts include *Hystrichokolpoma rigaudiae*
89C-433	Point Sal	Benthic and planktic foraminifers: assemblage not zoned, with rare and very small specimens of *Bolivina advena, Buliminella subfusiformis, Globigerina concinna*	Early and (or) middle Miocene	Upper to middle bathyal	Includes taxa believed to indicate low-oxygen conditions, and common fish remains
		Calcareous nannofossils: assemblage not zoned, with *Coccolithus pelagicus, Helicosphaera carteri, Dictyococcites* sp., *Reticulofenestra pseudoumbilica*	Miocene		Poorly preserved specimens
		Palynomorphs: assemblage	Early and (or) early middle Miocene		Abundant marine dinoflagellate cysts include *Hystrichokolpoma rigaudiae*
89C-438	Lospe	Barren of foraminifers, calcareous nannofossils, and palynomorphs			Rare pyrite
89C-432	Lospe	Barren of foraminifers, calcareous nannofossils, and palynomorphs			Rare, poorly preserved radiolarians
89C-437	Lospe	Foraminifers: assemblage of indeterminate age Barren of calcareous nannofossils and palynomorphs			Possibly marine on the basis of rare arenaceous foraminifera; also includes rare oxidized radiolarians, possibly reworked from Cretaceous strata
89C-431	Lospe	Barren of foraminifers, calcareous nannofossils, and palynomorphs			Common pyrite
89C-439	Lospe	Barren of foraminifers, calcareous nannofossils, and palynomorphs			

Table 3. Continued

Sample number	Formation	Age-diagnostic and associated taxa	Age or zone	Paleobathymetry	Remarks
		CHUTE CREEK			
89C-332B	Point Sal	Benthic and planktic foraminifers: *Bolivina advena, Valvulineria ornata, Globorotaloides suteri, Globigerina concinna*	Relizian	Upper to middle bathyal	Abundant foraminifers and common fish remains
		Calcareous nannofossils: assemblage not zoned, with *Coccolithus pelagicus, Helicosphaera carteri, Dictyococcites* sp., *Sphenolithus abies, Braarudosphaera bigelowii*	Miocene		Poorly preserved specimens
		Palynomorphs: assemblage with common *Carya* sp.	Probable early and (or) early middle Miocene		Abundant marine dinoflagellate cysts include *Hystrichokolpoma rigaudiae*
89C-332A	Point Sal	Benthic foraminifers: assemblage with rare *Valvulineria casitasensis*	Saucesian	Outer neritic to upper bathyal	Abundant foraminifers, rare pyrite and rare fish fragments
		Planktic foraminifers: *Catapsydrax dissimilis, Globorotaloides suteri*	N4-N6		
		Calcareous nannofossils: assemblage not zoned, includes *Coccolithus pelagicus, Helicosphaera carteri, Dictyococcites* sp., *Sphenolithus abies, Braarudosphaera bigelowii*	Miocene		Poorly preserved specimens
		Palynomorphs: assemblage with common *Carya* sp.	Probable early and (or) early middle Miocene		Abundant marine dinoflagellate cysts include *Hystrichokolpoma rigaudiae*
89C-330	Point Sal	Benthic foraminifers: *Valvulineria casitasensis, Valvulineria depressa, Valvulineria williami, Nonion incisum, Plectofrondicularia miocenica*	Saucesian	Outer neritic to upper bathyal	Stratigraphically lowest sample in Point Sal Formation. Includes common pyrite and rare fish remains
		Planktic foraminifers: *Catapsydrax dissimilis, Globigerina concinna, Globorotaloides suteri*	N4-N6		Abundant planktic foraminifers
		Calcareous nannofossils: assemblage not zoned, with *Coccolithus pelagicus, Helicosphaera carteri, Dictyococcites* sp., *Sphenolithus abies, Braarudosphaera bigelowii*	Miocene		Specimens poorly preserved
		Palynomorphs: assemblage with abundant *Carya* sp.	Early and (or) middle Miocene		Common marine dinoflagellate cysts
89C-329	Lospe	Barren of foraminifers and calcareous nannofossils			Common pyrite
		Palynomorphs: assemblage with abundant *Carya* sp.	Early and (or) middle Miocene		Includes very rare marine dinoflagellate cysts

Table 3. Continued

Sample number	Formation	Age-diagnostic and associated taxa	Age or zone	Paleobathymetry	Remarks
89C-328	Lospe	Benthic foraminifers: *Nonion incisum, Nonionella miocenica, Buliminella elegantissima, Elphidium* spp. Barren of calcareous nannofossils Palynomorphs: assemblage with abundant *Carya* sp.	Probable Saucesian Early and (or) middle Miocene	Neritic	Includes several specimens of redeposited palynomorphs of Jurassic(?) and (or) Cretaceous(?) age
89C-327	Lospe	Benthic foraminifers: *Nonion incisum, Nonionella miocenica, Buliminella elegantissima, Elphidium* spp. Barren of calcareous nannofossils Palynomorphs: assemblage with abundant *Carya* sp.	Probable Saucesian Early and (or) middle Miocene	Neritic	
89C-325	Lospe	Foraminifers: assemblage of indeterminate age Barren of calcareous nannofossils Palynomorphs: assemblage with abundant *Carya* sp.	 Early and (or) middle Miocene		Includes rare specimens of *Globigerina* spp.
89C-337	Lospe	Barren of foraminifers and calcareous nannofossils Palynomorphs: assemblage with abundant *Carya* sp.	 Early and (or) middle Miocene		Includes very rare marine dinoflagellate cysts
89C-336	Lospe	Foraminifers: assemblage of indeterminate age Barren of calcareous nannofossils Barren of palynomorphs			Includes rare specimens of *Globigerina* spp., and common to abundant pyrite
89C-335	Lospe	Barren of foraminifers, calcareous nannofossils, and palynomorphs			Common to abundant pyrite
89C-334	Lospe	Barren of foraminifers and calcareous nannofossils Palynomorphs: assemblage with abundant *Carya* sp.	 Early and (or) middle Miocene(?)		Common to abundant pyrite
89C-333	Lospe	Foraminifers: assemblage of indeterminate age Barren of calcareous nannofossils Palynomorphs: assemblage with abundant *Carya* sp.	 Early and (or) middle Miocene		Includes rare specimens of *Globigerina* spp., and common to abundant pyrite
89C-324, 89C-323	Lospe	Barren of foraminifers, calcareous nannofossils, and palynomorphs			Calcitic concretion
89C-316	Lospe	Barren of foraminifers, calcareous nannofossils, and palynomorphs			Includes one possible silicified radiolarian, one possible fish fragment, one possible arenaceous foraminifer, and common gypsum

Table 3. Continued

Sample number	Formation	Age-diagnostic and associated taxa	Age or zone	Paleobathymetry	Remarks
89C-311	Lospe	Barren of foraminifers, calcareous nannofossils, and palynomorphs			Abundant gypsum
89C-301	Lospe	Barren of foraminifers, calcareous nannofossils, and palynomorphs			
		CORRALITOS CANYON AREA			
89C-441	Point Sal	Benthic foraminifers: assemblage with *Bolivina advena*	Relizian	Upper to middle bathyal	Abundant foraminifers, common fish remains
		Planktic foraminifers: *Globigerina concinna, Globorotaloides suteri, Catapsydrax dissimilis*	N4-N6		
		Calcareous nannofossils: assemblage not zoned, includes *Coccolithus pelagicus, Coronocyclus nitescens, Helicosphaera carteri, Sphenolithus abies*	Miocene		Poorly preserved specimens
		Palynomorphs: assemblage with rare *Carya* sp.	Early and (or) early middle Miocene(?)		Includes several specimens of the marine dinoflagellate cyst *Hystrichokolpoma* sp.
89C-404	Lospe	Barren of foraminifers, calcareous nannofossils, and palynomorphs			Red mudstone interbed in conglomerate along Brown Road

(alder), *Pterocarya* (trees related to walnut and hickory), *Ilex* (holly), *Salix* (willows), *Ephedra* (Mormon tea), Pinaceae (pines), Bombacaceae (tropical trees, including baobab and balsa), Malvaceae (mallow family; e.g., cotton), and Astereaceae (sunflower family). This assemblage is generally similar to that found in early Miocene strata of the Monterey Formation at Lions Head (Srivastava, 1984) and suggests a deciduous hardwood forest and warm temperate climate with wet summers; the pines may have lived in elevated areas, whereas the willows probably grew along streams and in swamps. Also found in the Lospe and Point Sal samples were palynomorphs of the Chenopodiaceae (goosefoot family, including spinach, beets, and saltbush), which may indicate alkaline soils.

Common to abundant specimens of marine dinoflagellate cysts, mainly *Hystrichokolpoma* sp., were found in six samples of the Point Sal Formation (89C-436 and 89C-433 near Point Sal; 89C-332B, 89C-332A, and 89C-330 at Chute Creek; 89C-441 near Corralitos Canyon; see table 3). Rare to very rare specimens of marine dinoflagellate cysts, including *Lejeunecysta* sp., *Lingulodinium machaerophorum*, *Operculodinium* sp., and *Spiniferites* sp., were found in five Lospe Formation samples (DRV-6, 88C-122, and 88C-116 at North Beach; 89C-329 and 89C-337 at Chute Creek; see table 3). The marine dinoflagellate cysts in all Point Sal samples and three samples from the uppermost Lospe (DRV-6, 89C-329, 89C-337) occur in strata that contain other marine microfossils (including benthic and planktic foraminifers) and clearly were deposited in neritic to bathyal marine environments on the basis of paleobathymetric analysis (table 3) and sedimentology (Stanley and others, 1990). However, the presence of marine dinoflagellate cysts in two samples from stratigraphically lower in the Lospe (88C-122, 88C-116) is puzzling because the dinoflagellate cysts are not associated with other marine fossils and occur in strata interpreted as probable nonmarine and lacustrine on the basis of sedimentological evidence (Stanley and others, 1991, 1992a). These rogue dinoflagellate cysts may be reworked from older marine strata, or they may indicate that the Lospe lake was at times connected to the ocean.

AGE OF THE TYPE LOSPE FORMATION

The isotopic and biostratigraphic data discussed above demonstrate that the Lospe Formation in its type area in the northwestern Casmalia Hills is of late early Miocene age. According to the geomagnetic polarity time scale of Cande and Kent (1992, 1995), the early Miocene began about 23.8 Ma and ended about 16.0 Ma. The age of the base of the

Lospe can be estimated from isotopic dating of sample 88C-100, a tuff bed near the base of the Lospe at North Beach, which (as discussed earlier in this report) gave a single crystal laser fusion $^{40}Ar/^{39}Ar$ age on sanidine of about 17.7 Ma. Because this tuff is 30 m stratigraphically above the base of the Lospe, we suggest that deposition of the Lospe in its type area began earlier than 17.7 Ma, perhaps about 18 Ma.

Our analysis of benthic foraminiferal assemblages shows that the boundary between the Saucesian and Relizian Stages occurs within the Point Sal Formation about 2 m above the top of the Lospe Formation at North Beach (fig. 5) and about 1 m above the top of the Lospe at Chute Creek (fig. 7). The age of the top of the Lospe is therefore nearly the same or slightly older than the Saucesian-Relizian boundary, which in southern California is approximately dated at 17.0 Ma (fig. 14; Bartow, 1992). This age is consistent with our $^{40}Ar/^{39}Ar$ results, discussed earlier in this report, which show that the top of the Lospe at North Beach is about 203 m stratigraphically above a tuff dated at about 17.4 Ma (sample 88C-113; see fig. 4).

The contact between the Lospe and the Point Sal Formations is abrupt, implying a rapid change in the conditions of deposition. Anderson (1980, p. 26-27) argued that this contact is a "marked unconformity" representing a long period of erosion or nondeposition. However, our analysis of benthic foraminifers and palynomorphs in samples collected across this contact found no evidence of missing biostratigraphic zones. Furthermore, we found no physical indications for a hiatus, such as glauconite, phosphorite, bone beds, erosional scours, or borings, which are commonly associated with unconformities in other California Tertiary sequences (for example, in the Santa Cruz Mountains as noted by Brabb, 1964, and Stanley, 1985, 1990). We infer that the Lospe–Point Sal contact records rapid deepening from well-oxygenated neritic environments to oxygen-poor bathyal environments (figs. 4, 5, 6, 7) that occurred when the rate of subsidence exceeded the rate of sediment deposition.

We conclude that the Lospe Formation in its type area in the Casmalia Hills represents a time interval of about 1 m.y., beginning with initial subsidence and deposition of alluvial fan conglomerates about 18 Ma and ending with an episode of abrupt bathymetric deepening and deposition of bathyal marine shale about 17 Ma. The implied average rate of rock accumulation for the type Lospe, using the measured thickness from the Chute Creek section, is 830 m/m.y. This relatively high rate is comparable to rates in other tectonically active basins in the Cenozoic of California—for example, the Miocene and Pliocene Ridge basin (Crowell, 1974; Howell and Von Huene, 1981, p. 2), and the Pliocene and Pleistocene of the Santa Barbara–Ventura basin (Ingle, 1980, p. 182).

No biostratigraphic data or isotopic age dates are available from any of the numerous reported penetrations of the Lospe Formation by exploratory wells in the onshore Santa Maria basin. However, available well records and published cross-sections (see, for example, Woodring and Bramlette, 1950; American Association of Petroleum Geologists, 1959; Crawford, 1971; Namson and Davis, 1990) suggest that much of the Lospe in the subsurface is laterally contiguous with, and lithologically similar to, the outcrops of the type Lospe in the Casmalia Hills and therefore probably the same age.

COMPARISON OF THE LOSPE FORMATION WITH OTHER ROCK UNITS IN THE SANTA MARIA REGION

Rock Units Correlative with the Type Lospe Formation

Sedimentary and volcanic rocks that are the about the same age as the type Lospe Formation are widespread in the southern Coast Ranges (including the Santa Lucia Range and San Rafael Mountains) and western Transverse Ranges (figs. 1, 15), suggesting that a major regional episode of sedimentary basin formation and volcanism occurred in south-central coastal California during the late early Miocene.

The type Lospe Formation appears to be the about the same age as the Tranquillon Volcanics (Dibblee, 1950), a succession of rhyolitic tuff and minor basalt and sedimentary rocks exposed on and near Tranquillon Mountain (figs. 1, 15). The volcanic sequence is about 100–150 m thick (Robyn, 1980) and rests in angular unconformity on the Rincon Shale (Dibblee, 1988b). The upper part of the Rincon in this area is of Saucesian age, on the basis of an assemblage of benthic foraminifers in a sample from a roadcut about 240 m northwest of the peak of Tranquillon Mountain (R.G. Stanley and M.L. Cotton, unpub. data). In roadcuts about 3.9 km west of the peak of Tranquillon Mountain, the contact between the Rincon and the Tranquillon is abrupt and clearly erosional. The lower 30 cm of the Tranquillon is a pebble-granule conglomerate composed mainly of angular to rounded clasts of brown mudstone and dolomite, with abundant robust molluscan fossils. The dolomite clasts have been intensely bored by rock-boring marine invertebrates and appear to be recycled concretions derived from the underlying Rincon Shale. The fossils, identified by J.G. Vedder (oral commun., 1993), include *Turritella ocoyana topangensis* Merriam, *Turritella temblorensis* Wiedey, and *Spondylus perrini* Wiedey, which are representative of the uppermost "Vaqueros Stage" and (or) "Temblor Stage" of Addicott (1972). The basal Tranquillon conglomerate grades upward into nonwelded and then welded rhyolitic tuff. As noted earlier in this report, sample 89C-57 from tuff near the top of Tranquillon Mountain yielded a $^{40}Ar/^{39}Ar$ age of 17.80±0.05 Ma (table 1). The volcanic rocks in the Tranquillon Mountain area are overlain in apparent angular unconformity by the Monterey Formation; a sample from the lower part of the Monterey yielded diatoms of the early and middle Miocene *Denticulopsis lauta* zone as well as Relizian(?) foraminifers (Dunham and Blake, 1987, p. 31).

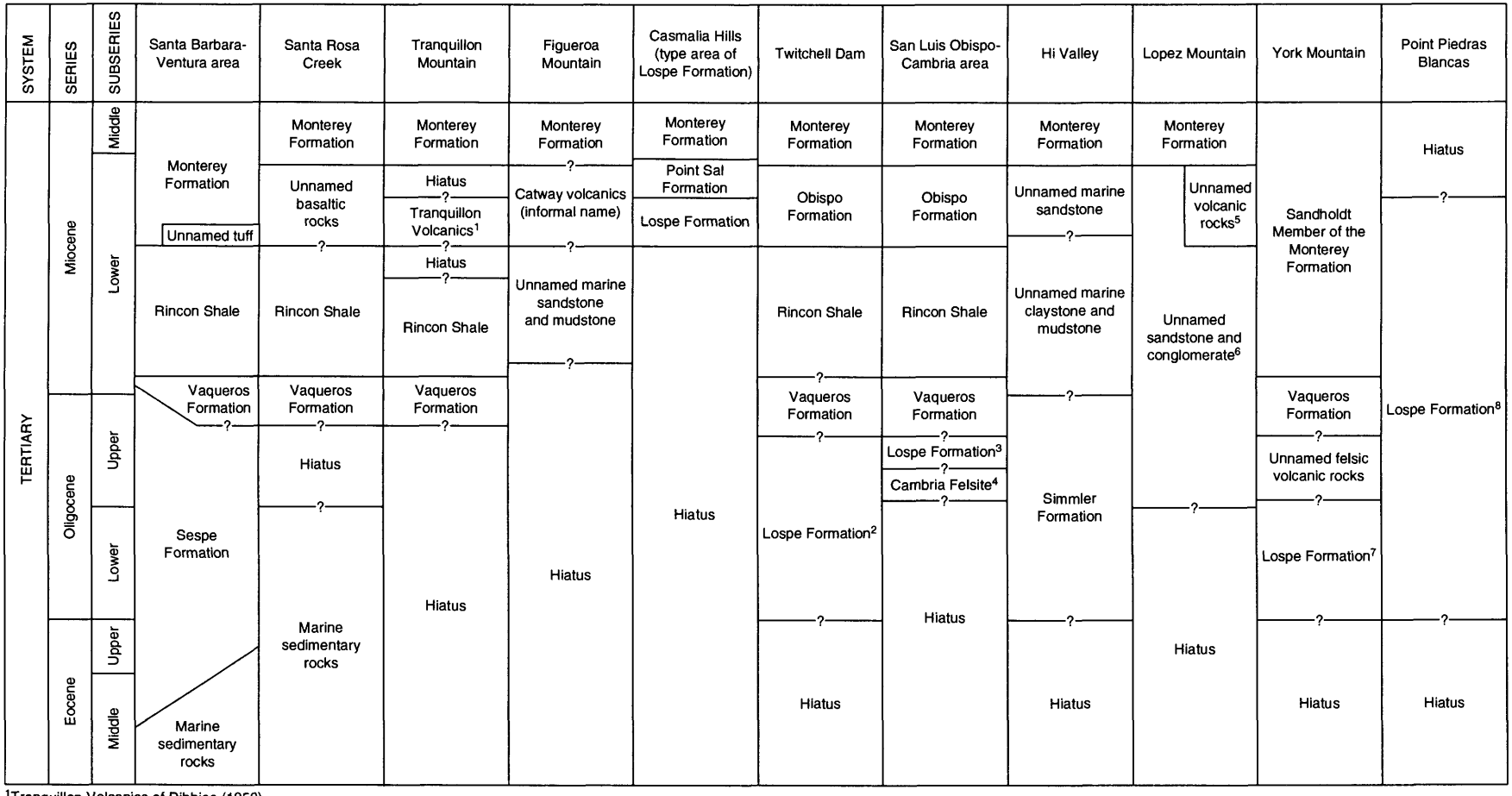

[1]Tranquillon Volcanics of Dibblee (1950)
[2]Lospe Formation(?) of Hall (1978b)
[3]Lospe Formation of Hall (1974), Ernst and Hall (1974), Hall and Prior (1975), and Hall and others (1979)
[4]Cambria Felsite of Ernst and Hall (1974)
[5]Unnamed volcanic rocks of McLean (1994, map units Tvt and Tvf)
[6]Unnamed sandstone and conglomerate of McLean (1994, map unit Tsc)
[7]Lospe Formation of Seiders (1982)
[8]Lospe Formation of Hall (1975, 1976) and Hall and others (1979)

Figure 15. Stratigraphic chart showing correlation of middle Tertiary rock units in the Santa Maria region; see text for discussion and sources of information.

The type Lospe Formation is partly correlative with a 150-m-thick sequence of basaltic rocks along Santa Rosa Creek, about 12 km east of Tranquillon Mountain (figs. 1, 15). The basaltic rocks rest in angular unconformity on the Rincon Shale, are conformably(?) overlain by the Monterey Formation, and yielded a whole-rock potassium-argon age of 17.4±1.2 Ma (age from Turner, 1970, corrected for changes in decay constants using the method of Dalrymple, 1979). The basaltic rocks occupy a similar stratigraphic position as the type Tranquillon Volcanics (Dibblee, 1950) of Tranquillon Mountain and were mapped by Dibblee (1988a) as Tranquillon Volcanic Formation; however, the name Tranquillon seems inappropriate for the basaltic rocks of Santa Rosa Creek because (1) the type Tranquillon Volcanics are predominantly rhyolitic, not basaltic; and (2) the basaltic rocks of Santa Rosa Creek are not physically contiguous with the type Tranquillon Volcanics.

The type Lospe Formation is correlative with an unknown thickness of rock within the lower part of the Monterey Formation along the coast near Santa Barbara (figs. 1, 15). In this area an interval of felsic tuff occurs sporadically along the contact between the Monterey Formation and the underlying Rincon Shale; the tuff has no formal name and is included by Dibblee (1966, p. 46) within the lowest part of the Monterey Formation, but it is known by several local and informal names, including the "Bentonite Bed" (Kleinpell and Weaver, 1963, p. 11), the Tranquillon bentonite (Hornafius, 1994, p. 52), the Tranquillon tuff (Hornafius, 1994, p. 52), and the Summerland rhyolite tuff (Turner, 1970, p. 118). The unnamed tuff is of upper Saucesian age, for it conformably overlies upper Saucesian strata within the upper part of the Rincon Shale and is conformably overlain by upper Saucesian strata within the lower part of the Monterey Formation (Dibblee, 1950, p. 34; Kleinpell and Weaver, 1963, p. 11-12; Dibblee, 1966, p. 50; Turner, 1970, p. 105; DePaolo and Finger, 1991; Stanley and others, 1992b, 1994). As noted earlier in this report, sample 122734 from the unnamed tuff at the base of the Monterey Formation near Naples yielded a $^{40}Ar/^{39}Ar$ age on sanidine of 18.42±0.06 Ma (table 2). Samples of tuff from the base of the Monterey Formation near Summerland, about 9 km east of Santa Barbara (fig. 1), yielded potassium-argon ages on plagioclase of 16.5±0.6 Ma and 17.2±0.5 Ma (ages from Turner, 1970, corrected for changes in decay constants using the method of Dalrymple, 1979). In the Santa Barbara coastal area, the boundary between the Saucesian and Relizian benthic foraminiferal stages occurs within the Monterey Formation "as much as several hundred feet" stratigraphically above the unnamed tuff (Dibblee, 1966, p. 50). Near Naples, for example, the Saucesian-Relizian boundary is about 125 m stratigraphically above the unnamed tuff (see DePaolo and Finger, 1991, their table 3); therefore, it appears that part or perhaps all of the lower 125 m of the Monterey Formation at Naples was deposited at about the same time as the 830-m-thick Lospe Formation in the Casmalia Hills. Thickness trends, available paleocurrents, and similarities in age, petrography, and major and trace element composition indicate that the basal Monterey tuff of the Santa Barbara coast, the Tranquillon Volcanics of Dibblee (1950), and tuff in the Lospe Formation in the Casmalia Hills may have been derived from a single volcanic source located somewhere in the vicinity of Tranquillon Mountain (Stanley and others, 1991, 1992a; Cole and others, 1991a, b; Hornafius, 1994).

The type Lospe Formation is partly correlative with the Obispo Formation (Hall and others, 1966), which is widespread in the region north and northeast of Santa Maria (figs. 1, 15; Hall and Corbató, 1967; Hall, 1973, 1978b). The Obispo is as thick as 1,500 m (Hall, 1981b) and includes rhyolitic and dacitic tuffs, basaltic and andesitic lavas, sandstones, shales, and diabase sills and dikes. The Obispo Formation is of late early and early middle Miocene age on the basis of potassium-argon ages on plagioclase ranging from 15.7±0.5 Ma to 16.9±1.2 Ma (ages from Turner, 1970, corrected for changes in decay constants using the method of Dalrymple, 1979). According to Hall and Corbató (1967, p. 570) and Hall (1973, p. 3), molluscan fossils from the Obispo suggest an age of Saucesian to Relizian. The Obispo conformably overlies Saucesian strata within the upper part of the Rincon Shale. The Obispo is overlain by fine-grained sedimentary rocks of Relizian age, which in most places are included within the lower part of the Monterey Formation but locally are mapped as the Point Sal Formation (Hall and Corbató, 1967; Turner, 1970, p. 103; Hall, 1973, 1978b; Hall and others, 1979).

The type Lospe Formation may correlate in part with a sequence of Miocene volcanic rocks, informally referred to as the Catway volcanics, near Figueroa Mountain (figs. 1, 15). A sample of pillow basalt from the Catway volcanics yielded a potassium-argon age on plagioclase of 18.8±1.5 Ma (Vedder and others, 1994). The Catway volcanics rest conformably and gradationally on a sequence of shallow(?)-marine sandstone and mudstone that contain *Turritella ocoyana* and therefore may be of Saucesian and (or) Relizian age (J.G. Vedder, oral commun., 1993). The volcanic sequence is overlain by the Monterey Formation, which in this area has yielded assemblages of benthic foraminifers of the Relizian and (or) Luisian Stages (J.G. Vedder, oral commun., 1993).

The type Lospe Formation may be partly correlative with Miocene marine sedimentary rocks mapped by Vedder and others (1988) near Hi Valley (figs. 1, 15). Here, the nonmarine Simmler Formation is overlain by unnamed marine claystone and mudstone containing benthic foraminifers of probable Saucesian age (R.G. Stanley and M.L. Cotton, unpub. data). The unnamed marine claystone and mudstone unit grades upward into an unnamed shallow-marine sandstone unit that may correlate, in whole or in part, with the Lospe and (or) Point Sal Formations in the Casmalia Hills. This sandstone, in turn, is conformably overlain by the Monterey Formation. Samples from the lower part of the Monterey in this area have yielded benthic foraminifers of the Relizian Stage and calcareous nannofossils of Miocene zones CN3 and (or) CN4 (R.G. Stanley, M.L. Cotton, and M.V. Filewicz, unpub. data).

The type Lospe Formation may be about the same age as unnamed volcanic rocks (mainly vitric tuffs and basaltic to dacitic lava flows) and unnamed sandstone and conglomerate mapped by McLean (1994) along the West Huasna fault near Lopez Mountain (figs. 1, 15). The volcanic rocks (map units Tvt and Tvf of McLean, 1994) apparently overlie Mesozoic sedimentary rocks and are in turn overlain by the Monterey Formation, which in this area contains calcareous nannofossils of middle Miocene zone CN4 as well as assemblages of benthic foraminifers ranging in age from Saucesian(?) to late Mohnian (McLean, 1994). A basaltic interbed in tuff (map unit Tvt) yielded a potassium-argon age on plagioclase of 17.0±0.5 Ma (McLean, 1994). In the same general area, but not in contact with the volcanic rocks, are patches of unnamed, poorly dated, marine and nonmarine sandstone and conglomerate to which McLean (1994, map unit Tsc) assigned an age of Miocene and (or) Oligocene. These strata are as thick as 220 m, rest unconformably on Mesozoic sedimentary rocks, and grade upward into shale of the Monterey Formation.

Along the West Huasna fault near Arroyo Grande (fig. 1), Hall (1973) mapped several small patches of brown to cream-colored conglomerate, red and green sandstone, red and gray siltstone, and gray tuff as Lospe Formation(?). Hall's mapping suggests that these rocks rest unconformably on the Franciscan Complex and on Cretaceous(?) volcanic rocks, and that they are overlain by the Miocene Monterey Formation. Hall (1973) assigned the Lospe(?) in this area an age of Oligocene or early Miocene on the basis of possible correlations with Oligocene volcanic rocks of the informally named Morro Rock–Islay Hill complex of Ernst and Hall (1974), the Miocene Obispo Formation, and the Lospe Formation of the Santa Maria basin. The conglomerate includes clasts of serpentinite and chert derived from the Franciscan Complex, fragments of hornblende monzonite derived from an unknown source, and clasts of dacite derived from Oligocene intrusive rocks near San Luis Obispo (fig. 1; Ernst and Hall, 1974, p. 526).

The type Lospe Formation may be partly correlative with an unknown thickness of the Sandholdt Member of the Monterey Formation near York Mountain (figs. 1, 15), which includes benthic foraminiferal assemblages of Saucesian and early Relizian age (Seiders, 1982). The type Lospe may also be correlative with parts of several units in the Cuyama basin (fig. 1) that include strata of upper Saucesian age, including the Saltos Shale Member of the Monterey Formation, the Painted Rock Sandstone Member of the Vaqueros Formation, and the lower part of the Caliente Formation (Hill and others, 1968; Vedder, 1973; Lagoe, 1981, 1984, 1985, 1987).

The type Lospe Formation may be correlative with certain volcanic and sedimentary rocks in the offshore. The Chevron P-0450-1 well in the offshore Point Arguello oil field (fig. 1) penetrated a 213-m-thick sequence of rhyolitic tuffs, volcaniclastic sandstones, and interbedded Saucesian marine siltstones correlated by Crain and others (1987, p. 416) with the onshore Tranquillon Volcanics. In the offshore about 25 km northwest of Point Sal, the Chevron P-060-1 well (fig. 1) penetrated at least 390 m of andesitic and rhyolitic tuffs, flow rocks, and volcaniclastic strata that overlie Mesozoic rocks and are overlain by the Monterey Formation (Epstein and Nary, 1982; Ogle and others, 1987; McCulloch, 1987). Seismic reflection data show that these volcanic rocks are widespread in the offshore Santa Maria basin (McCulloch, 1989; Clark and others, 1991).

Previous Miscorrelation of Type Lospe Formation with Sespe Formation

On the basis of similarities in conglomeratic texture, reddish coloration, inferred nonmarine origin, and general stratigraphic position, many geologists have correlated the type Lospe Formation of the Santa Maria basin with the Sespe Formation of the Santa Barbara–Ventura region (for example, see Wissler and Dreyer, 1943; Hall, 1978a, 1982; Anderson, 1980). However, recent work shows that the type Lospe is younger than the Sespe, and that the two were deposited in geographically separate basins in disparate depositional environments and contrasting tectonic settings.

Isotopic and biostratigraphic results discussed earlier in this report demonstrate that the type Lospe is of late early Miocene age. In contrast, the Sespe is of middle Eocene to early Miocene age (fig. 15) on the basis of fossil land mammals of late Uintan to Arikareean age, a potassium-argon age of 28.2±0.2 Ma on a tuff interbed, paleomagnetic polarity zonation, and stratigraphic relations with overlying, underlying, and laterally interfingering units that contain well-dated marine fossils (Dibblee, 1950, 1966; Lander, 1983, 1994; Mason, 1988; Mason and Swisher, 1989; Howard, 1995; Prothero and others, 1996).

In the Casmalia Hills, the type Lospe is as thick as 830 m and was deposited in alluvial fan, fan-delta, lacustrine, and shallow-marine environments in a small, rapidly subsiding, fault-bounded basin in a transtensional tectonic setting (Stanley and others, 1990, 1991, 1992a; Johnson and Stanley, 1994; Cole and Stanley, 1994; McCrory and others, 1991, 1993, 1995). In contrast, the Sespe Formation of the Santa Barbara–Ventura area is as thick as 1,700 m and consists of two fining-upward megasequences separated by a regional unconformity that represents much or all of the early Oligocene (Howard, 1988, 1989, 1995; Lander, 1994; Prothero and others, 1996). The lower megasequence accumulated mainly during the middle and late Eocene and consists of braided fluvial and deltaic deposits, whereas the upper megasequence accumulated during the late Oligocene and early Miocene and grades upsection from braided to meandering fluvial deposits (Howard, 1987, 1988, 1989, 1995; Lander, 1994). On the basis of detailed studies of paleocurrents and provenance, Howard and Lowry (1995) suggested that the Sespe Formation was deposited by several ancient rivers that flowed from the Mojave Desert and Arizona to coastal southern California. The Sespe accumulated in a subduction-related forearc basin, but the rela-

tive roles of tectonics and eustasy in controlling Sespe sedimentation remain unclear and controversial (Lander, 1994; Howard, 1995).

Older Conglomeratic Units Also Called the Lospe Formation

The name Lospe has been applied to several occurrences of nonmarine conglomeratic rocks that crop out in widely separated localities in the south-central Coast Ranges. Nearly all of these occurrences are clearly older and thinner than the type Lospe Formation of the Casmalia Hills, and they are lithologically distinct from each other and from the type Lospe.

Along both sides of the West Huasna fault near Twitchell Dam (figs. 1, 15), Hall (1978b) mapped several small, poorly exposed patches of nonmarine conglomerate and sandstone as Lospe Formation(?) and assigned these rocks an Oligocene age. West of the West Huasna fault, the conglomeratic sequence is about 40–50 m thick, rests unconformably on the Franciscan Complex, and contains angular clasts of greenstone, green sandstone, red and green chert, serpentinite, and blueschist that apparently were derived from the Franciscan. This conglomeratic unit apparently is overlain by bioturbated marine sandstone of the Vaqueros Formation; samples from fine-grained rocks within the Vaqueros yielded benthic foraminifers of the Saucesian Stage and calcareous nannofossils of early Miocene zone CN2 (Tennyson and others, 1991). East of the West Huasna fault in the Twitchell Dam area, the conglomeratic sequence mapped as Lospe Formation(?) by Hall (1978b) was called Sespe Formation by Hall and Corbató (1967). This sequence is at least 300 m thick and apparently is overlain by shallow-marine sandstone of the Vaqueros Formation, followed in turn by the lower Miocene Rincon Shale and the lower Miocene Obispo Formation (Hall and Corbató, 1967).

Along the Oceanic–West Huasna fault system in the San Luis Obispo–Cambria area, Hall (1974), Ernst and Hall (1974), Hall and Prior (1975), and Hall and others (1979) mapped several patches of nonmarine conglomerate, sandstone, and silty claystone as Lospe Formation and assigned these rocks an Oligocene age (figs. 1, 15). The so-called Lospe in this area has a maximum thickness of about 200 m, rests unconformably on the Franciscan Complex and locally on the upper Oligocene Cambria Felsite (of Ernst and Hall, 1974), and grades upward into shallow-marine sandstone of the Vaqueros Formation, which in this area contains molluscan fossils of the "Vaqueros Stage" of Addicott (1972) that yielded $^{87}Sr/^{86}Sr$ ratios indicating an age of about 25 Ma (Tennyson and others, 1991; M.E. Tennyson, oral commun., 1992). In turn, the Vaqueros is overlain by Rincon Shale (of Hall and others, 1979) containing Saucesian benthic foraminifers as well as calcareous nannofossils of early Miocene zones CN1 and (or) CN2 (Tennyson and others, 1991; M.E. Tennyson, oral commun., 1992). Conglomerate clasts in the so-called Lospe include (1) sandstone, chert, blueschist, metavolcanics, and serpentinite presumably derived from the Franciscan Complex; (2) granitic clasts of unknown derivation; and (3) fragments of Oligocene volcanic rocks derived from the Cambria Felsite or the Morro Rock–Islay Hill complex (Ernst and Hall, 1974; Hall, 1974, 1975; Hall and Prior, 1975).

West of the San Simeon fault near Pt. Piedras Blancas (figs. 1, 15), Hall (1975, 1976) and Hall and others (1979) mapped a sequence about 330 m thick of nonmarine, red, green, and gray conglomerate and sandstone as Lospe Formation and assigned it an Oligocene age; they did not discuss the basis for this age. This sequence rests nonconformably on ophiolitic rocks of Jurassic age and is unconformably overlain by Quaternary deposits. Hall (1975) proposed that the conglomeratic strata were offset from the type Lospe of the Casmalia Hills by post-late Miocene right-lateral displacement of 80 km or more along the San Simeon–Hosgri fault system (fig. 1); a detailed evaluation of this hypothesis is underway (R.G. Stanley, S.Y. Johnson, M.E. Tennyson, and M.A. Keller, unpub. data). The following preliminary observations suggest that the sequences mapped as Lospe at Pt. Piedras Blancas and in the Casmalia Hills may not have been formerly contiguous: (1) The conglomerates at Pt. Piedras Blancas consist almost entirely of ophiolitic debris, whereas those in the type Lospe of the Casmalia Hills include a mixture of ophiolitic material with sandstones and other clast types derived from the Franciscan Complex, the Great Valley sequence, and unidentified Paleogene units (McLean and Stanley, 1994). (2) The type Lospe in the Casmalia Hills includes a thick upper member composed of greenish-gray sandstone and mudstone with minor gypsum, but similar rocks do not occur at Pt. Piedras Blancas. (3) Interbeds of rhyolitic tuff occur in both the lower and upper members of the Lospe in the Casmalia Hills but are not present at Pt. Piedras Blancas.

Near York Mountain (figs. 1, 15), Seiders (1982) mapped red and green sandstone, conglomerate, and mudstone of largely nonmarine origin as Lospe Formation of Oligocene age. This unit is as thick as 30 m, rests unconformably on Jurassic and Cretaceous sedimentary rocks, and is overlain by felsic volcanic rocks that in turn are overlain by the Oligocene and Miocene Vaqueros Formation and the lower Miocene Sandholdt Member of the Monterey Formation. In this area, the Sandholdt contains benthic foraminifers of the early Saucesian Stage (Seiders, 1982) and is itself intruded by basalt that is undated but may be the same age as volcanic rocks in the type Lospe Formation of the Casmalia Hills.

The name Lospe Formation seems inappropriate for the aforementioned nonmarine conglomeratic sequences in the Twitchell Dam, San Luis Obispo, Cambria, Pt. Piedras Blancas, and York Mountain areas. The conglomeratic strata in these places are physically separated and geographically distant from the type Lospe in the Casmalia Hills, and (with the possible exception of Pt. Piedras Blancas) they are clearly older than, and lithologically distinct from, the type Lospe (fig. 15). We suggest that the name Lospe be restricted to sedimentary and

volcanic strata in the type area as originally defined by Wissler and Dreyer (1943), and to laterally contiguous and lithologically similar rocks in the subsurface Santa Maria basin.

ORIGIN OF THE SANTA MARIA BASIN

The type Lospe Formation, because it occurs at the bottom of the Neogene sequence in the Santa Maria basin and rests depositionally on Mesozoic rocks, is the geologic record of the origin and early history of the basin. The age of the base of the Lospe, about 18 Ma, establishes the time of initial subsidence and sedimentation in the Neogene Santa Maria basin. The Lospe records a progressive change from alluvial fan to fan-delta, lacustrine, and shallow-marine environments, culminating in bathyal marine deposition of the Point Sal Formation beginning about 17 Ma. Movement along the Lions Head fault and other faults during Lospe deposition is suggested by the coarse, angular, and lithologically diverse alluvial fan deposits in the lower member of the Lospe (Stanley and others, 1992a; Johnson and Stanley, 1994, p. D19). Volcanic rocks in the Lospe and correlative units around the perimeter of the Santa Maria basin (including the Obispo Formation, Tranquillon Volcanics, the informally named Catway volcanics, and others discussed earlier in this report) indicate that the origin of the basin was accompanied by regional volcanism. Rapid tectonic subsidence about 18–16 Ma is indicated by geohistory diagrams that incorporate our new age data from the Lospe and Point Sal Formations (McCrory and others, 1991, 1993, 1995). These findings provide important constraints on tectonic models for the origin of the Santa Maria basin. Four such models are discussed below.

Hall (1977, 1978a, 1981a, c) proposed that the Santa Maria basin originated as a pull-apart structure that formed by a combination of right-lateral strike-slip and counterclockwise rotation of the western Transverse Ranges with respect to the southern Coast Ranges. Hall suggested that crustal extension beneath the Santa Maria basin was accommodated by "stretching" and "mass flowage" of structurally incompetent Franciscan mélange, with only minor volcanic activity (for example, the diabase sills in the lower part of the Point Sal Formation near Point Sal). In this model, the pull-apart structure began to form during the middle Miocene about 14 Ma (Hall, 1978a, p. 25) or possibly as early as 16 Ma (Hall, 1981c, p. 565), after emplacement of the Obispo and Tranquillon volcanic rocks and deposition of part of the Point Sal Formation. This model is inconsistent with new information about the age and depositional setting of the Lospe Formation. Hall's model assumes that both the Lospe and Sespe Formations are of Oligocene age and were formerly contiguous parts of a regional blanket of nonmarine strata; however, it is now clear (as discussed earlier in this report) that the type Lospe is younger than the Sespe, and that the two were deposited in separate depositional basins. Furthermore, Hall's model proposes that Obispo and Tranquillon volcanism occurred prior to formation of the Santa Maria basin; however, the type Lospe includes volcanic rocks that are the same age as those in the Obispo Formation and Tranquillon Volcanics, demonstrating that initial subsidence and sedimentation in the Santa Maria basin occurred at the same time as regional volcanism. Finally, Hall's model requires counterclockwise rotation of the western Transverse Ranges, contrary to abundant paleomagnetic data that indicate clockwise rotation of 90° or more since the early Miocene (fig. 16; Luyendyk and others, 1980, 1985;

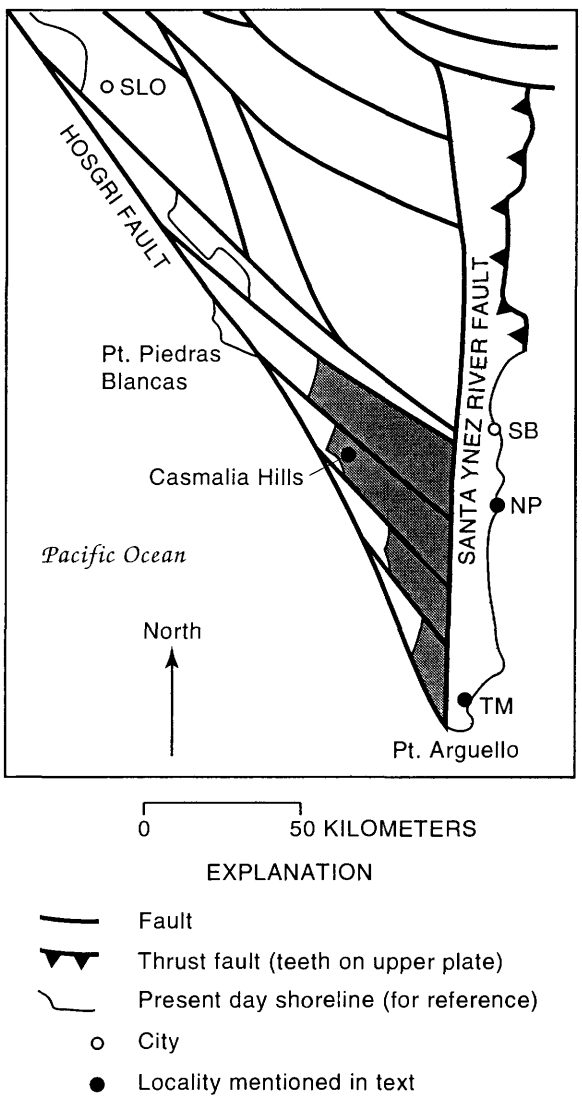

Figure 16. Early Miocene paleogeography of the Santa Maria region, prior to clockwise rotation of the western Transverse Ranges (stippled), subsidence of the onshore Santa Maria basin (shaded), and right-lateral strike-slip offset of varying amounts along northwest-trending faults (after Hornafius, 1985). NP, Naples; SB, Santa Barbara; SLO, San Luis Obispo; TM, Tranquillon Mountain.

Hornafius 1985; Hornafius and others, 1986; Luyendyk and Hornafius, 1987; Luyendyk, 1989, 1991; Liddicoat, 1990; Prothero and others, 1996).

The geometric implications of the paleomagnetic data led Hornafius (1985) and Luyendyk and Hornafius (1987) to propose an alternative model for the origin of the Santa Maria basin. In this model (fig. 17*A*), clockwise rotation of the western Transverse Ranges about a pivot near Point Arguello was accompanied by dilation and subsidence of the area bounded by the Hosgri, Santa Maria River, and Santa Ynez River faults. The time of initial rotation (and, by implication, initial subsidence of the onshore Santa Maria basin) is constrained as early Miocene by the paleomagnetic data and was thought by Luyendyk and Hornafius (1987, p. 263), on the basis of geologic evidence, to have occurred about 16 Ma, somewhat later than our estimate of about 18 Ma based on dating of the Lospe Formation in the Casmalia Hills. This clockwise rotation model predicts the creation of small grabens bounded by northeast-trending faults; such grabens may correspond to Lospe depocenters, but this hypothesis has not been tested by detailed mapping of the thickness of the Lospe. The clockwise rotation model also implies the formation of a number of triangular crustal gaps such as those along the Santa Ynez River fault at the southern margin of the Santa Maria basin (fig. 17*A*), which may have been the sites of mantle upwelling and volcanism (Cole and others, 1991a). Several northwest-trending faults located north and south of the western Transverse Ranges may have been right-lateral strike-slip faults, with calculated displacements ranging as high as 130–140 km for the Hosgri fault (Hornafius, 1985, p. 12,519; Luyendyk and Hornafius, 1987, p. 271). The postulated fault offsets are controversial because no piercing points such as offset shorelines or submarine fans have been identified. Additionally, the clockwise rotation model assumes that crustal slivers within the Santa Maria basin itself have not rotated, but this assumption has been challenged because paleomagnetic data from the central part of the basin are sparse and may have been affected by remagnetization (C.C. Sorlien, written commun., 1991; Sorlien and others, 1994).

A subsequent model suggested by Luyendyk (1991) fits well with current knowledge of the earliest history of the Santa Maria basin. Luyendyk proposed that initial rotation of the western Transverse Ranges occurred within a broad, northwest-trending zone of transtension in which the relative dextral shear between the Pacific and North American plates was accompanied by a component of extension. In this model (fig. 17*B*), crustal extension, oblique-slip faulting, and basin formation in the Santa Maria area occurred about 18–17 Ma, followed shortly thereafter by clockwise rotation of the western Transverse Ranges as the deforming zone widened between the Pacific and North American plates. This hypothesis is consistent with our estimate of about 18 Ma for initial subsidence of the Santa Maria basin, and it also fits well with an episode during the late early Miocene (late Saucesian) of rapid bathymetric deepening in the nearby Cuyama basin (Lagoe, 1987).

Luyendyk's (1991) model further indicates that nonrotating crust within the deforming zone was extended orthogonal to the zone, resulting in the initiation of long, linear, fault-bounded, northwest-trending sedimentary basins. Unfortunately, the early Miocene geometry of the Santa Maria basin is poorly understood because the Lospe Formation is mostly covered by younger deposits. Even so, the known subsurface distribution of the Lospe (fig. 1) suggests the presence of at least two northwest-trending depocenters, consistent with Luyendyk's prediction. Detailed mapping of the subsurface thickness and facies of the Lospe Formation could provide an important new test of the model. Luyendyk's model also suggests that certain northwest-trending faults within the Santa Maria basin were oblique-slip (dextral and normal) during the early history of the basin, but this prediction remains to be tested by a systematic investigation of piercing points and other kinematic indicators.

Crouch and Suppe (1993) proposed a model in which the Santa Maria region was affected by large-magnitude crustal extension beginning about 27 Ma. This event may be recorded in the San Luis Obispo area by sedimentary and volcanic rocks dated at about 27–22 Ma (Turner, 1970; Tennyson and others, 1991; M.A. Mason and C.C. Swisher, unpub. data), but rocks of this age are unknown within the central Santa Maria basin. It is possible that sedimentary and volcanic strata were laid down about 27–22 Ma in the central Santa Maria basin and then removed by uplift and erosion prior to deposition of the type Lospe Formation, but no erosional remnants or other physical evidence of such older strata have been identified.

In summary, it appears that the origin of the Santa Maria basin occurred at about the same time as regional transtension and initial rotation of the western Transverse Ranges, and that these events were causally related. In the Santa Maria area, subduction ended and transtension began about 20–19 Ma (or shortly thereafter) when the Pacific-Monterey segment of the old Farallon-Pacific mid-oceanic ridge encountered the continental margin and stopped spreading, and the partially subducted Monterey microplate (a fragment of the old Farallon plate) apparently was "captured" by and attached to the Pacific plate (Nicholson and others, 1994; McCrory and others, 1995; Bohannon and Parsons, 1995). Transtensional deformation of the crust in the Santa Maria area may have been the result of strong traction imposed on the lower part of the crust by the subducted Monterey microplate as it moved to the northwest relative to the continent (Bohannon and Parsons, 1995). Transtension was accompanied about 19–16 Ma by regional bimodal volcanism in which the magmas apparently were derived from depleted mantle and melted continental crustal sources (Cole and Basu, 1992, 1995). However, the exact mechanisms by which transtension resulted in magma genesis, clockwise rotation of the western Transverse Ranges, and subsequent dilation and subsidence of the Santa Maria basin are unclear.

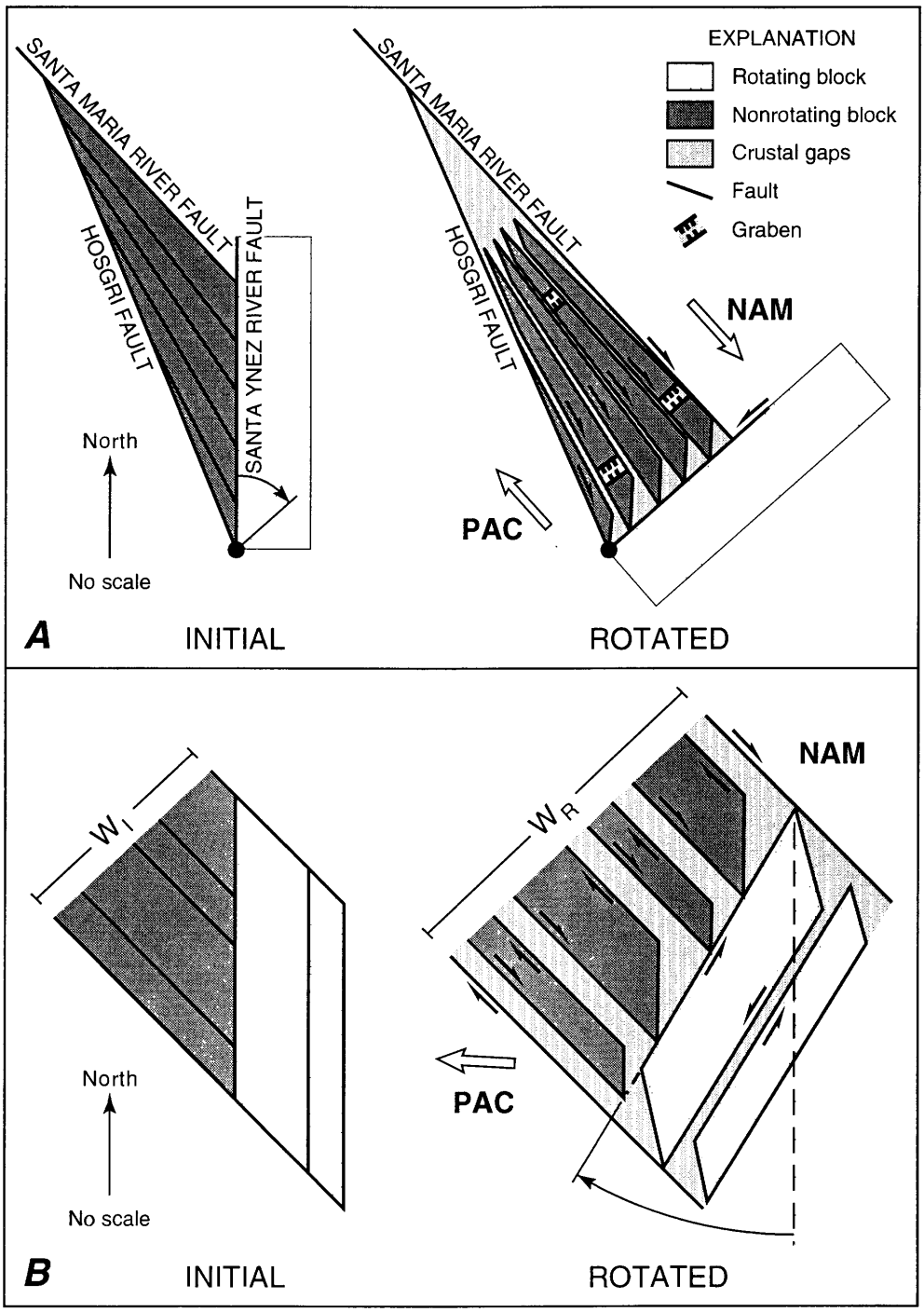

Figure 17. Schematic geometric models showing clockwise rotation and simultaneous faulting. *A*, Clockwise rotation of the Santa Ynez River fault and western Transverse Ranges (stippled) about a pivot near Pt. Arguello (filled circle) causes extension and formation of crustal gaps and grabens in the onshore Santa Maria basin (dark and light shaded areas), and oblique right-lateral offset along northwest-trending faults, including the Hosgri and Santa Maria River faults; diagram modified from Hornafius (1985) and Luyendyk and Hornafius (1987). This model assumes right-lateral simple shear (shown by large hollow arrows) between the North American plate (NAM) and the Pacific plate (PAC). *B*, Clockwise rotation and faulting in a widening zone of deformation caused by oblique right-lateral shear (transtension) between the Pacific plate and a fixed North American plate; diagram modified from Luyendyk (1991). W_I, initial width of deforming zone; W_R, resulting width of deforming zone.

CONCLUSIONS

The origin of the Neogene Santa Maria basin is recorded by the 830-m-thick Lospe Formation. In its type area in the Casmalia Hills, the Lospe is a sequence of sedimentary and minor volcanic rocks that record deposition in alluvial fan, fan-delta, lacustrine, and shallow-marine environments. Isotopic dating of rhyolitic tuffs near the base of the type Lospe indicates that basin subsidence and sedimentation began about 18 Ma. Biostratigraphic analysis of microfossils suggests that accumulation of the type Lospe ended about 17 Ma with abrupt deepening to bathyal marine deposition of the Point Sal Formation. The type Lospe is younger than the Sespe Formation with which it was previously correlated, and it is also younger than several occurrences north of the Santa Maria basin of Oligocene conglomeratic strata that previously were miscorrelated with the Lospe and called by that name.

The Neogene Santa Maria basin originated about 18 Ma and was accompanied by rapid tectonic subsidence, active faulting, regional volcanism, and rapid bathymetric deepening. These events appear to be consistent with a tectonic model which holds that the basin originated during the late early Miocene by crustal dilation and oblique-slip faulting related to regional transtension and the beginning of clockwise rotation of the western Transverse Ranges.

REFERENCES CITED

American Association of Petroleum Geologists, 1959, Correlation section across Santa Maria basin from Cretaceous outcrop in Santa Ynez Mountains northerly to Franciscan outcrop north of Santa Maria River, California: Pacific Section, American Association of Petroleum Geologists (AAPG), Correlation Section 12, scales 1:12,000 and 1:48,000.

Addicott, W.O., 1972, Provincial middle and late Tertiary molluscan stages, Temblor Range, California: Bakersfield, Calif., Pacific Section, Society of Economic Paleontologists and Mineralogists, Proceedings of the Pacific Coast Miocene Biostratigraphic Symposium, p. 1-26.

Anderson, D.S., 1980, Provenance and tectonic implications of mid-Tertiary nonmarine deposits, Santa Maria basin and vicinity, California: Los Angeles, Calif., University of California, M.S. thesis, 218 p.

Ballog, R.A., and Malloy, R.E., 1981, Neogene palynology from the southern California continental borderland, site 467, Deep Sea Drilling Project Leg 63, *in* Yeats, R.S., Haq, B.U., and others, Initial reports of the Deep Sea Drilling Project, v. 63: Washington, D.C., U.S. Government Printing Office, p. 565-573.

Bandy, O.L., and Ingle, J.C., Jr., 1970, Neogene planktonic events and radiometric scale, California: Geological Society of America Special Paper 124, p. 131-172.

Bartow, J.A., 1978, Oligocene continental sedimentation in the Caliente Range area, California: Journal of Sedimentary Petrology, v. 48, no. 1, p. 75-98.

———1992, Paleogene and Neogene time scales for southern California: U.S. Geological Survey Open-File Report 92-212, 2 sheets.

Bernhard, J.M., 1992, Benthic foraminiferal distribution and biomass related to pore-water oxygen content: central California continental slope and rise: Deep-Sea Research, v. 39, no. 3/4, p. 585-605.

Blake, G.H., 1991, Review of the Neogene biostratigraphy and stratigraphy of the Los Angeles basin and implications for basin evolution, *in* Biddle, K.T., ed., Active margin basins: American Association of Petroleum Geologists Memoir 52, p. 135-184.

Bohannon, R.G., and Parsons, Tom, 1995, Tectonic implications of post-30 Ma Pacific and North American relative plate motions: Geological Society of America Bulletin, v. 107, no. 8, p. 937-959.

Bolli, H.M., and Saunders, J.B., 1985, Oligocene to Holocene low latitude planktic foraminifera, *in* Bolli, H.M., Saunders, J.B., and Perch-Nielsen, K.E., eds., Plankton stratigraphy: Cambridge, Engl., Cambridge University Press, p. 155-262.

Brabb, E.E., 1964, Subdivision of the San Lorenzo Formation (Eocene-Oligocene), west-central California: American Association of Petroleum Geologists Bulletin, v. 48, p. 670-679.

Bukry, David, 1973, Low-latitude coccolith biostratigraphic zonation, *in* Edgar, N.T., Saunders, J.B., and others, 1973, Initial reports of the Deep Sea Drilling Project, v. 15: Washington, D.C., U.S. Government Printing Office, p. 685-703.

———1975, Coccolith and silicoflagellate stratigraphy, northwestern Pacific Ocean, Deep Sea Drilling Project Leg 12, *in* Larson, R.L., Moberly, R., and others, 1975, Initial reports of the Deep Sea Drilling Project, v. 27: Washington, D.C., U.S. Government Printing Office, p. 677-701.

California Division of Oil and Gas, 1991, California oil and gas fields, volume II, southern, central, and coastal California (3d ed.): Sacramento, Calif., California Department of Conservation, Publication TR12, 689 p.

Cande, S.C., and Kent, D.V., 1992, A new geomagnetic polarity time scale for the Late Cretaceous and Cenozoic: Journal of Geophysical Research, v. 97, no. B10, p. 13,917-13,951.

———1995, Revised calibration of the geomagnetic polarity timescale for the Late Cretaceous and Cenozoic: Journal of Geophysical Research, v. 100, no. B4, p. 6,093-6,095.

Clark, D.H., Hall, N.T., and Hamilton, D.H., 1991, Structural analysis of late Neogene deformation in the central offshore Santa Maria basin, California: Journal of Geophysical Research, v. 96, no. B4, p. 6,435-6,457.

Cole, R.B., and Basu, A.R., 1992, Middle Tertiary volcanism during ridge-trench interactions in western California: Science, v. 258, p. 793-796.

———1995, Nd-Sr isotopic geochemistry and tectonics of ridge subduction and middle Cenozoic volcanism in western California: Geological Society of America Bulletin, v. 107, no. 2, p. 167-179.

Cole, R.B., and Stanley, R.G., 1994, Sedimentology and origin of subaqueous pyroclastic sediment gravity flows in the Neogene Santa Maria basin, California: Sedimentology, v. 41, p. 37-54.

Cole, R.B., Stanley, R.G., and Basu, A.R., 1991a, Stratigraphy and origin of lower Miocene volcanic rocks, onshore and offshore Santa Maria province, California [abs.]: Geological Society of America Abstracts with Programs, v. 23, no. 5, p. A476.

Cole, R.B., Stanley, R.G., and Johnson, S.Y., 1991b, Origin of tuff deposits in the lower Miocene Lospe Formation, Santa Maria basin, California [abs.]: American Association of Petroleum Geologists Bulletin, v. 75, no. 2, p. 359-360.

Crain, W.E., Mero, W.E., and Patterson, Don, 1987, Geology of the Point Arguello field, *in* Ingersoll, R.V., and Ernst, W.G., eds., Cenozoic basin development of coastal California, Rubey Volume 6: Englewood Cliffs, N.J., Prentice-Hall, p. 407-426.

Crawford, F.D., 1971, Petroleum potential of Santa Maria province, California, *in* Cram, I.H., ed., Future petroleum provinces of the United States—their geology and potential: American Association of Petroleum Geologists Memoir 15, p. 316-328.

Crouch, J.K., and Suppe, John, 1993, Late Cenozoic tectonic evolution of the Los Angeles basin and inner California borderland—a model for core-complex-like crustal extension: Geological Society of America Bulletin, v. 105, p. 1,415-1,434.

Crowell, J.C., 1974, Sedimentation along the San Andreas fault, California, *in* Dott, R.H., and Shaver, R.H., eds., Modern and ancient geosynclinal sedimentation: Tulsa, Okla., Society of Economic Paleontologists and Mineralogists Special Publication 19, p. 292-303.

Dalrymple, G.B., 1979, Critical tables for conversion of K-Ar ages from old to new constants: Geology, v. 7, p. 558-560.

DePaolo, D.J., and Finger, K.L., 1991, High-resolution strontium-isotope stratigraphy and biostratigraphy of the Miocene Monterey Formation, central California: Geological Society of America Bulletin, v. 103, p. 112-124.

Dibblee, T.W., Jr., 1950, Geology of southwestern Santa Barbara County, California: California Division of Mines Bulletin 150, 95 p.

———1966, Geology of the central Santa Ynez Mountains, Santa Barbara County, California: California Division of Mines and Geology Bulletin 186, 99 p.

———1988a, Geologic map of the Santa Rosa Hills and Sacate quadrangles, Santa Barbara County, California: Santa Barbara, Calif., Dibblee Geological Foundation Map DF-17, scale 1:24,000.

———1988b, Geologic map of the Tranquillon Mtn. and Point Arguello quadrangles, Santa Barbara County, California: Santa Barbara, Calif., Dibblee Geological Foundation Map DF-19, scale 1:24,000.

———1989a, Geologic map of the Casmalia and Orcutt quadrangles, Santa Barbara County, California: Santa Barbara, Calif., Dibblee Geological Foundation Map DF-24, scale 1:24,000.

———1989b, Geologic map of the Point Sal and Guadalupe quadrangles, Santa Barbara County, California: Santa Barbara, Calif., Dibblee Geological Foundation Map DF-25, scale 1:24,000.

Dunham, J.B., and Blake, G.H., 1987, Guide to coastal outcrops of the Monterey Formation of western Santa Barbara County, California: Los Angeles, Calif., Pacific Section, Society of Economic Paleontologists and Mineralogists, 36 p.

Epstein, S.A., and Nary, Q.L., 1982, A look at the geology of the hot Santa Maria basin area off California: Oil and Gas Journal, Nov. 15, 1982, p. 162-168.

Ernst, W.G., and Hall, C.A., Jr., 1974, Geology and petrology of the Cambria Felsite, a new Oligocene formation, west-central California Coast Ranges: Geological Society of America Bulletin, v. 85, p. 523-532.

Fairbanks, H.W., 1896, The geology of Point Sal: Berkeley, Calif., University of California, Bulletin of the Department of Geology, v. 2, no. 1, p. 1-92.

Garrison, R.E., 1981, Pelagic and hemipelagic sedimentation in active margin basins, *in* Douglas, R.G., Colburn, I.P., and Gorsline, D.S., eds., Depositional systems of active continental margin basins—short course notes: Los Angeles, Calif., Pacific Section, Society of Economic Paleontologists and Mineralogists, p. 15-38.

Gooday, A.J., 1994, The biology of deep-sea foraminifera: a review of some advances and their applications in paleoceanography: Palaios, v. 9, no. 1, p. 14-31.

Gudde, E.G., 1960, California place names: Berkeley and Los Angeles, Calif., University of California Press, 383 p.

Hall, C.A., Jr., 1973, Geology of the Arroyo Grande 15-minute quadrangle, San Luis Obispo County, California: California Division of Mines and Geology Map Sheet 24, scale 1:48,000.

———1974, Geologic map of the Cambria region, San Luis Obispo County, California: U.S. Geological Survey Miscellaneous Field Studies Map MF-599, 2 sheets, scale 1:24,000.

———1975, San Simeon-Hosgri fault system, coastal California—economic and environmental implications: Science, v. 190, p. 1291-1294.

———1976, Geologic map of the San Simeon-Piedras Blancas region, San Luis Obispo County, California: U.S. Geological Survey Miscellaneous Field Studies Map MF-784, scale 1:24,000.

———1977, Origin and development of the Lompoc-Santa Maria pull-apart basin and its relation to the San Simeon-Hosgri fault, California [abs]: Cordilleran Section, Geological Society of America Abstracts with Programs, v. 9, no. 4, p. 428.

———1978a, Origin and development of the Lompoc-Santa Maria pull-apart basin and its relation to the San Simeon-Hosgri strike-slip fault, western California, *in* Silver, E.A., and Normark, W.R., eds., San Gregorio-Hosgri fault zone, California: California Division of Mines and Geology Special Report 137, p. 25-31.

———1978b, Geologic map of Twitchell Dam and parts of Santa Maria and Tepusquet Canyon quadrangles, Santa Barbara County, California: U.S. Geological Survey Miscellaneous Field Studies Map MF-963, 2 sheets, scale 1:24,000.

———1981a, San Luis Obispo transform fault and middle Miocene rotation of the western Transverse Ranges, California: Journal of Geophysical Research, v. 86, no. B2, p. 1015-1031.

———1981b, Map of geology along the Little Pine fault, parts of the Sisquoc, Foxen Canyon, Zaca Lake, Bald Mountain, Los Olivos, and Figueroa Mountain quadrangles, Santa Barbara County, California: U.S. Geological Survey Miscellaneous Field Studies Map MF-1285, two sheets, scale 1:24,000.

———1981c, Evolution of the western Transverse Ranges microplate: late Cenozoic faulting and basinal development, *in* Ernst, W.G., ed., The geotectonic development of California, Rubey Volume 1: Englewood Cliffs, N.J., Prentice-Hall, p. 559-582.

———1982, Pre-Monterey subcrop and structure contour maps, western San Luis Obispo and Santa Barbara Counties, south-central California: U.S. Geological Survey Miscellaneous Field Studies Map MF-1384, six sheets, scale 1:62,500.

Hall, C.A., Jr., and Corbató, C.E., 1967, Stratigraphy and structure of Mesozoic and Cenozoic rocks, Nipomo quadrangle, southern Coast Ranges, California: Geological Society of America Bulletin, v. 78, p. 559-582.

Hall, C.A., Jr., Ernst, W.G., Prior, S.W., and Wiese, J.W., 1979, Geologic map of the San Luis Obispo-San Simeon region, Califor-

nia: U.S. Geological Survey Miscellaneous Investigations Series Map I-1097, 3 sheets, scale 1:48,000.

Hall, C.A., Jr., and Prior, S.W., 1975, Geologic map of the Cayucos-San Luis Obispo region, San Luis Obispo County, California: U.S. Geological Survey Miscellaneous Field Studies Map MF-686, 2 sheets, scale 1:24,000.

Hall, C.A., Jr., Turner, D.L., and Surdam, R.C., 1966, Potassium-argon age of the Obispo Formation with *Pecten lompocensis* Arnold, southern Coast Ranges, California: Geological Society of America Bulletin, v. 77, p. 443-446.

Hill, M.L., Carlson, S.A., and Dibblee, T.W., Jr., 1968, Stratigraphy of Cuyama Valley-Caliente Range area, California: American Association of Petroleum Geologists Bulletin, v. 42, no. 12, p. 2973-3000.

Hopson, C.A., and Frano, C.J., 1977, Igneous history of the Point Sal ophiolite, southern California, *in* Coleman, R.G., and Irwin, W.P., eds., North American ophiolites: Oregon Department of Geology and Mineral Industries Bulletin 95, p. 161-183.

Hornafius, J.S., 1985, Neogene tectonic rotation of the Santa Ynez Range, western Transverse Ranges, California, suggested by paleomagnetic investigation of the Monterey Formation: Journal of Geophysical Research, v. 90, no. B14, p. 12,503-12,522.

———1994, Correlation of volcanic ashes in the Monterey Formation between Naples Beach and Gaviota Beach, California, *in* Hornafius, J.S., ed., Field guide to the Monterey Formation between Santa Barbara and Gaviota, California: Bakersfield, Calif., Pacific Section, American Association of Petroleum Geologists, p. 45-58.

Hornafius, J.S., Luyendyk, B.P., Terres, R.R., and Kamerling, M.J., 1986, Timing and extent of Neogene tectonic rotation in the western Transverse Ranges, California: Geological Society of America Bulletin, v. 97, p. 1476-1487.

Howard, J.L., 1987, Paleoenvironments, provenance, and tectonic implications of the Sespe Formation, southern California: Santa Barbara, Calif., University of California, Ph.D. dissertation, 306 p.

———1988, Sedimentation of the Sespe Formation in southern California, *in* Sylvester, A.G., and Brown, G.C., eds., Santa Barbara and Ventura basins—tectonics, structure, sedimentation, oilfields along an east-west transect: Ventura, Calif., Coast Geological Society Guidebook 64, p. 53-69.

———1989, Conglomerate clast populations of the upper Paleogene Sespe Formation, southern California, *in* Colburn, I.P., Abbott, P.L., and Minch, John, eds., Conglomerates in basin analysis—a symposium dedicated to A.O. Woodford: Pacific Section, Society of Economic Paleontologists and Mineralogists, v. 62, p. 269-280.

———1995, Conglomerates of the upper middle Eocene to lower Miocene Sespe Formation along the Santa Ynez fault—implications for the geologic history of the eastern Santa Maria basin area, California: U.S. Geological Survey Bulletin 1995-H, p. H1-H37.

Howard, J.L., and Lowry, W.D., 1995, Middle Cenozoic paleogeography of the Los Angeles area, southwestern California, and adjacent parts of the United States, *in* Fritsche, A.E., ed., Cenozoic paleogeography of the western United States—II: Bakersfield, Calif., Pacific Section, SEPM (Society for Sedimentary Geology), v. 75, p. 22-41.

Howell, D.G., and Von Huene, Roland, 1981, Tectonics and sediment, along active continental margins, *in* Douglas, R.G., Colburn, I.P., and Gorsline, D.S., eds., Depositional systems of active continental margin basins—short course notes: Los Angeles, Calif., Pacific Section, Society of Economic Paleontologists and Mineralogists, p. 1-13.

Ingle, J.C., Jr., 1973, Summary comments on Neogene biostratigraphy, physical stratigraphy, and paleo-oceanography in the marginal northeastern Pacific Ocean, *in* Kulm, L.D., von Huene, Roland, and others, 1973, Initial reports of the Deep Sea Drilling Project, v. 18: Washington, D.C., U.S. Government Printing Office, p. 949-960.

———1980, Cenozoic paleobathymetry and depositional history of selected sequences within the southern California continental borderland: Cushman Foundation for Foraminiferal Research Special Publication no. 19, p. 163-195.

Johnson, S.Y., and Stanley, R.G., 1994, Sedimentology of the conglomeratic lower member of the Lospe Formation (lower Miocene), Santa Maria basin, California: U.S. Geological Survey Bulletin 1995-D, p. D1-D21.

Kleinpell, R.M., 1938, Miocene stratigraphy of California: Tulsa, Okla., American Association of Petroleum Geologists, 450 p.

———1980, The Miocene stratigraphy of California revisited: Tulsa, Okla., American Association of Petroleum Geologists Studies in Geology No. 11, p. 1-53.

Kleinpell, R.M., and Weaver, D.W., 1963, Foraminiferal faunas from the Gaviota and Alegria Formations: Berkeley and Los Angeles, Calif., University of California Publications in Geological Sciences, v. 43, p. 1-77.

Lagoe, M.B., 1981, Subsurface facies analysis of the Saltos Shale Member, Monterey Formation (Miocene) and associated rocks, Cuyama Valley, California, *in* Garrison, R.E., and others, eds., The Monterey Formation and related siliceous rocks of California: Los Angeles, Calif., Pacific Section, Society of Economic Paleontologists and Mineralogists, p. 199-211.

———1984, Paleogeography of Monterey Formation, Cuyama basin, California: American Association of Petroleum Geologists Bulletin, v. 68, no. 5, p. 610-627.

———1985, Depositional environments in the Monterey Formation, Cuyama basin, California: Geological Society of America Bulletin, v. 96, p. 1296-1312.

———1987, Middle Cenozoic basin development, Cuyama basin, California, *in* Ingersoll, R.V., and Ernst, W.G., eds., Cenozoic basin development of coastal California, Rubey Volume 6: Englewood Cliffs, N.J., Prentice-Hall, p. 172-206.

Lander, E.B., 1983, Continental vertebrate faunas from the upper member of the Sespe Formation, Simi Valley, California, and the terminal Eocene event, *in* Squires, R.R., and Filewicz, M.V., eds., Cenozoic geology of the Simi Valley area, southern California: Los Angeles, Calif., Pacific Section, Society of Economic Paleontologists and Mineralogists, p. 142-153.

———1994, Recalibration and causes of marine regressive-transgressive cycle recorded by middle Eocene to lower Miocene nonmarine Sespe Formation, southern California continental plate margin, *in* Fritsche, A.E., ed., Sedimentology and paleontology of Eocene rocks in the Sespe Creek area, Ventura County, California: Bakersfield, Calif., Pacific Section, SEPM (Society for Sedimentary Geology), v. 74, p. 79-88.

Liddicoat, J.C., 1990, Tectonic rotation of the Santa Ynez Range, California, recorded in the Sespe Formation: Geophysical Journal International, v. 102, p. 739-745.

Luyendyk, B.P., 1989, Crustal rotation and fault slip in the continental transform zone in southern California, *in* Kissel, Catherine, and Laj, Carlo, eds., Paleomagnetic rotations and continental deformation: Dordrecht, The Netherlands, Kluwer Academic Publishers, p. 229-246.

———1991, A model for Neogene crustal rotations, transtension, and transpression in southern California: Geological Society of America Bulletin, v. 103, p. 1528-1536.

Luyendyk, B.P., and Hornafius, J.S., 1987, Neogene crustal rotations, fault slip, and basin development in southern California, *in* Ingersoll, R.V., and Ernst, W.G., eds., Cenozoic basin development of coastal California, Rubey Volume 6: Englewood Cliffs, N.J., Prentice-Hall, p. 259-283.

Luyendyk, B.P., Kamerling, M.J., and Terres, R.R., 1980, Geometric model for Neogene crustal rotations in southern California: Geological Society of America Bulletin, pt. 1, v. 91, p. 211-217.

Luyendyk, B.P., Kamerling, M.J., Terres, R.R., and Hornafius, J.S., 1985, Simple shear of southern California during Neogene time suggested by paleomagnetic declinations: Journal of Geophysical Research, v. 90, no. B14, p. 12,454-12,466.

Mason, M.A., 1988, Mammalian paleontology and stratigraphy of the early to middle Tertiary Sespe and Titus Canyon Formations, southern California: Berkeley, Calif., University of California, Ph.D. dissertation, 257 p.

Mason, M.A., and Swisher, C.C., III, 1989, New evidence for the age of the South Mountain local fauna, Ventura County, California: Natural History Museum of Los Angeles County Contributions in Science No. 410, p. 1-9.

Mayer, L.F., Pisias, N.G., Janecek, T.R., and others, 1992, Explanatory notes, *in* Mayer, L.F., Pisias, N.G., Janecek, T.R., and others, Proceedings of the Ocean Drilling Program, Initial Reports, v. 138: College Station, Tex., Ocean Drilling Program, p. 13-42.

McCrory, P.A., Arends, R.G., Ingle, J.C., Jr., Isaacs, C.M., Stanley, R.G., and Cotton Thornton, M.L., 1991, Geohistory analysis of the Santa Maria basin, California, and its relationship to tectonic evolution of the continental margin [abs.]: American Association of Petroleum Geologists Bulletin, v. 75, no. 2, p. 374.

McCrory, P.A., Ingle, J.C., Jr., Wilson, D.S., and Stanley, R.G., 1993, Neogene transfer of central California to the Pacific Plate: implications for evolution of the San Andreas fault [abs.]: Eos (American Geophysical Union, Transactions), v. 74, no. 43, p. 586.

———1995, Neogene geohistory analysis of Santa Maria basin, California, and its relationship to transfer of central California to the Pacific plate: U.S. Geological Survey Bulletin 1995-J, p. J1-J38.

McCulloch, D.S., 1987, Regional geology and hydrocarbon potential of offshore central California, *in* Scholl, D.W., Grantz, Arthur, and Vedder, J.G., eds., Geology and resource potential of the continental margin of western North America and adjacent ocean basins—Beaufort Sea to Baja California: Houston, Tex., Circum-Pacific Council for Energy and Mineral Resources, Earth Science Series, v. 6, p. 353-401.

———1989, Evolution of the offshore central California margin, *in* Winterer, E.L., Hussong, D.M., and Decker, R.W., eds., The eastern Pacific Ocean and Hawaii: Boulder, Colo., Geological Society of America, The Geology of North America, v. N, p. 439-470.

McLean, Hugh, 1991, Distribution and juxtaposition of Mesozoic lithotectonic elements in the basement of the Santa Maria basin, California: U.S. Geological Survey Bulletin 1995-B, p. B1-B12.

———1994, Geologic map of the Lopez Mountain quadrangle, San Luis Obispo County, California: U.S. Geological Survey Geologic Quadrangle Map GQ-1723, scale 1:24,000.

McLean, Hugh, and Stanley, R.G., 1994, Provenance of sandstone clasts in the lower Miocene Lospe Formation near Point Sal, California: U.S. Geological Survey Bulletin 1995-E, p. E1-E7.

Namson, Jay, and Davis, T.L., 1990, Late Cenozoic fold and thrust belt of the southern Coast Ranges and Santa Maria basin, California: American Association of Petroleum Geologists Bulletin, v. 74, no. 4, p. 467-492.

Nicholson, Craig, Sorlien, C.C., Atwater, Tanya, Crowell, J.C., and Luyendyk, B.P., 1994, Microplate capture, rotation of the western Transverse Ranges, and initiation of the San Andreas as a low-angle fault system: Geology, v. 22, no. 6, p. 491-495.

Obradovich, J.D., 1993, A Cretaceous time scale, *in* Caldwell, W.G.E., and Kauffman, E.G., eds., Evolution of the western interior basin: Geological Association of Canada Special Paper 39, p. 379-396.

Ogle, B.A., Wallis, W.S., Heck, R.G., and Edwards, E.B., 1987, Petroleum geology of the Monterey Formation in the offshore Santa Maria/Santa Barbara areas, *in* Ingersoll, R.V., and Ernst, W.G., eds., Cenozoic basin development of coastal California, Rubey Volume 6: Englewood Cliffs, N.J., Prentice-Hall, p. 382-406.

Okada, Hisatake, and Bukry, David, 1980, Supplementary modification and introduction of code numbers to the low-latitude coccolith biostratigraphic zonation (Bukry, 1973; 1975): Marine Micropaleontology, v. 5, p. 321-325.

Page, B.M., 1981, The southern Coast Ranges, *in* Ernst, W.G., ed., The geotectonic development of California, Rubey Volume 1: Englewood Cliffs, N.J., Prentice-Hall, p. 329-417.

Perch-Nielsen, Katharina, 1985a, Mesozoic calcareous nannofossils, *in* Bolli, H.M., Saunders, J.B., and Perch-Nielsen, K.E., eds., Plankton stratigraphy: Cambridge, Engl., Cambridge University Press, p. 329-426.

———1985b, Cenozoic calcareous nannofossils, *in* Bolli, H.M., Saunders, J.B., and Perch-Nielsen, K.E., eds., Plankton stratigraphy: Cambridge, Engl., Cambridge University Press, p. 427-554.

Pisciotto, K.E., and Garrison, R.E., 1981, Lithofacies and depositional environments of the Monterey Formation, California, *in* Garrison, R.E., and Douglas, R.G., eds., The Monterey Formation and related siliceous rocks of California: Los Angeles, Calif., Pacific Section, Society of Economic Paleontologists and Mineralogists, p. 97-122.

Prothero, D.R., Howard, J.L., and Dozier, T.H.D., 1996, Stratigraphy and paleomagnetism of the upper middle Eocene to lower Miocene (Uintan to Arikareean) Sespe Formation, Ventura County, California, *in* Prothero, D.R., and Emry, R.J., eds., Terrestrial Eocene-Oligocene transition in North America: New York, Cambridge University Press, p. 171-188.

Rathburn, A.E., and Corliss, B.H., 1994, The ecology of living (stained) deep-sea benthic foraminifera from the Sulu Sea: Paleoceanography, v. 9, no. 1, p. 87-150.

Robyn, E.S., 1980, A description of the Miocene Tranquillon volcanics and a comparison with the Miocene Obispo tuff: Santa Barbara, Calif., University of California, M.A. thesis, 110 p.

Seiders, V.M., 1982, Geologic map of an area near York Mountain, San Luis Obispo County, California: U.S. Geological Survey Miscellaneous Investigations Series Map I-1369, 1 sheet, scale 1:24,000.

Sorlien, C.C., Nicholson, Craig, Luyendyk, B.P., Cisowski, S., Bird, K.J., and Tennyson, M.E., 1994, Miocene extension and rotation

of south-central California [abs.]: American Association of Petroleum Geologists Bulletin, v. 78, no. 4, p. 675.

Soutar, Andrew, Johnson, S.R., and Baumgartner, T.R., 1981, In search of modern depositional analogs to the Monterey Formation, *in* Garrison, R.E., and Douglas, R.G., eds., The Monterey Formation and related siliceous rocks of California: Los Angeles, Calif., Pacific Section, Society of Economic Paleontologists and Mineralogists, p. 123-147.

Srinivasan, M.S., and Kennett, J.P., 1981, Neogene planktonic foraminiferal biostratigraphy and evolution: equatorial to subantarctic, South Pacific: Micropaleontology, v. 6, p. 499-533.

Srivastava, S.K., 1984, Palynology of the Monterey Formation (Miocene) phosphatic facies at Lions Head, Santa Maria area, California: Palynology, v. 8, p. 33-49.

Stanley, R.G., 1985, Middle Tertiary sedimentation and tectonics of the La Honda basin, central California: U.S. Geological Survey Open-File Report 85-596, 263 p.

———1990, Evolution of the Tertiary La Honda basin, central California, *in* Garrison, R.E., Greene, H.G., Hicks, K.R., Weber, G.E., and Wright, T.L., eds., Geology and tectonics of the central California coast region, San Francisco to Monterey, volume and guidebook: Bakersfield, Calif., Pacific Section, American Association of Petroleum Geologists, Book GB67, p. 1-29.

Stanley, R.G., Cotton, M.L., Bukry, David, Filewicz, M.V., Valin, Z.C., and Vork, D.R., 1994, Stratigraphic revelations regarding the Rincon Shale (lower Miocene) in the Santa Barbara coastal area, California [abs.]: American Association of Petroleum Geologists Bulletin, v. 78, no. 4, p. 675-676.

Stanley, R.G., Johnson, S.Y., Cole, R.B., Mason, M.A., Swisher, C.C., III, Cotton Thornton, M.L., Filewicz, M.V., Vork, D.R., Tuttle, M.L., and Obradovich, J.D., 1992a, Origin of the Santa Maria basin, California [abs.], *in* Carter, L.M.H., ed., USGS Research on Energy Resources—1992 Program and Abstracts, Eighth V.E. McKelvey Forum on Mineral and Energy Resources: U.S. Geological Survey Circular 1074, p. 73.

Stanley, R.G., Johnson, S.Y., Obradovich, J.D., Tuttle, M.L., Cotton Thornton, M.L., Vork, D.R., Filewicz, M.V., Mason, M.A., and Swisher, C.C., III, 1990, Age, facies, and depositional environments of the lower Miocene Lospe Formation, Santa Maria basin, central California [abs.], *in* Carter, L.M.H., ed., USGS Research on Energy Resources—1990 Program and Abstracts, Sixth V.E. McKelvey Forum on Mineral and Energy Resources: U.S. Geological Survey Circular 1060, p. 78-79.

Stanley, R.G., Johnson, S.Y., Tuttle, M.L., Mason, M.A., Swisher, C.C., III, Cotton Thornton, M.L., Vork, D.R., Filewicz, M.V., Cole, R.B., and Obradovich, J.D., 1991, Age, correlation, and origin of the type Lospe Formation (lower Miocene), Santa Maria basin, central California [abs.]: American Association of Petroleum Geologists Bulletin, v. 75, no. 2, p. 382.

Stanley, R.G., Pawlewicz, M.J., Vork, D.R., Johnson, S.Y., and Valin, Z.C., 1995, Preliminary report on petroleum source potential and thermal maturity of the Lospe Formation (lower Miocene) near Point Sal, onshore Santa Maria basin, California: U.S. Geological Open-File Report 95-530, 36 p.

Stanley, R.G., Valin, Z.C., and Pawlewicz, M.J., 1992b, Rock-Eval pyrolysis and vitrinite reflectance results from outcrop samples of the Rincon Shale (lower Miocene) collected at the Tajiguas Landfill, Santa Barbara County, California: U.S. Geological Survey Open-File Report 92-571, 27 p.

Steritz, J.W., 1986, The southern termination of the Hosgri fault zone, offshore south-central California: Santa Barbara, Calif., University of California, M.S. thesis, 78 p., 22 pl.

Swisher, C.C., III, Dingus, Lowell, and Butler, R.F., 1993, $^{40}Ar/^{39}Ar$ dating and magnetostratigraphic correlation of the terrestrial Cretaceous-Paleogene boundary and Puercan Mammal Age, Hell Creek-Tullock formations, eastern Montana: Canadian Journal of Earth Sciences, v. 30, no. 9, p. 1981-1996.

Sylvester, A.G., and Darrow, A.C., 1979, Structure and neotectonics of the western Santa Ynez fault system in southern California: Tectonophysics, v. 52, p. 389-405.

Tennyson, M.E., Keller, M.A., Filewicz, M.V., and Cotton-Thornton, M.L., 1991, Contrasts in early Miocene subsidence history across Oceanic-West Huasna fault system, northern Santa Maria province, California [abs.]: American Association of Petroleum Geologists Bulletin, v. 75, no. 2, p. 383.

Tolman, C.F., 1927, Biogenesis of hydrocarbons by diatoms: Economic Geology, v. 22, no. 5, p. 454-474.

Turner, D.L., 1970, Potassium-argon dating of Pacific coast Miocene foraminiferal stages, *in* Bandy, O.L., ed., Radiometric dating and paleontologic zonation: Geological Society of America Special Paper 124, p. 91-129.

Tysdal, R.G., Zimmerman, R.A., Wallace, A.R., and Snee, L.W., 1990, Geologic and fission-track evidence for Late Cretaceous faulting and mineralization, northeastern flank of Blacktail Mountains, southwestern Montana: U.S. Geological Survey Bulletin 1922, 20 p.

Vedder, J.G., 1973, Geologic framework and correlation of Miocene rocks in the Caliente Range, *in* Sedimentary facies changes in Tertiary rocks—California Transverse and southern Coast Ranges: Society of Economic Paleontologists and Mineralogists Field Trip 2 Guidebook, p. 42-54.

Vedder, J.G., Howell, D.G., McLean, Hugh, and Wiley, T.J., 1988, Geologic map of Los Machos Hills and Caldwell Mesa quadrangles and part of Tar Spring Ridge quadrangle, California: U.S. Geological Survey Open-File Report 88-253, scale 1:24,000.

Vedder, J.G., McLean, Hugh, and Stanley, R.G., 1994, New 1:24,000-scale geologic maps show stratigraphic and structural relations that require reinterpretation of Cretaceous and Cenozoic tectonic events in the Sierra Madre-San Rafael Mountains area, California [abs]: Geological Society of America Abstracts with Programs, v. 26, no. 2, p. 100-101.

Wissler, S.G., and Dreyer, F.E., 1943, Correlation of the oil fields of the Santa Maria district, *in* Jenkins, O.P., ed., Geologic formations and economic development of the oil and gas fields of California: California Division of Mines Bulletin 118, p. 235-238.

Woodring, W.P., and Bramlette, M.N, 1950, Geology and paleontology of the Santa Maria district, California: U.S. Geological Survey Professional Paper 222, 185 p.

Chapter N

Petroleum Source Potential and Thermal Maturity of the Lospe Formation (Lower Miocene) near Point Sal, Onshore Santa Maria Basin, California

By RICHARD G. STANLEY, MARK J. PAWLEWICZ, DAVID R. VORK, SAMUEL Y. JOHNSON, and ZENON VALIN

U.S. GEOLOGICAL SURVEY BULLETIN 1995–N

EVOLUTION OF SEDIMENTARY BASINS/ONSHORE OIL AND GAS INVESTIGATIONS—SANTA MARIA PROVINCE

Edited by Margaret A. Keller

CONTENTS

FIGURES

TABLES

Petroleum Source Potential and Thermal Maturity of the Lospe Formation (Lower Miocene) near Point Sal, Onshore Santa Maria Basin, California

By Richard G. Stanley, Mark J. Pawlewicz, David R. Vork[1], Samuel Y. Johnson, *and* Zenon C. Valin

Abstract

The Lospe Formation is an 830-m-thick sequence of sedimentary and minor volcanic rocks at the base of the onshore Neogene Santa Maria basin of central California. Eighteen outcrop samples (14 from lacustrine and shallow-marine mudstones of the Lospe Formation, and 4 from bathyal marine shales of the overlying Point Sal Formation) were collected from a measured stratigraphic section at North Beach (informal name) near Point Sal and analyzed using Rock-Eval pyrolysis and vitrinite reflectance. The Rock-Eval data indicate that mudstones of the Lospe are low in organic carbon (range 0.18 to 0.80 weight percent, mean about 0.35 percent) and therefore are generally poor potential source rocks of petroleum. In contrast, shales of the Point Sal Formation exhibit much higher total organic carbon (range 1.47 to 3.63 weight percent, mean about 2.4 percent) and therefore are good to very good potential source rocks. These results should be regarded as preliminary because only a small number of samples were analyzed, and because interpretation of the data is complicated by weathering effects, relatively high thermal maturity, and evidence of migrated bitumen in some samples.

Vitrinite reflectance values (range 0.68–1.56 percent R_0, mean 1.29 percent R_0) and calculated maximum burial temperatures (range 106–192°C, mean 172°C) of the Lospe and Point Sal Formations in the North Beach section are the highest ever observed and reported for Neogene rocks of the onshore Santa Maria basin. These high values can be explained by a combination of burial heating plus a local heat source such as a nearby gabbro sill and (or) a high-temperature hydrothermal system. The local heating event is poorly dated but was probably late early or early middle Miocene, and it may have stimulated thermal generation of oil and gas from organic-rich strata of the Point Sal Formation.

INTRODUCTION

The onshore Santa Maria basin is an important petroleum-producing region in coastal California (fig. 1). Since the first commercial discovery in 1901, more than 820 million barrels of oil and 810 billion cubic feet of associated gas have been produced from this area (California Division of Oil and Gas, 1993). Most of the hydrocarbon accumulations are trapped in anticlines bounded by reverse faults, but a major stratigraphic trap occurs in the western Santa Maria Valley field (Dunham and others, 1991). The most important producing reservoirs are fractured siliceous rocks and dolomites of Miocene age and sandstones of Miocene and Pliocene age (Woodring and Bramlette, 1950; Dryden and others, 1968; Crawford, 1971; Redwine, 1981; Roehl, 1981; California Division of Oil and Gas, 1991).

The principal petroleum source rocks in the Santa Maria basin are widely believed to be organic-rich strata within the Miocene Monterey and Point Sal Formations (Woodring and Bramlette, 1950; Crawford, 1971; Isaacs and Petersen, 1987; Dunham and others, 1991; Lillis and King, 1991). However, some geologists have speculated privately that stratigraphic units beneath the Monterey and Point Sal Formations—including the Lospe Formation—might be minor sources of hydrocarbons. The purpose of this report is to present the results and implications of a reconnaissance study, using Rock-Eval pyrolysis and vitrinite reflectance, of the petroleum source potential and thermal maturity of the Lospe Formation in a measured stratigraphic section at North Beach (informal name) near Point Sal (figs. 1, 2). The Rock-Eval data show that mudstones of the Lospe are organically lean and unlikely to be significant sources of oil or gas. The vitrinite reflectance results indicate that both the Lospe and Point Sal Formations at North Beach are thermally mature to overmature with respect to the oil-generative window. These thermal maturities are the highest ever observed and reported for Neogene rocks of the onshore Santa Maria basin and probably record heating

[1]Unocal Corporation, P.O. Box 4551, Houston, TX 77210.

associated with emplacement of a gabbro sill and (or) a local high-temperature hydrothermal system.

ACKNOWLEDGMENTS

We thank the United States Air Force for permission to work on Vandenberg Air Force Base. Much of the laboratory work was ably performed by T.A. Daws and G.M. Frost. We also thank K.J. Bird, R.B. Cole, T.A. Daws, D.W. Houseknecht, C. E. Katherman, D.G. McCubbin, and K.E. Peters for stimulating discussions. Comments by P.M. Lillis and M.E. Tennyson were helpful in revising an early draft of this report.

STRATIGRAPHIC AND SEDIMENTOLOGIC SETTING

The Lospe Formation (Tolman, 1927; Wissler and Dreyer, 1943) consists of nonmarine and shallow-marine sedimentary rocks and minor rhyolitic tuffs that crop out sporadically in the Casmalia Hills near Point Sal (fig. 1). The Lospe also is present in the subsurface of the Santa Maria basin, where it has been penetrated by numerous exploratory wells (Woodring and Bramlette, 1950; Hall, 1978a, 1982; McLean, 1991; California Division of Oil and Gas, 1991). Sandstones of the Lospe Formation are minor producing reservoirs in the Casmalia and Orcutt oil fields (Woodring and Bramlette, 1950; California Division of Oil and Gas, 1991).

The Lospe Formation records initial tectonic subsidence of the Neogene Santa Maria basin during an episode of crustal extension or transtension beginning about 18 Ma (Stanley and others, 1992a; McCrory and others, 1995). In its type area in the Casmalia Hills, the Lospe is as much as 830 m thick, rests unconformably on the Jurassic Point Sal ophiolite (Hopson and Frano, 1977), and is of late early Miocene age (Saucesian Stage of Kleinpell, 1938, 1980) on the basis of microfossils and isotopic dates (Stanley and others, 1991, 1992a). The Lospe is conformably overlain by the Point Sal Formation (Canfield, 1939, p. 66-67; Wissler and Dreyer, 1943, p. 237; Woodring and others, 1943, p. 1344), which also is of late early Miocene age (Saucesian and Relizian Stages of Kleinpell, 1938, 1980) on the basis of microfossils (Stanley and others, 1991, 1992a).

In the North Beach section (fig. 2) the Lospe is about 410 m thick, but the section is cut by numerous normal(?) faults of unknown displacement, so the original thickness may have been greater. Alluvial fan and fan-delta facies within the basal part of the Lospe consist mainly of reddish-brown and greenish-gray conglomerate and sandstone derived from nearby fault-bounded uplifts of Mesozoic sedimentary and igneous rocks (Stanley and others, 1990, 1991; Johnson and Stanley, 1994; McLean and Stanley, 1994). The alluvial fan and fan-delta deposits grade upward into a sequence of interbedded mudstone and sandstone that accumulated in a lake with possible intermittent connections to the ocean (Stanley and others, 1991). The mudstones are gray brown when fresh, weather gray green, are bioturbated to laminated, and locally display scattered mud cracks that indicate infrequent desiccation. Primary and secondary gypsum occurs locally in the lake deposits; isotopic studies suggest that the sulfur in this gypsum was derived from hydrothermal springs on the floor of the lake (M.L. Tuttle, U.S. Geological Survey, oral commun., 1991; Stanley and others, 1992a). Lenses of nonwelded rhyolitic tuff as much as 20 m thick are interspersed throughout this interval and were deposited primarily as subaqueous pyroclastic flows and high-concentration turbidites that may have originated from eruptive centers in the vicinity of the Santa Ynez River fault (Cole and others, 1991a, b; Cole and Stanley, 1994).

The uppermost 30 m of the Lospe consists of storm-deposited, plane-laminated to bioturbated sandstone and bioturbated mudstone containing shallow-marine microfossils. These shallow-marine deposits are abruptly overlain by the Point Sal Formation, indicating rapid deepening from shelf to bathyal marine environments (Stanley and others, 1991).

In the Point Sal area, the Point Sal Formation is more than 450 m thick and consists mainly of dark-gray to black silty shale with interbeds of turbidite sandstone. Generally, the shale is hard, fissile, and calcareous, with laminations and calcareous microfossils that suggest deposition in oxygen-poor environments at bathyal water depths (Stanley and others, 1991). At some localities, freshly broken surfaces of the shale smell strongly of petroleum. Permeable sandstone beds of the Point Sal Formation are petroleum reservoirs in the Orcutt, Casmalia, and Santa Maria Valley fields (Woodring and Bramlette, 1950; California Division of Oil and Gas, 1991).

Sedimentary rocks of the Point Sal Formation are intruded by basic igneous intrusions mapped as "augite teschenite" by Fairbanks (1896) and as "diabase" by Woodring and Bramlette (1950) and Dibblee (1989). In the North Beach area, one such intrusion is a sill about 25–30 m thick that occurs about 40–50 m stratigraphically above the base of the Point Sal Formation (fig. 2). According to Fairbanks (1896), contact metamorphism has turned shales of the Point Sal Formation to slate for a distance of about 3 m beyond the margin of the sill. The sill rock is composed mainly of plagioclase, pyroxene, and altered olivine, and it has a silica (SiO_2) content of 47.64, corresponding to a basic (gabbroic or basaltic) composition (Cole and Basu, 1995). No isotopic date has been obtained from this sill, but it intrudes strata of the Point Sal Formation that contain benthic foraminifers of the lower part of the Relizian Stage (Woodring and Bramlette, 1950) and therefore can be no older than latest early Miocene (Bartow, 1992). The youngest isotopically dated igneous rocks in the Santa Maria province occur in the Obispo Formation of Hall and others (1966), and yield potassium-argon ages of about 15–18 Ma (ages from Turner, 1970, corrected using the technique of Dalrymple, 1979). On the basis of these regional ages, we suggest that

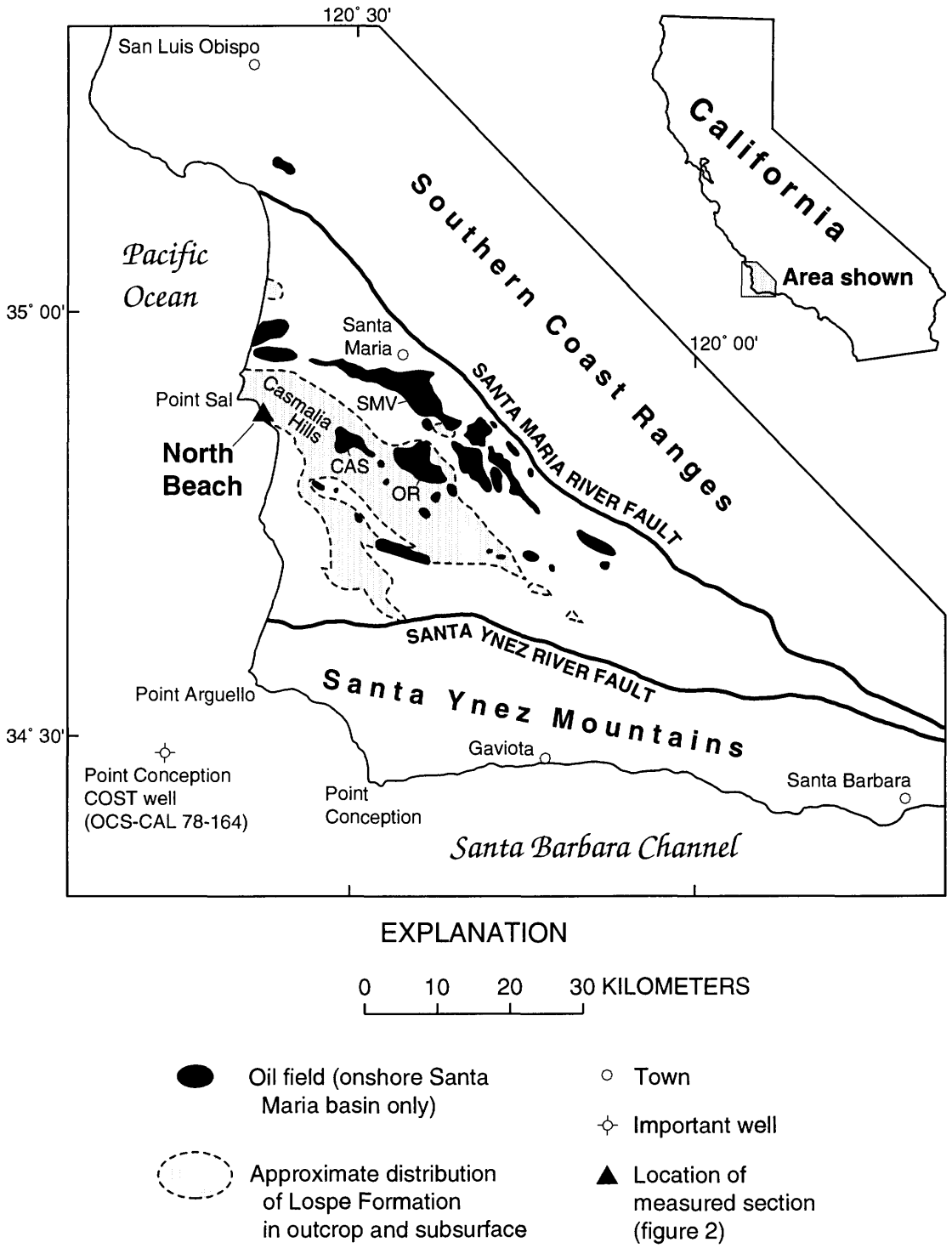

Figure 1. Location map of the Santa Maria area. Generally, the onshore Santa Maria basin is the triangular area bounded by the Santa Maria River fault (Hall, 1978a), the Santa Ynez River fault (Sylvester and Darrow, 1979), and the present shoreline. Shaded areas show the onshore surface and subsurface distribution of the Lospe Formation according to Hall (1982) with modifications from McLean (1991). Oil and gas fields in the Santa Maria basin area are shown in black and include the Casmalia (CAS), Orcutt (OR), and Santa Maria Valley (SMV) fields.

the sill in the North Beach area was most likely emplaced during the late early or early middle Miocene.

METHODS

Eighteen rock samples (14 from the Lospe Formation and, for comparison, 4 from the Point Sal Formation) were collected from the North Beach section along the sea cliff about 3.5 km southeast of Point Sal (figs. 1, 2). The rock samples were taken from about 10 cm to 30 cm back from the outcrop faces in order to obtain the freshest available material. All 18 samples were analyzed using a Rock-Eval II pyroanalyzer, and 16 of these were examined for vitrinite reflectance, in the laboratories of the U.S. Geological Survey, Branch of Petroleum Geology, in Denver, Colorado. Duplicate vitrinite slides were prepared and analyzed from 14 of the samples. Organic carbon was measured on all 18 samples in the laboratories of the U.S. Geological Survey, Branch of Pacific Marine Geology, in Palo Alto, California. The results of the Rock-Eval pyrolysis, vitrinite reflectance, and organic carbon analyses are shown in tables 1, 2, and 3 and summarized in table 4. Processing and examination of samples for palynomorphs were conducted in the laboratories of Unocal Oil and Gas Division in Ventura, California.

Rock-Eval pyrolysis is a widely used method of rapidly evaluating the quality and thermal maturity of prospective petroleum source rocks (Espitalié and others, 1977, 1984; Clementz and others, 1979; Tissot and Welte, 1984; Peters, 1986). The procedure mimics, in some respects, the natural hydrocarbon-generation processes that occur at much slower rates within the earth when sediments containing kerogen (sedimentary organic matter) are buried progressively deeper and subjected to increasing temperatures (Waples, 1985). Pulverized samples of rock are held at 250°C for 3 minutes (the so-called isothermal period), then gradually heated from 250°C to 600°C at 25°C per minute in an oxygen-free atmosphere, causing the release of water, carbon dioxide, and hydrocar-

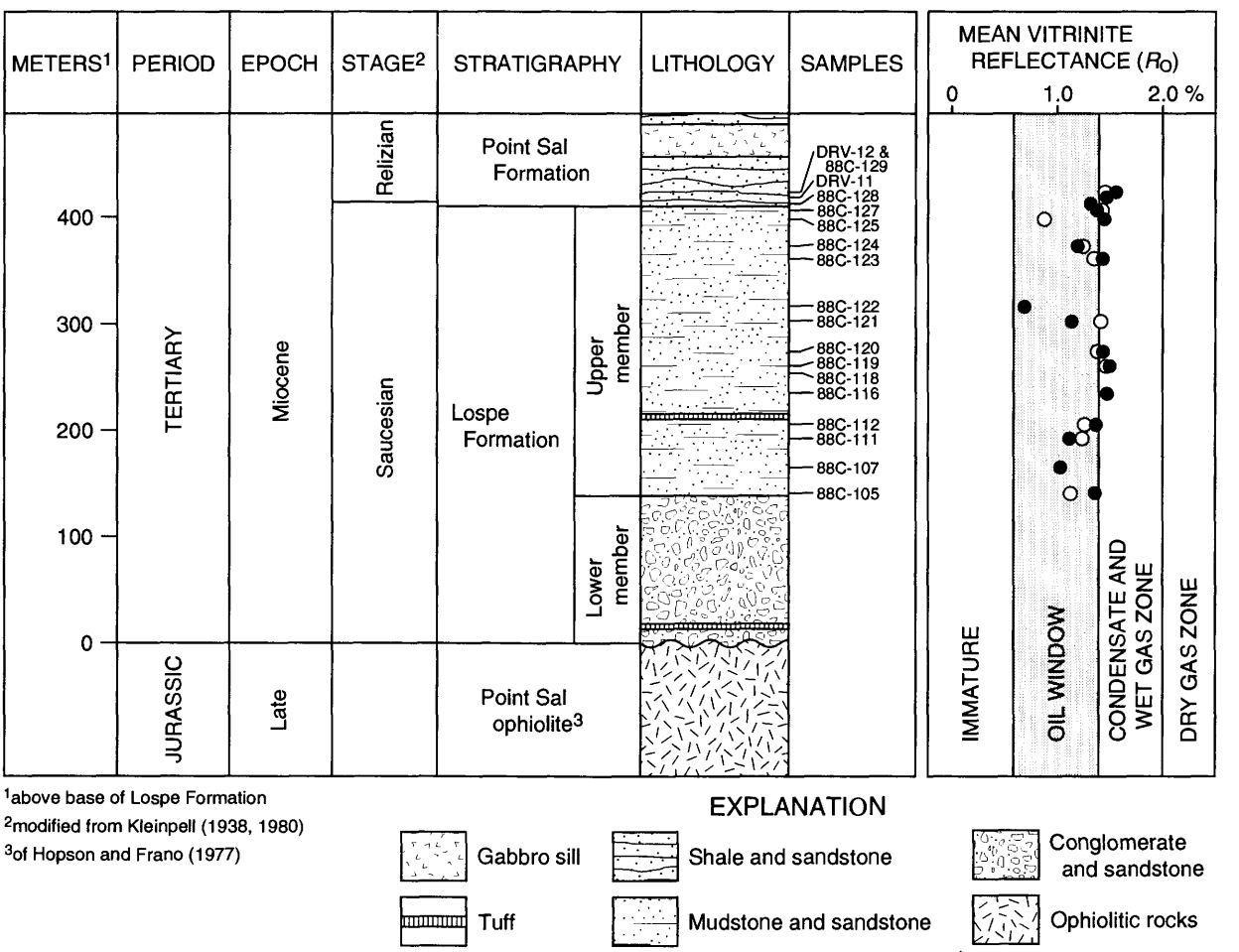

Figure 2. Generalized stratigraphy of the North Beach section, showing sample locations and mean values of vitrinite reflectance (on a linear scale) for run 1 (empty circles) and run 2 (filled circles). Top and base of oil-generative window from Peters (1986); base of condensate and wet gas zone from Tissot and Welte (1984). Numerous normal(?) faults of unknown displacement are present in the outcrops but are not shown on this figure.

Table 1. Rock-Eval pyrolysis data from the Lospe and Point Sal Formations in the North Beach section

[T_{max} values for samples with S2 less than 0.2 mg HC/g rock were rejected as unreliable, following the recommendation of Peters (1986). T_{max} value for sample 88C-105 was not reported by the laboratory. Rock-Eval parameters are discussed in the text. mdst, mudstone]

Sample number	Formation	Meters above base[1]	Rock type	Depositional environment	Sample weight (mg)	TOC (weight percent)	S1 (mg HC/ g rock)	S2 mg HC/ g rock)	S3 (mg CO_2/ g rock)	S2/S3	PI [S1/ S1+S2]	HI	OI	T_{max} (°C)
88C-129	Point Sal	426.65	shale	Bathyal marine	72.1	1.47	1.10	0.58	0.76	0.76	0.65	39	51	374
DRV-12	Point Sal	426.30	shale	Bathyal marine	51.2	1.81	2.42	2.22	1.44	1.54	.52	122	79	395
DRV-11	Point Sal	423.70	shale	Bathyal marine	56.3	3.57	3.35	2.96	1.77	1.67	.53	82	49	454
88C-128	Point Sal	416.15	shale	Bathyal marine	49.9	2.67	2.28	2.94	1.44	2.04	.44	110	53	447
88C-127	Lospe	409.55	mdst	Shallow marine	191.8	.24	.15	.51	.31	1.64	.23	212	129	493
88C-125	Lospe	401.25	mdst	Shallow marine	187.7	.46	.04	.37	.18	2.05	.10	80	39	442
88C-124	Lospe	378.05	mdst	Lacustrine	202.3	.39	.25	.44	.48	.91	.37	112	123	334
88C-123	Lospe	364.55	mdst	Lacustrine	234.9	.41	.48	.84	.54	1.55	.36	204	131	346
88C-122	Lospe	319.65	mdst	Lacustrine	204.5	.68	.01	.41	.21	1.95	.02	60	30	423
88C-121	Lospe	305.95	mdst	Lacustrine	192.0	.37	.96	1.42	.77	1.84	.40	383	208	364
88C-120	Lospe	277.30	mdst	Lacustrine	185.7	.26	.01	.08	.12	.66	.12	30	46	
88C-119	Lospe	260.45	mdst	Lacustrine	211.2	.20	0	.02	.08	.25	0	10	40	
88C-118	Lospe	255.65	mdst	Lacustrine	221.6	.34	0	.08	.18	.44	0	23	52	
88C-116	Lospe	237.90	mdst	Lacustrine	220.9	.34	.02	.13	.16	.81	.14	38	47	
88C-112	Lospe	209.80	mdst	Lacustrine	201.3	.43	.09	.42	.25	1.68	.18	97	58	363
88C-111	Lospe	196.30	mdst	Lacustrine	206.5	.18	.07	.42	.09	4.66	.15	233	50	401
88C-107	Lospe	167.95	mdst	Lacustrine	206.7	.24	.08	.19	.23	.82	.31	79	95	
88C-105	Lospe	142.95	mdst	Lacustrine	145.3	.30	.16	.91	.26	3.50	.15	303	86	

[1]Above base of Lospe Formation in the measured stratigraphic section at North Beach. Numerous normal(?) faults of unknown displacement probably have removed parts of the section (Johnson and Stanley, 1994).

Table 2. Total carbon obtained by dry combustion, carbonate carbon obtained by coulometric titration, and organic carbon determined by the difference between total carbon and carbonate carbon, for samples from the Lospe and Point Sal Formations in the North Beach section

[Also shown, for comparison with organic carbon results, are values of Rock-Eval TOC (from table 1). See text for discussion]

Sample number	Formation	Total carbon (weight percent)	Carbonate carbon (weight percent)	Organic carbon (weight percent)	Rock-Eval TOC (weight percent)
88C-129	Point Sal	3.76	1.48	2.28	1.47
DRV-12	Point Sal	2.85	1.03	1.82	1.81
DRV-11	Point Sal	4.79	1.16	3.63	3.57
88C-128	Point Sal	2.76	1.07	1.69	2.67
88C-127	Lospe	.52	.32	.20	.24
88C-125	Lospe	.61	.16	.45	.46
88C-124	Lospe	.74	.27	.47	.39
88C-123	Lospe	.73	.36	.37	.41
88C-122	Lospe	1.05	.24	.81	.68
88C-121	Lospe	.49	.26	.23	.37
88C-120	Lospe	.44	.17	.27	.26
88C-119	Lospe	.62	.40	.22	.20
88C-118	Lospe	.64	.29	.35	.34
88C-116	Lospe	.48	.13	.35	.34
88C-112	Lospe	.52	.16	.36	.43
88C-111	Lospe	.21	.03	.18	.18
88C-107	Lospe	.27	.06	.21	.24
88C-105	Lospe	.41	.13	.28	.30

bons from the rock. Several parameters are measured automatically by the Rock-Eval apparatus (table 1). The quantity S1 is the amount of hydrocarbons (HC), measured in milligrams HC per gram of rock, that is released upon initial heating to 250°C; this quantity includes the bitumen (free organic compounds, including gas and oil) already present in the rock. The quantity S2 (also measured in milligrams HC per gram of rock) is the amount of hydrocarbons generated by pyrolytic

Table 3. Vitrinite reflectance (R_o) data from the Lospe and Point Sal Formations in the North Beach section

Sample number	Formation	Vitrinite reflectance (R_o) run 1: Number of measurements	Range of R_o (percent)	Mean R_o (percent)	Standard deviation	Vitrinite reflectance (R_o) run 2: Number of measurements	Range of R_o (percent)	Mean R_o (percent)	Standard deviation
88C-129	Point Sal	16	1.02-1.73	1.46	0.18	5	1.52-1.60	1.56	0.04
DRV-12	Point Sal								
DRV-11	Point Sal	25	1.26-1.72	1.47	.11	4	1.40-1.62	1.47	.10
88C-128	Point Sal					3	1.25-1.45	1.32	.12
88C-127	Lospe	14	0.98-1.89	1.43	.23	5	1.25-1.44	1.38	.08
88C-125	Lospe	8	0.74-1.28	.87	.18	3	1.43-1.47	1.44	.03
88C-124	Lospe	12	1.03-1.46	1.24	.12	1	1.20-1.20	1.20	.00
88C-123	Lospe	27	1.00-1.62	1.37	.16	21	1.15-1.65	1.43	.12
88C-122	Lospe	11	0.60-0.82	.68	.07	25	0.58-0.87	.69	.06
88C-121	Lospe	20	1.15-1.53	1.41	.11	1	1.14-1.14	1.14	.00
88C-120	Lospe	31	1.17-1.54	1.37	.10	51	1.17-1.63	1.43	.10
88C-119	Lospe	23	1.28-1.65	1.43	.09	45	1.28-1.66	1.49	.08
88C-118	Lospe								
88C-116	Lospe	35	1.23-1.71	1.48	.11	51	1.17-1.76	1.47	.12
88C-112	Lospe	27	1.03-1.57	1.27	.13	41	1.20-1.66	1.38	.10
88C-111	Lospe	24	0.98-1.58	1.23	.14	1	1.59-1.59	1.11	.00
88C-107	Lospe					55	0.89-1.17	1.03	.07
88C-105	Lospe	2	1.06-1.19	1.13	.09	7	1.21-1.52	1.36	.11

Table 4. Summary of Rock-Eval pyrolysis, organic carbon, and vitrinite reflectance (R_o) data from the Lospe and Point Sal Formations in the North Beach section

Subset	Number of Rock-Eval/ organic carbon/ R_o analyses	Rock-Eval TOC (weight percent)	Organic carbon (weight percent)	S1 (mg HC/ g rock)	S2 (mg HC/ g rock)	S3 (mg HC/ g rock)	S2/S3	PI	HI	OI	T_{max} (° C)	Mean R_o (percent) (run 1)	Mean R_o (percent) (run 2)	Mean R_o (percent) (runs 1 & 2)
All samples	18/18/30[1]													
minimum		0.18	.18	0	0.02	0.08	0.25	0	10	30	334	0.68	0.69	0.68
maximum		3.57	3.63	3.35	2.96	1.77	4.66	.65	383	208	493	1.48	1.56	1.56
mean		.80	.79	.64	.83	.52	1.60	.26	123	76	403	1.27	1.31	1.29
Point Sal Fm.	4/4/5[2]													
minimum		1.47	1.69	1.10	.58	.76	.76	.44	39	49	374	1.46	1.32	1.32
maximum		3.57	3.63	3.35	2.96	1.77	2.04	.65	122	79	454	1.47	1.56	1.56
mean		2.38	2.36	2.29	2.18	1.35	1.50	.54	88	58	418	1.47	1.45	1.46
Lospe Fm.	14/14/25[3]													
minimum		.18	.18	0	.02	.08	.25	0	10	30	334	.68	.69	.68
maximum		.68	.80	.96	1.42	.77	4.66	.4	383	208	493	1.48	1.49	1.49
mean		.35	.34	.17	.45	.28	1.63	.18	133	81	396	1.24	1.27	1.26

[1] Includes 14 R_o analyses for run 1 and 16 R_o analyses for run 2.
[2] Includes 2 R_o analyses for run 1 and 3 R_o analyses for run 2.
[3] Includes 12 R_o analyses for run 1 and 13 R_o analyses for run 2.

Table 5. Geochemical parameters describing source rock generative potential (from Peters, 1986)

Potential	TOC (weight percent)	S1 (mg HC/g rock)	S2 (mg HC/g rock)
Poor	0-0.5	0-0.5	0-2.5
Fair	0.5-1.0	0.5-1.0	2.5-5.0
Good	1.0-2.0	1.0-2.0	5.0-10.0
Very good	2.0+	2.0+	10.0+

degradation (or "cracking") of the remaining organic matter in the rock and is an indicator of the potential of the rock to generate additional oil and gas. T_{max} is the temperature—generally about 400°C to 500°C—at which S2 is at a maximum and is regarded as a rough indicator of thermal maturity. S3 is the amount of carbon dioxide (in milligrams of CO_2 per gram of rock) generated during pyrolysis and is thought to be related to the amount of oxygen in the pyrolyzed organic matter. Calculated Rock-Eval parameters include (1) the total organic carbon (TOC), in weight percent; (2) the hydrogen index (HI), defined as the product 100(S2/TOC) and sometimes expressed as mg HC/g C; (3) the oxygen index (OI), defined as the product 100(S3/TOC) and sometimes expressed as mg CO_2/g C; and (4) the production index (PI), defined as the ratio S1/(S1 + S2).

Vitrinite reflectance (R_o) is a common method of determining thermal maturity and is obtained by measuring the percentage of light reflected by vitrinite, a type of kerogen formed from woody terrestrial plant material (Tissot and Welte, 1984; Waples, 1985). Higher values of vitrinite reflectance correspond to higher levels of thermal maturity. The maturation of vitrinite is irreversible and related to maximum burial temperature (Barker and Pawlewicz, 1986) and perhaps also to elapsed heating time (P.G. Lillis, U.S. Geological Survey, written commun., 1992).

Carbon was measured by methods described by Jackson and others (1987). Total carbon was determined by dry combustion with a Coulometrics, Inc. Model 5020 Total Carbon Apparatus. Carbonate carbon was measured by automated coulometric titration of carbon dioxide (Huffman, 1977) using a Coulometrics, Inc. Model 5010 Carbon Dioxide Coulometer. Organic carbon was then determined by the difference between total carbon and carbonate carbon.

Although the Rock-Eval, vitrinite reflectance, and organic carbon techniques are widely used and accepted, there is a high degree of variability in the sample preparation steps, analytical procedures, and units of measurement employed in various laboratories. Therefore, caution must be used when comparing source rock data from different laboratories (Dembicki, 1984).

QUANTITY OF ORGANIC MATTER

The quantity of organic matter in the samples is indicated by the Rock-Eval TOC (total organic carbon, in weight percent), organic carbon determined from combustion and coulometry, and the Rock-Eval quantities S1 and S2. The Rock-Eval TOC of mudstones in the Lospe Formation ranges from 0.18 to 0.68 percent with a mean of about 0.35 percent (tables 1, 4); these results are generally close to the amounts of organic carbon determined from combustion and coulometry (tables 2, 4). Only one of the 14 Lospe samples exhibits a Rock-Eval TOC or organic carbon value greater than 0.5 percent (table 2), which is regarded as the lower limit for potential source rocks of petroleum by Tissot and Welte (1984). Comparison with table 5 shows that, on the basis of Rock-Eval TOC and organic carbon, 13 of the 14 Lospe samples have poor hydrocarbon generative potential, while one sample has fair generative potential. In contrast, the Rock-Eval TOC values for mudstones of the Point Sal Formation range from 1.47 to 3.57 percent and average 2.38 percent (tables 1, 4); these results are comparable to the amounts of organic carbon measured by combustion and coulometry (tables 2, 4) and indicate that the Point Sal samples have good to very good hydrocarbon generative potential (table 5). The Rock-Eval TOC and organic carbon results from both the Lospe and Point Sal Formations should be viewed with caution, however, because the amount of organic material in rocks can be significantly reduced by oxidation during outcrop weathering (Leythaeuser, 1973; Clayton and Swetland, 1978; Peters, 1986; Stanley, 1987) and, in thermally mature and overmature rocks, by losses due to hydrocarbon generation and expulsion (Daly and Edman, 1987). Vitrinite reflectance results (discussed later in this report) from the North Beach samples suggest thermal maturities within the oil-generative window and the upper part of the condensate and wet gas zone (table 3, fig. 2); organic carbon reductions at such levels of thermal maturity are generally small (10–20 percent) for type III and IV kerogens, which are common in samples from the Lospe and Point Sal Formations, but may be as much as 50 percent for type II kerogens (A.R. Daly and J.D. Edman, Exlog and Brown and Ruth Laboratories, Englewood, Colorado, written commun. to D.W. Houseknecht, 1987). A further complication is that organic carbon can be increased by contamination due to migrated bitumen (K.E. Peters, Chevron Oil Field Research Co., Richmond, Calif., written commun., 1992), which may be significant in some of our Point Sal samples, as noted below.

Values of S1 for mudstones from the Lospe Formation range from 0 to 0.96, with a mean of about 0.17 (tables 1, 4). Thirteen of the 14 Lospe samples exhibit values of S1 less than 0.5 (table 1), suggesting poor generative potential (table 5). All Lospe samples exhibit values of S2 of less than 2.5 (table 1), also indicating poor generative potential (table 5). Samples from the Point Sal Formation exhibit S1 values ranging from 1.10 to 3.35 (table 1), suggesting good to very good hydrocarbon generative potential (table 5); however, these high values most likely reflect the presence of indigenous or migrated oil, which is also indicated by the strong oily odor emitted by freshly broken surfaces of these rocks. Values of S2 from the Point Sal Formation range from 0.58 to 2.96 (table 1), are generally higher than from the Lospe, and indicate poor to fair generative potential for the Point Sal (table 5).

We suggest that the generally low values of S1 and S2 in the Lospe samples indicate initially poor generative potential due to a large proportion of woody (humic) and oxidized (inertinitic and recycled) kerogens, as discussed below in the section on "Types of Organic Matter." The values of S1 and S2 in the Lospe also may have been lowered by oxidation of organic matter during surface weathering of the sampled out-

crops, by adsorption on clay minerals of the hydrocarbons produced during pyrolysis, and by hydrocarbon generation and expulsion during thermal maturation (Peters, 1986; Daly and Edman, 1987). The amounts of such losses, however, are unknown.

Both the quantity of organic matter and the inferred hydrocarbon generative potential in the samples appear to correlate with depositional environment. Mudstones of the Point Sal Formation that were deposited in bathyal, oxygen-poor marine environments have generally higher values of TOC, S1, and S2 than mudstones of the Lospe Formation that accumulated in a lacustrine setting (table 1). The reasons for these differences in values are unclear but may include one or more of the following: (1) Rates of consumption of organic matter by bottom-dwelling invertebrates and microorganisms may have been higher in the Lospe lake than in the Point Sal sea; this hypothesis is consistent with our field observation that burrowed intervals are more common in the Lospe than in the Point Sal Formation, while laminated intervals are more common in the Point Sal. (2) Accumulation rates of terrigenous debris (silt and clay) may have been higher than accumulation rates of organic matter during deposition of the Lospe Formation, resulting in relatively greater dilution of organic material in the Lospe than in the Point Sal. (3) Rates of organic productivity may have been higher in the bathyal marine setting of the Point Sal Formation than in the lacustrine setting of the Lospe, perhaps because coastal upwelling made the marine environments more nutrient rich and therefore more fertile.

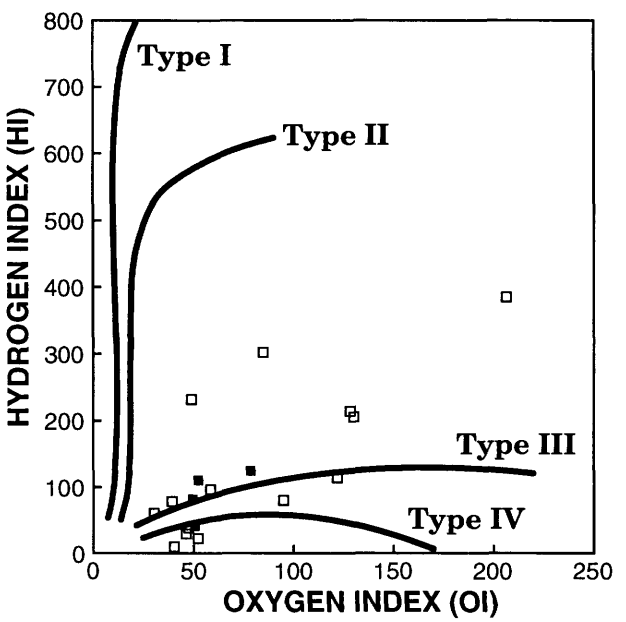

Figure 3. Modified van Krevelen diagram (Peters, 1986) showing idealized kerogen types (solid lines) and results for mudstones from the Lospe Formation (empty squares) and the Point Sal Formation (filled squares) from the North Beach section (table 1). Type I and type II kerogens are oil prone, type III kerogens are gas prone, and type IV kerogens are inert (Peters, 1986).

TYPES OF ORGANIC MATTER

Plots of hydrogen index (HI) versus oxygen index (OI) on a modified van Krevelen diagram (fig. 3) show a range of kerogen compositions in samples from the Lospe and Point Sal Formations. These plots also indicate considerable overlap between the two formations. Most of the Lospe and Point Sal samples are types III and IV, but some appear to be intermediate between types II and III. Type II kerogens are generally considered to be potential sources of both oil and gas, whereas type III kerogens are sources mainly of gas (Tissot and Welte, 1984; Peters, 1986). Type IV kerogens are generally regarded as inert, with little or no hydrocarbon source potential (Peters, 1986; K.E. Peters, written commun., 1992).

A wide range in kerogen compositions also is suggested by variations in the values of HI and the ratio S2/S3. HI ranges from 39 to 122 in the Point Sal Formation, and from 10 to 383 in the Lospe Formation (tables 1, 4). All 4 samples from the Point Sal Formation and 9 of the 14 Lospe samples exhibit HI less than 150 and values of S2/S3 less than 3 (table 1), suggesting gas generative potential (table 6). These results should be viewed with caution because both HI and S2/S3 can be reduced by (1) thermal maturation accompanied by generation and subsequent escape of hydrocarbons, (2) adsorption of pyrolytic organic compounds onto the clay mineral matrix during pyrolysis, and (3) oxidation of organic matter during transport, sedimentation, diagenesis, or outcrop weathering (Peters, 1986). Taken at face value, however, the Rock-Eval data suggest that kerogens in the Lospe Formation are variable in composition and mostly gas prone. Three Lospe samples (88C-105, 88C-111, and 88C-121) are clearly anomalous, with HI greater than 300 and (or) S2/S3 between 3 and 5 (table 1). The reasons for these anomalously high values are unknown, but they may reflect the presence of migrated bitumen.

Analysis of palynomorphs in samples from the North Beach section suggests that much of the organic matter in the Lospe is of terrestrial (humic and herbaceous) origin. (Four samples from the Point Sal Formation were processed for palynomorphs but were barren.) The palynomorphs from the Lospe show signs of oxidation but yield evidence of a diverse terrestrial vascular plant flora including *Carya* (hickory), *Quercus* (oaks), *Juglans* (walnuts), *Ulmus* (elms), *Betula* (birch), Pinaceae (pines), *Alnus* (alder), *Pterocarya* (trees related to walnut and hickory), Bombacaceae (tropical trees, including baobab and balsa), *Ilex* (holly), *Ephedra* (Mormon tea), *Salix* (willows), Malvaceae (mallow family; e.g., cotton), and Astereaceae (sunflower family). This assemblage suggests a deciduous hardwood forest and temperate climate with wet summers. Also found were palynomorphs of the

Table 6. Geochemical parameters describing type of hydrocarbon generated (from Peters, 1986)

Type	Hydrogen Index (HI)	S2/S3
Gas	0-150	0-3
Gas and oil	150-300	3-5
Oil	300+	5+

Chenopodiaceae (goosefoot family; e.g., spinach, beets, and saltbush), which may indicate alkaline soil. Several Lospe samples contained reworked pollen of Late Cretaceous and Paleogene age. A few samples yielded sparse marine dinoflagellate cysts, which may indicate that the Lospe lake was at times marine influenced; alternatively, the dinoflagellate cysts may have been reworked from older marine strata.

One of the samples from the Lospe Formation (table 1, sample 88C-121) shows an oxygen index (OI) value of 208. Values over 150 are unusually high (Katz, 1983) and can be caused by oxidation of organic matter in the samples during outcrop weathering (Peters, 1986; Stanley, 1987) or by generation of carbon dioxide during pyrolysis by thermal degradation of carbonate minerals such as calcite, dolomite, and siderite (Katz, 1983; Peters, 1986). Either or both of these problems may have affected our data because the samples were collected from surface exposures susceptible to weathering and because the samples were not treated with acid to remove carbonate before pyrolysis.

THERMAL MATURITY

The thermal maturity of organic matter in our samples is indicated by the vitrinite reflectance (percent R_o); however, these results should be viewed with caution because of the low numbers of vitrinite reflectance measurements in some samples (table 3). The mean vitrinite reflectance of samples from the Lospe Formation ranges from 0.68 to 1.49 percent R_o, with a total sample mean of 1.26 percent R_o (tables 3, 4). Comparison of these values with the thermal maturity range chart (table 7) indicates that the thermal maturity of Lospe samples falls within the oil-generative window and the upper part of the condensate and wet gas zone (fig. 2). The mean vitrinite reflectance of samples from the Point Sal Formation ranges from 1.32 to 1.56 percent R_o with a total sample mean of 1.45 percent R_o (tables 3, 4), falling within the lower part of the oil-generative window and the upper part of the condensate and wet gas zone (fig. 2). Thus, on the basis of the ranges and mean values of vitrinite reflectance, it appears that the thermal maturity of the Point Sal Formation is about the same to somewhat higher than the underlying Lospe Formation. Inspection of figure 2 shows that the relationship between vitrinite reflectance and stratigraphic position is not a simple linear trend, and that there is an apparent increase in vitrinite reflectance in the part of the section above 225 m from the base of the Lospe.

The vitrinite in most samples is consistent in appearance, with some plant structure visible and some evidence of weathering. No obviously recycled vitrinite was noted. In most of our samples, histograms of the reflectance measurements exhibit unimodal populations with well-defined peaks. None of the histograms show the bimodal distribution expected from samples that contain both primary and recycled vitrinite (e.g., Hunt, 1979).

Nevertheless, the vitrinite reflectance values for sample 88C-122 are anomalously low compared with the other samples (fig. 2). The reason for these low values is unknown, but it may be related to retardation of vitrinite maturation due to the absorption of thermally generated bitumen into the vitrinite, as proposed by Peters and others (1978) for a similar anomaly noted in samples of Cretaceous rocks from the Atlantic Ocean. Another possibility is that this sample was somehow shielded from the high temperatures that affected the other samples. If the high temperatures were related to migrating hot fluids in the subsurface, shielding may have been provided by local permeability barriers such as faults, clayey intervals, or zones of early cementation in the surrounding strata.

Six of the 14 Lospe samples and 2 of the 4 Point Sal samples exhibit values of T_{max} less than 435°C (table 1), suggesting that these rocks are thermally immature with respect to the oil-generative window (table 7)—a result that is inconsistent with the high thermal maturities indicated by the vitrinite reflectance data. Anomalously low T_{max} values can be caused by the occurrence of resinite (fossil tree resin) and by oil that has been generated in place or migrated into the rock (Peters, 1986). The presence of oil is an obvious explanation for low values of T_{max} in some samples (88C-121, 88C-123, 88C-124, 88C-129, and DRV-12) that also exhibit high production index (PI) values. Further organic geochemical analysis—for example, organic petrography, and extraction prior to Rock-Eval pyrolysis (Peters, 1986)—may resolve the problem of anomalously low values of T_{max} relative to vitrinite reflectance in the other samples.

INFERRED PALEOTEMPERATURES IN THE NORTH BEACH SECTION

Vitrinite reflectance data can be used to estimate maximum burial temperatures using the following equation (Barker, 1988):

$$\ln(R_o)=0.0096(T_{burial})-1.4, \quad (1)$$

where R_o is the vitrinite reflectance (in percent), and T_{burial} is the maximum burial temperature in degrees Celsius. Potential errors may be as great as ±30°C (Laughland and others, 1990). Using equation 1 and the observed vitrinite reflectance values from the Point Sal area, we calculate maximum burial temperatures for the Lospe Formation ranging from 106°C to 187°C, with a mean of 170°C (table 8). The calcu-

Table 7. Geochemical parameters describing level of thermal maturation (from Peters, 1986), and corresponding estimated burial temperatures (T_{burial}) calculated from vitrinite reflectance using the following equation (Barker, 1988): ln (R_o)=0.0096 (T_{burial})–1.4

Maturation	Production Index (PI)[1] [S1/(S1 + S2)]	T_{max}[1] (° C)	Vitrinite reflectance (percent R_o)	T_{burial} (°C)
Top of oil-generative window	ca. 0.1	ca. 435-445	ca. 0.6	ca. 93
Bottom of oil-generative window	ca. 0.4	ca. 470	ca. 1.4	ca. 181

[1] T_{max} and PI are crude measurements of thermal maturation and are partly dependent on other factors, including the type of organic matter (Peters, 1986).

lated temperatures for the Point Sal Formation are generally higher, ranging from 175°C to 192°C, with a mean of 185°C. Recent work by Barker and Pawlewicz (1994) suggests that maximum temperatures may have been as much as 20°C higher if one assumes that the vitrinite reflectance values reflect peak heating during hydrothermal metamorphism, rather than burial heating.

These results are noteworthy for two reasons. First, our vitrinite reflectance values and calculated paleotemperatures are, to the best of our knowledge, the highest ever observed and reported for rocks of Miocene and younger age in the Santa Maria province. Second, our results suggest an inverted thermal maturity profile, in which the Lospe Formation appears to be less thermally mature than the overlying Point Sal Formation. This is contrary to the usual case in which rocks that are stratigraphically and (or) structurally lower exhibit higher levels of thermal maturity because they have been buried deeper and experienced correspondingly higher temperatures (e.g., Hunt, 1979; Tissot and Welte, 1984). These issues are further discussed below.

Table 8. Maximum burial temperatures (T_{burial}) calculated from vitrinite reflectance results using the following equation (Barker, 1988): ln (R_o) = 0.0096 (T_{burial}) - 1.4. See text for discussion

Subset	Mean R_o[1] (percent)	T_{burial} (°C)
All samples		
minimum	0.68	106
maximum	1.56	192
mean	1.29	172
Point Sal Fm.		
minimum	1.32	175
maximum	1.56	192
mean	1.46	185
Lospe Fm.		
minimum	.68	106
maximum	1.49	187
mean	1.26	170

[1]From table 3.

COMPARISON WITH PREVIOUS THERMAL MATURITY RESULTS FROM THE SANTA MARIA BASIN

For several reasons, little information is available to the public on the thermal maturity of strata in the Santa Maria basin. Research done by the petroleum industry is largely unpublished (Isaacs and Petersen, 1987). Most studies have focused on the Monterey Formation, but experience suggests that conventional techniques of measuring thermal maturity—including vitrinite reflectance, Rock-Eval pyrolysis T_{max}, Thermal Alteration Index (TAI, a measurement of kerogen on a color scale), and others—may be unreliable or difficult to interpret in the Monterey (Isaacs and Petersen, 1987; Isaacs, 1988). Another problem is that vitrinite particles are sparse or absent from the Monterey in many areas (Isaacs and Petersen, 1987). Some evidence suggests that the Monterey Formation in some areas generates oil at lower than expected levels of thermal maturity, perhaps at vitrinite reflectance values less than 0.4 percent R_o (McCulloh, 1979; Petersen and Hickey, 1987; Isaacs and Petersen, 1987; Isaacs, 1987, 1988). Low-temperature generation of petroleum in the Monterey, if it occurs, may be related to the unusual chemistry of some Monterey kerogens, particularly the high sulfur content (Orr, 1984; Petersen and Hickey, 1987; Isaacs, 1988; Baskin and Peters, 1992). The notion of low-temperature generation of petroleum in the Monterey is not universally accepted, however (for example, see Dunham and others, 1991, p. 442-443).

Currently available information, summarized here, indicates that the Monterey Formation and other Neogene strata in the Santa Maria basin and surrounding areas are thermally immature to mature with respect to the conventional oil-generative window (table 7). Studies of silica diagenesis in the Santa Maria basin and surrounding areas show that, in places, siliceous strata of the Monterey Formation have been buried at least as deep as the zone of transformation of opal-CT to quartz. The top of this zone corresponds to temperatures of about 75–85°C (Isaacs, 1988, and references therein), slightly less than the top of the oil-generative window at about 93°C (table 7). In some parts of the Santa Maria basin, the Monterey Formation presently is situated at depths where temperatures exceed 120°C, well within the conventional oil window (Dunham and others, 1991, p. 443). Studies of illite/smectite geothermometry of the Monterey Formation in a well in the Orcutt field (fig. 1) suggest temperatures greater than 100–

105°C (Pollastro, 1990), which fall within the oil-generative window (table 7). In the Point Arguello oil field about 10 km southwest of Point Arguello (fig. 1), the highest measured temperature was about 128.8°C at a depth of about 2,255 m (Williams and others, 1994, p. F6; Colin Williams, oral commun., 1995), also within the oil window (table 7). A reconnaissance study of 43 well and outcrop samples from the Miocene Point Sal and Monterey Formations and the Miocene and Pliocene Sisquoc Formation of the onshore Santa Maria basin and the Miocene Monterey Formation of the Santa Barbara coast showed vitrinite reflectance values of 0.21–0.6 percent R_o and TAI values of 1.1–2.5, indicating that these rocks are thermally immature to marginally mature (Isaacs and Magoon, 1984; Isaacs and Tomson, 1990). A regional study of more than 200 outcrop and subsurface samples from the Santa Maria and Ventura basins concluded (on the basis of TAI, R_o, Rock-Eval pyrolysis T_{max}, sapropel fluorescence, and silica diagenetic grade) that the Point Sal and Monterey Formations are generally immature to marginally mature but are fully mature in certain areas, such as subthrust sections and deep synclines (Global Geochemistry Corporation, 1985). In a study of the Monterey Formation, Keller (1984) reported that 16 outcrop samples from the Santa Barbara coast and 2 subsurface samples from the onshore Santa Maria basin showed Rock-Eval pyrolysis T_{max} values ranging from 397–436°C, or immature to marginally mature (table 7). Six outcrop samples of the Monterey Formation along the Santa Barbara coast showed several organic geochemical characteristics consistent with thermal immaturity (G.E. Claypool *in* Taylor, 1976, p. 25). Also from the Santa Barbara coast, unpublished analyses of atomic hydrogen/carbon ratios in organic matter in 37 samples indicate that the Monterey Formation in this area is thermally immature (C.M. Isaacs, written commun., 1991). A sample of the Monterey Formation collected from near Gaviota (fig. 1) showed a vitrinite reflectance of 0.38 percent R_o (Pytte, 1989). The lower Miocene Rincon Shale of the Santa Barbara coast also is thermally immature, on the basis of Rock-Eval pyrolysis T_{max} values (Stanley and others, 1992b, 1993). In the Point Conception COST well (fig. 1), the highest average vitrinite reflectance values reported were 0.68 percent R_o for Mesozoic rocks near the bottom of the well, and 0.34 percent R_o for the oldest Neogene rocks (Bostick, 1979). In the same well, similarly low levels of thermal maturity also were suggested by studies of molecular composition of saturated hydrocarbons, pyrolysis characteristics, elemental analysis of solid organic matter, TAI values, and thermal history modeling (Claypool and others, 1979; Petersen and Hickey, 1987). In the San Luis Obispo area (fig. 1), samples of the Monterey Formation from outcrops and wells are immature to marginally mature on the basis of Rock-Eval pyrolysis T_{max} values ranging from 410°–429°C (Frizzell and Claypool, 1983), and TAI results that correspond to vitrinite reflectance values of about 0.3-0.7 percent R_o (Surdam and Stanley, 1984). Kablanow and Surdam (1984) and Isaacs and Tomson (1990) reported additional pyrolysis results (using techniques other than Rock-Eval) indicating that the Monterey Formation is thermally immature in the San Luis Obispo and Santa Maria areas.

Higher levels of thermal maturity occur sporadically in the Santa Maria area in rocks older than Miocene. In the Santa Ynez Mountains and southern Coast Ranges (fig. 1), TAI results from 115 outcrop samples and 20 core samples show that Mesozoic and Paleogene rocks are thermally immature to mature with respect to the oil-generative window (Frederiksen, 1985). Also in the Santa Ynez Mountains, vitrinite reflectance values from 20 outcrop samples and 25 subsurface samples of Mesozoic and Paleogene rocks range from 0.23 to 2.44 percent R_o, or thermally immature to overmature with respect to the oil-generative window (Helmold, 1980; Helmold and van de Kamp, 1984). Frizzell and Claypool (1983) reported Rock-Eval pyrolysis results from 17 samples of Mesozoic and Paleogene strata in the San Luis Obispo and Cuyama River gorge areas (fig. 1); however, only two of these samples showed S2 peaks greater than 0.2 mg HC/g (Peters, 1986), and these samples had T_{max} values of 430°C and 444°C, or immature to marginally mature with respect to the oil-generative window (table 7). Howell and Claypool (1977) suggested, on the basis of pyrolysis data (technique of Claypool and Reed, 1976), that three mudstone samples from the Lower Cretaceous of the southern Coast Ranges had reached maximum paleotemperatures of 230–200°C, or overmature with respect to the oil-generative window; however, these estimates of paleotemperature may not be reliable because all three samples had low pyrolytic hydrocarbon yields (Howell and Claypool, 1977).

In summary, previous investigations have found that Neogene strata in the Santa Maria basin and surrounding region are thermally immature to marginally mature, whereas Mesozoic and Paleogene strata range from immature to overmature. Our vitrinite reflectance results (range 0.68–1.56 percent R_o, mean 1.29 percent R_o) and inferred paleotemperatures (range 106–192°C, mean 172°C) for the Lospe and Point Sal Formations in the North Beach section appear to include the highest values ever observed and reported from Neogene rocks in the Santa Maria area.

GEOLOGIC SIGNIFICANCE OF HIGH THERMAL MATURITIES AND PALEOTEMPERATURES

To better understand the possible geologic significance of the high thermal maturities and corresponding high paleotemperatures in the North Beach section, we compared our observed vitrinite reflectance values with those predicted by a commercial computer program, BasinMod™ version 2.95 (Platte River Associates, Inc., 1992). The BasinMod™ program constructs geological models of thermal maturity from stratigraphic and geothermal data provided by the user, and it relies on a variety of assumptions regarding physical parameters—such as compaction, thermal conductivity, heat capacity, and kinetics—that are built into the program.

We used BasinMod™ to construct three models that predict vitrinite reflectance versus stratigraphic position for the North Beach section (fig. 4). All three models incorporate data on lithology, thickness, age, and paleobathymetry from McCrory and others (1995, table A3). Present-day geothermal gradients in the Santa Maria basin are markedly variable from place to place and from formation to formation, but they are generally in the range of 45–60°C/km for the Foxen Mudstone and older units, and 20–40°C/km for the Careaga Sandstone and units younger than the Careaga (Williams and others,

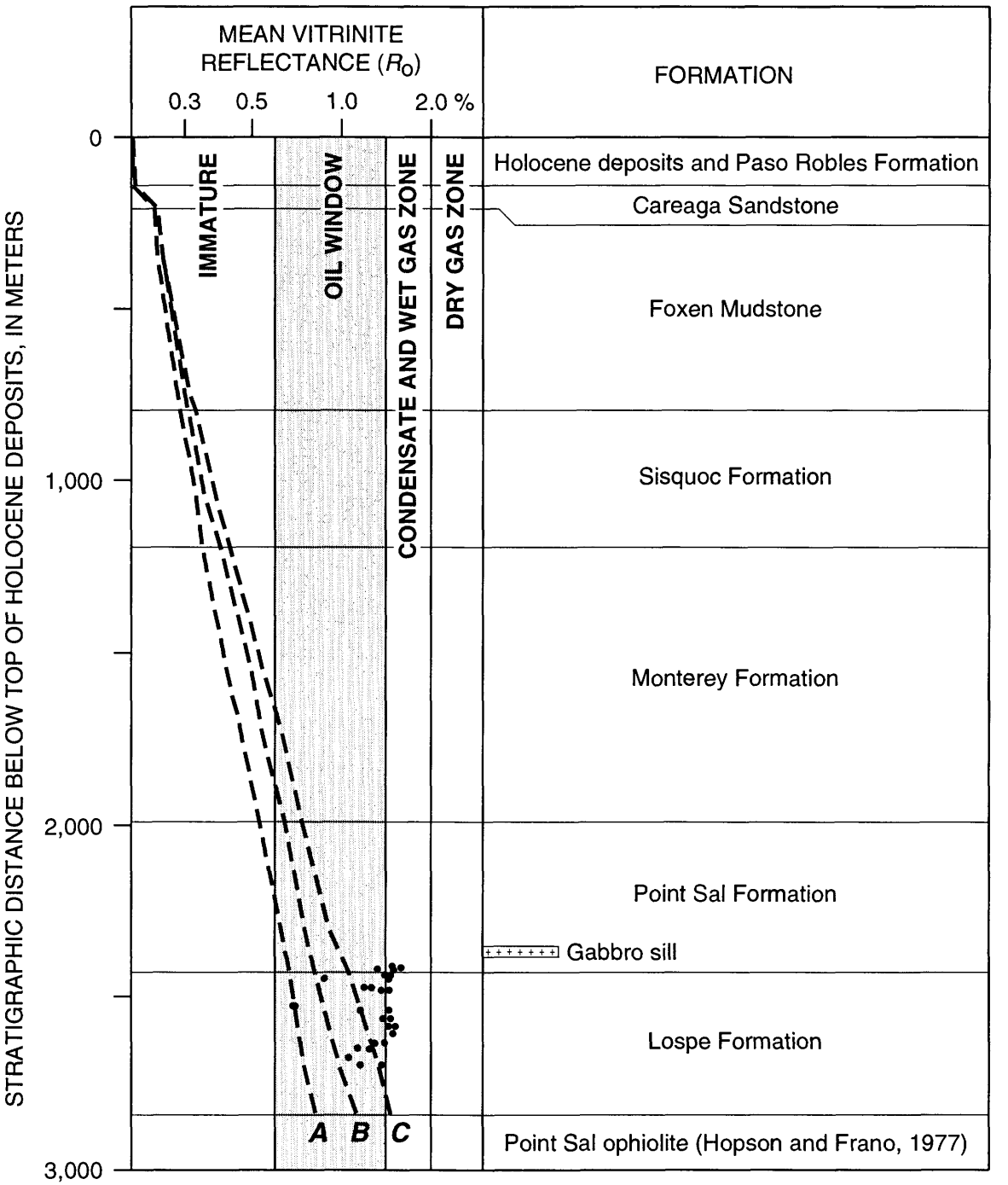

Figure 4. Values of vitrinite reflectance (on a logarithmic scale) calculated by BasinMod™ in the North Beach area (dashed lines), for three different sets of assumed geothermal gradients: *A*, 20°C/km for the Careaga Sandstone and younger units, and 45°C/km for the Foxen Mudstone and older units; *B*, 30°C/km for the Careaga Sandstone and younger units, and 52.5°C/km for the Foxen Mudstone and older units; and *C*, 40°C/km for the Careaga Sandstone and younger units, and 60°C/km for the Foxen Mudstone and older units. Compare the calculated values with actual observed values of vitrinite reflectance from table 3 (dots). See text for discussion.

1994, p. F6). The three predictive models in figure 4 were calculated by BasinMod™ from the minimum (curve *A*), mean (curve *B*), and maximum (curve *C*) geothermal gradients reported by Williams and others (1994).

Inspection of figure 4 shows that most of the observed values of vitrinite reflectance in the upper part of the Lospe Formation and in the Point Sal Formation are higher than predicted by BasinMod™ for even the maximum geothermal gradients. Furthermore, the observed values suggest an inverted thermal maturity profile (mentioned earlier in this report), which contrasts with BasinMod's prediction of a smooth increase in thermal maturity with depth (fig. 4). We suggest that the anomalously high observed values of vitrinite reflectance and the apparent inverted thermal maturity profile at North Beach resulted from a local heat source such as the gabbro sill in the lower part of the Point Sal Formation (fig. 2), or a zone of high-temperature hydrothermal waters in the lower part of the Point Sal Formation and upper part of the Lospe Formation. The temperatures and thermal effects presumably were greatest in the rocks immediately adjacent to the heat source and decreased with distance away from it, resulting in the apparent inverted thermal maturity profile. The observed and predicted values of vitrinite reflectance (assuming mean and maximum geothermal gradients) seem to converge about 250 m below the base of the gabbro sill (fig. 4). On the basis of this convergence, we suggest that the observed values of vitrinite reflectance in the middle of the Lospe Formation might reflect thermal maturation during burial with geothermal gradients similar to present-day ones.

Most basic magmas crystallize at temperatures of about 900–1,200°C (Macdonald, 1972; Hyndman, 1985). High levels of thermal maturity and unusual thermal maturity profiles in mudrocks and coals that have been invaded by hot igneous intrusions have been widely reported (Briggs, 1935; Dapples, 1939; Dutcher and others, 1966; Schopf and Long, 1966; Bostick, 1971; Dow, 1977; Peters and others, 1978, 1983; Simoneit and others, 1978, 1981; Dypvik, 1979; Perregaard and Schiener, 1979; Bostick and Pawlewicz, 1984; Clayton and Bostick, 1985; Niem and Niem, 1985). Igneous intrusions can cause a large increase in the vitrinite reflectance of the intruded rocks by providing high temperatures over short time ranges (Hunt, 1979). Reflectance values above 3 percent R_o are common in contact metamorphism but decrease with increasing distance away from the intrusive body (Dow, 1977; Peters and others, 1978, 1983; Hunt, 1979; Bostick and Pawlewicz, 1984; Clayton and Bostick, 1985). A traditional rule of thumb is that contact metamorphism affects the intruded rocks for a distance of about one to two times the thickness of the intrusive body (Dow, 1977; K.E. Peters, oral commun., 1992). The actual distance, however, depends on the size of the intrusive body, the temperature difference between the magma and the intruded rock, the rate of cooling, the depth at which the intrusive body was emplaced, the amount of volatiles emitted from the magma, the amount of pore water in the intruded rocks, and the thermal conductivity of the intruded rocks (Dow, 1977; Hunt, 1979, Simoneit and others, 1981; Peters and others, 1983).

In the North Beach section, the observed values of vitrinite reflectance differ significantly from the ones predicted by BasinMod™ for a distance of about 250 m below the gabbro sill (assuming maximum present day geothermal gradients, represented by curve C on fig. 4). This may mean that contact metamorphism extended as far as 250 m from the sill. However, the rule of thumb noted above predicts that the zone of contact metamorphism should extend only about 25–60 m from the sill, which is about 25–30 m thick. Perhaps the width of the apparent zone of contact metamorphism was enhanced by hot hydrothermal waters that either accompanied the gabbro intrusion or circulated during a separate event before or after the intrusion. Hot fluids may have found conduits along the ubiquitous faults and fractures in the area, and also along permeable horizons of sandstone within the Point Sal and Lospe Formations. Hydrocarbons may have been thermally generated in organic-rich strata of the Point Sal Formation and may have circulated with the hydrothermal waters. High-temperature hydrothermal systems associated with volcanism have been recognized in many parts of the world and are known to have resulted in geologically rapid thermal maturation of sedimentary strata over thicknesses of hundreds of meters (see, for example, Barker and Pawlewicz, 1990, and references therein; Summer and Verosub, 1992, and references therein).

It is possible that geothermal gradients in the Santa Maria basin were higher in the geologic past. Several tectonic and thermal models invoking subcrustal slabless windows, with asthenospheric upwelling resulting in high heat flow and high geothermal gradients, have been proposed for the Santa Maria area (Heasler and Surdam, 1983, 1985, 1989; Compton, 1991; Howie, 1991). It is also possible that higher temperatures could have been reached during deep burial beneath one or more thrust sheets during late Cenozoic compressional tectonism in the area, but we believe this is unlikely because available structural cross sections show that the Casmalia Hills (including the North Beach section) are on the structurally highest block in the Santa Maria basin (Woodring and Bramlette, 1950) and not in the lower plate beneath any recognized thrust fault. While tectonic models invoking higher ancient geothermal gradients or deeper burial may help explain some aspects of the high thermal maturity observed at North Beach, our analysis using BasinMod™ and modern geothermal gradients suggests that such models are not needed. Furthermore, the inverted thermal maturity profile found at North Beach can only be explained by a local thermal anomaly such as an igneous intrusion or hydrothermal system.

SUMMARY AND IMPLICATIONS FOR PETROLEUM EXPLORATION

Worldwide experience indicates that certain lakebed sediments can be prolific petroleum source rocks (Fouch and Dean,

1982; Powell, 1986; Katz, 1990). Nevertheless, results from Rock-Eval pyrolysis of a limited number of outcrop samples suggest that, at least locally, lacustrine and shallow-marine mudstones of the Lospe Formation contain too little organic matter (organic carbon generally less than 0.5 percent) to be potential source rocks of petroleum. In contrast to the Lospe, the amount of organic carbon in the Point Sal Formation ranges from about 1.5 to more than 3.5 percent (tables 2, 4). In the Monterey Formation, the principal source rock in the Santa Maria basin, organic carbon content averages about 5 percent and is as high as 23 percent in individual beds (Isaacs and Petersen, 1987). Kerogens in the Lospe are mainly gas-prone Type III and inert(?) Type IV. Monterey kerogens, however, are mostly oil-prone Type II and of mixed marine algal and terrestrial origin (Isaacs and Petersen, 1987; Isaacs, 1988).

The data set from the North Beach section is small and may not be representative of the Lospe Formation everywhere. It is possible that organic-rich mudstones occur in the Lospe elsewhere in the Santa Maria basin. Our preliminary conclusions can be tested by further investigations, including regional studies of subsurface cores and cuttings (rather than outcrop samples, which are susceptible to weathering); by using samples that are less thermally mature than those from the North Beach section; and by additional geochemical analyses such as hydrous pyrolysis (e.g., Lewan, 1985; Peters and others, 1990), and kerogen elemental composition (e.g. Tissot and Welte, 1984, and references therein).

Previous work by Lillis and King (1991) suggested two major periods of oil generation and migration in the Santa Maria basin: one during the late Miocene, in which low-gravity, high-sulfur oil was generated in the Monterey Formation and migrated into existing stratigraphic and structural traps; and a later episode in which high-gravity, low-sulfur oil generated at higher levels of thermal maturity moved into folds of Pliocene and Quaternary age. Our thermal maturity results from the North Beach section suggest the hypothesis that a third, earlier, and volumetrically less significant episode of oil generation (most likely in the Point Sal Formation) occurred locally near early to middle Miocene igneous intrusions and (or) hydrothermal systems.

Heat from igneous intrusions and high-temperature hydrothermal waters can cause thermal transformation of organic matter in petroleum source rocks near the intrusion, resulting in generation of oil and gas (Simoneit and others, 1978, 1981; Peters and others, 1983; Tissot and Welte, 1984; Kvenvolden and Simoneit, 1990). The exact time-temperature history of these processes is unknown, but one scenario suggests that petroleum can form by intense heating (at about 300–350°C) during periods as short as about 100 years (Kvenvolden and others, 1988; Simoneit and Kvenvolden, 1994). We suggest that at least some of the oil detected in our samples from the North Beach section could have been generated in organic-rich strata of the Point Sal Formation by heating during early or middle Miocene intrusion or hydrothermal activity. We further speculate that if similar intrusions or hydrothermal systems occur elsewhere in the Santa Maria basin, they may have caused generation of limited quantities of oil and gas in small areas. Subsequently, some of this petroleum may have accumulated in early-formed fault and stratigraphic traps (e.g., Namson and Davis, 1990; Lillis and King, 1991) in strata overlying the intrusions. Hydrocarbons may also have accumulated beneath thick, laterally extensive sills like the one near North Beach; such sills may have served not only as heat sources, but also as seals that trapped oil and gas generated in organic-rich shales of the Point Sal Formation.

Basic igneous dikes and sills of Miocene age have been recognized in outcrop along the fringes of the Santa Maria basin in the San Luis Obispo area (Hall, 1973; Hall and others, 1979), in the nearby southern Coast Ranges (Hall and Corbató, 1967; Hall, 1978b, 1981a, b; Vedder and others, 1988), and in the Santa Ynez Mountains (Robyn, 1980), but we know of no Miocene intrusions in the subsurface in the onshore Santa Maria basin. However, organic geochemical studies suggest that parts of the basin, including the Casmalia and Orcutt fields, may have experienced higher heat flow in the past (King and Lillis, 1990); the elevated heat flow may have resulted from crustal thinning and (or) emplacement of yet-unrecognized Miocene igneous intrusions or hydrothermal systems in the subsurface. Oil generated near such thermal anomalies might occur along the Santa Ynez River fault at the southern margin of the Santa Maria basin, where clockwise tectonic rotation of the Santa Ynez Mountains during the early and middle Miocene (Hornafius, 1985; Luyendyk, 1991) may have caused the creation of small triangular crustal gaps that were the sites of mantle upwelling (Cole and others, 1991b). These speculative ideas can be tested by further drilling, geophysical investigations, organic geochemical studies, and isotopic dating of intrusions.

REFERENCES CITED

Barker, C.E., 1988, Geothermics of petroleum systems: implications of the stabilization of kerogen thermal maturation after a geologically brief heating duration at peak temperatures, *in* Magoon, L.B., ed., Petroleum systems of the United States: U.S. Geological Survey Bulletin 1870, p. 26-29.

Barker, C.E., and Pawlewicz, M.J., 1986, The correlation of vitrinite reflectance with maximum temperature in humic organic matter, *in* Bunterbarth, G., and Stegena, L., eds., Paleogeothermics: Berlin, Springer-Verlag, Lecture Notes in Earth Sciences, v. 5, p. 79-93.

———1990, Vitrinite reflectance as an exploration tool in defining areas of recent and ancient heating: a case study of the Cerro Prieto geothermal system, Mexico, *in* Nuccio, V.F., and Barker, C.E., eds., Applications of thermal maturity studies to energy exploration: Denver, Colo., Rocky Mountain Section, Society of Economic Paleontologists and Mineralogists, p. 161-166.

———1994, Calculations of vitrinite reflectance from thermal histories and peak temperatures (Chapter 14), *in* Mukhopadhyay, P.K., and Dow, W.G., eds., Vitrinite reflectance as a maturity parameter—applications and limitations: Washington, D.C.,

American Chemical Society, p. 216-229.
Bartow, J.A., 1992, Paleogene and Neogene time scales for southern California: U.S. Geological Survey Open-File Report 92-212, 2 sheets.
Baskin, D.K., and Peters, K.E., 1992, Early generation characteristics of a sulfur-rich Monterey kerogen: American Association of Petroleum Geologists Bulletin, v. 76, no. 1, p. 1-13.
Bostick, N.H., 1971, Thermal alteration of clastic inorganic particles as an indicator of contact and burial metamorphism in sedimentary rocks: Geoscience and Man, v. 3, p. 83-92.
———1979, Vitrinite reflectance, *in* Cook, H.E., ed., Geologic studies of the Point Conception deep stratigraphic test well OCS-CAL 78-164 No. 1, outer continental shelf, southern California, United States: U.S. Geological Survey Open-File Report 79-218, p. 125-128.
Bostick, N.H., and Pawlewicz, M.J., 1984, Paleotemperatures based on vitrinite reflectance of shales and limestones in igneous dike aureoles in the Upper Cretaceous Pierre Shale, Walsenburg, Colorado, *in* Woodward, Jane, Meissner, F.F., and Clayton, J.L., eds., Hydrocarbon source rocks of the greater Rocky Mountain region: Denver, Colo., Rocky Mountain Association of Geologists, p. 387-392.
Briggs, Henry, 1935, Alteration of coal-seams in the vicinity of igneous intrusions, and associated problems: Transactions of the Institution of Mining Engineers, v. 89, pt. 4, p. 187-219.
California Division of Oil and Gas, 1991, California oil and gas fields, volume II, southern, central, and coastal California (3d ed.): Sacramento, Calif., California Department of Conservation, Publication TR12, 689 p.
———1993, 78th annual report of the State Oil and Gas Supervisor, 1992: Sacramento, Calif., California Department of Conservation, Publication PR06, 159 p.
Canfield, C.R., 1939, Subsurface stratigraphy of Santa Maria Valley oil field and adjacent parts of Santa Maria Valley, California: American Association of Petroleum Geologists Bulletin, v. 23, no. 1, p. 45-81.
Claypool, G.E., Baysinger, J.P., Lubeck, C.M., and Love, A.H., 1979, Organic geochemistry, *in* Cook, H.E., ed., Geologic studies of the Point Conception deep stratigraphic test well OCS-CAL 78-164 No. 1, outer continental shelf, southern California, United States: U.S. Geological Survey Open-File Report 79-218, p. 109-124.
Claypool, G.E., and Reed, P.R., 1976, Thermal-analysis technique for source-rock evaluation: quantitative estimate of organic richness and effects of lithologic variation: American Association of Petroleum Geologists Bulletin, v. 60, no. 4, p. 608-626.
Clayton, J.L., and Bostick, N.H., 1985, Temperature effects on kerogen and on molecular and isotopic composition of organic matter in Pierre Shale near an igneous dike: Organic Geochemistry, v. 10, nos. 1-3, p. 135-143.
Clayton, J.L., and Swetland, P.J., 1978, Subaerial weathering of sedimentary organic matter: Geochimica et Cosmochimica Acta, v. 42, no. 2, p. 305-312.
Clementz, D.M., Demaison, G.J., and Daly, A.R., 1979, Well site geochemistry by programmed pyrolysis: Proceedings, Eleventh Annual Offshore Technology Conference, v. 1, p. 465-470.
Cole, R.B., and Basu, A.R., 1995, Nd-Sr isotopic geochemistry and tectonics of ridge subduction and middle Cenozoic volcanism in western California: Geological Society of America Bulletin, v. 107, no. 2, p. 167-179.
Cole, R.B., and Stanley, R.G., 1994, Sedimentology and origin of subaqueous pyroclastic sediment gravity flows in the Neogene Santa Maria basin, California: Sedimentology, v. 41, p. 37-54.
Cole, R.B., Stanley, R.G., and Basu, A.R., 1991a, Stratigraphy and origin of lower Miocene volcanic rocks, onshore and offshore Santa Maria province, California [abs.]: Geological Society of America Abstracts with Programs, v. 23, no. 5, p. A476.
Cole, R.B., Stanley, R.G., and Johnson, S.Y., 1991b, Origin of tuff deposits in the lower Miocene Lospe Formation, Santa Maria basin, California [abs.]: American Association of Petroleum Geologists Bulletin, v. 75, no. 2, p. 359-360.
Compton, J.S., 1991, Porosity reduction and burial history of siliceous rocks from the Monterey and Sisquoc Formations, Point Pedernales area, California: Geological Society of America Bulletin, v. 103, no. 5, p. 625-636.
Crawford, F.D., 1971, Petroleum potential of Santa Maria province, California, *in* Cram, I.H., ed., Future petroleum provinces of the United States—their geology and potential: American Association of Petroleum Geologists Memoir 15, p. 316-328.
Dalrymple, G.B., 1979, Critical tables for conversion of K-Ar ages from old to new constants: Geology, v. 7, p. 558-560.
Daly, A.R., and Edman, J.D., 1987, Loss of organic carbon from source rocks during thermal maturation [abs.]: American Association of Petroleum Geologists Bulletin, v. 71, no. 5, p. 546.
Dapples, E.C., 1939, Coal metamorphism in the Anthracite-Crested Butte quadrangles, Colorado: Economic Geology, v. 34, no. 4, p. 369-398.
Dembicki, Harry, Jr., 1984, An interlaboratory comparison of source rock data: Geochimica et Cosmochimica Acta, v. 48, p. 2641-2649.
Dibblee, T.W., Jr., 1989, Geologic map of the Point Sal and Guadalupe quadrangles, Santa Barbara County, California: Santa Barbara, California, Dibblee Geological Foundation, scale 1:24,000.
Dow, W.G., 1977, Kerogen studies and geological interpretations: Journal of Geochemical Exploration, v. 7, p. 79-99.
Dryden, J.E., Erickson, R.C., Off, T., and Yost, S.W., 1968, Gas in Cenozoic rocks in Ventura-Santa Maria basins, California, *in* Beebe, B.W., ed., Natural gases of North America: American Association of Petroleum Geologists Memoir 9, v. 1, p. 135-148.
Dunham, J.B., Bromely, B.W., and Rosato, V.J., 1991, Geologic controls on hydrocarbon occurrence within the Santa Maria basin of western California, *in* Gluskoter, H.J., Rice, D.D., and Taylor, R.B., eds., Economic Geology, U.S.: Boulder, Colo., Geological Society of America, The Geology of North America, v. P-2, p. 431-446.
Dutcher, R.R., Campbell, D.L., and Thornton, C.P., 1966, Coal metamorphism and igneous intrusives in Colorado, *in* Given, P.H., ed., Coal science: American Chemical Society, Advances in Chemistry Series, v. 55, p. 708-723.
Dypvik, Henning, 1979, Major and minor element chemistry of Triassic black shales near a dolerite intrusion at Sassenfjorden, Spitsbergen: Chemical Geology, v. 25, p. 53-65.
Espitalié, J., Madec, M., Tissot, B., Mennig, J.J., and Leplat, P., 1977, Source rock characterization method for exploration: Proceedings, Ninth Annual Offshore Technology Conference, v. 3, p. 439-444.
Espitalié, J., Marquis, F., and Borsony, I., 1984, Geochemical logging, *in* Voorhees, K.J., ed., Analytical pyrolysis: London, Butterworth and Co., Ltd., p. 276-304.
Fairbanks, H.W., 1896, The geology of Point Sal: Berkeley, Calif.,

University of California, Bulletin of the Department of Geology, v. 2, no. 1, p. 1-92.

Fouch, T.D., and Dean, W.E., 1982, Lacustrine and associated clastic depositional environments, *in* Scholle, P.A., and Spearing, Darwin, eds., Sandstone depositional environments: American Association of Petroleum Geologists Memoir 31, p. 87-114.

Frederiksen, N.O., 1985, Map showing thermal-alteration indices in roadless areas and the Santa Lucia Wilderness in the Los Padres National Forest, southwestern California: U.S. Geological Survey Miscellaneous Field Studies Map MF-1655-F, scale 1:250,000.

Frizzell, V.A., Jr., and Claypool, G.E., 1983, Petroleum potential map of Mesozoic and Cenozoic rocks in roadless areas and the Santa Lucia Wilderness in the Los Padres National Forest, southwestern California: U.S. Geological Survey Miscellaneous Field Studies Map MF-1655-D, scale 1:250,000, 18 p.

Global Geochemistry Corporation, 1985, The geochemical and paleoenvironmental history of the Monterey Formation—sediments and hydrocarbons: Canoga Park, Calif., unpublished report, v. 1 (data synthesis and text), 459 p.

Hall, C.A., Jr., 1973, Geology of the Arroyo Grande 15-minute quadrangle, San Luis Obispo county, California: California Division of Mines and Geology Map Sheet 24, scale 1:48,000.

———1978a, Origin and development of the Lompoc-Santa Maria pull-apart basin and its relation to the San Simeon-Hosgri strike-slip fault, western California, *in* Silver, E.A., and Normark, W.R., eds., San Gregorio-Hosgri fault zone, California: California Division of Mines and Geology Special Report 137, p. 25-31.

———1978b, Geologic map of Twitchell Dam and parts of Santa Maria and Tepusquet Canyon quadrangles, Santa Barbara county, California: U.S. Geological Survey Miscellaneous Field Studies Map MF-963, 2 sheets, scale 1:24,000.

———1981a, San Luis Obispo transform fault and middle Miocene rotation of the western Transverse Ranges, California: Journal of Geophysical Research, v. 86, no. B2, p. 1015-1031.

———1981b, Map of geology along the Little Pine fault, parts of the Sisquoc, Foxen Canyon, Zaca Lake, Bald Mountain, Los Olivos, and Figueroa Mountain quadrangles, Santa Barbara County, California: U.S. Geological Survey Miscellaneous Field Studies Map MF-1285, two sheets, scale 1:24,000.

———1982, Pre-Monterey subcrop and structure contour maps, western San Luis Obispo and Santa Barbara Counties, south-central California: U.S. Geological Survey Miscellaneous Field Studies Map MF-1384, six sheets, scale 1:62,500.

Hall, C.A., Jr., and Corbató, C.E., 1967, Stratigraphy and structure of Mesozoic and Cenozoic rocks, Nipomo quadrangle, southern Coast Ranges, California: Geological Society of America Bulletin, v. 78, p. 559-582.

Hall, C.A., Jr., Ernst, W.G., Prior, S.W., and Wiese, J.W., 1979, Geologic map of the San Luis Obispo-San Simeon region, California: U.S. Geological Survey Miscellaneous Investigations Series Map I-1097, 3 sheets, scale 1:48,000.

Hall, C.A., Jr., Turner, D.L., and Surdam, R.C., 1966, Potassium-argon age of the Obispo Formation with *Pecten lompocensis* Arnold, southern Coast Ranges, California: Geological Society of America Bulletin, v. 77, p. 443-446.

Heasler, H.P., and Surdam, R.C., 1983, A thermally-subsiding basin model for the maturation of hydrocarbons in the Pismo basin, California, *in* Isaacs, C.M., and Garrison, R.E., eds., Petroleum generation and occurrence in the Miocene Monterey Formation, California: Los Angeles, Calif., Society of Economic Paleontologists and Mineralogists, Pacific Section, p. 69-74.

———1985, Thermal evolution of coastal California with application to hydrocarbon maturation: American Association of Petroleum Geologists Bulletin, v. 69, no. 9, p. 1386-1400.

———1989, Thermal and hydrocarbon maturation modeling of the Pismo and Santa Maria basins, coastal California, *in* Naeser, N.D., and McCulloh, T.H., eds., Thermal history of sedimentary basins: methods and case histories: New York, Springer-Verlag, p. 297-309.

Helmold, K.P., 1980, Diagenesis of Tertiary arkoses, Santa Ynez Mountains, California: Stanford, Calif., Stanford University, Ph.D. dissertation, 225 p.

Helmold, K.P., and van de Kamp, P.C., 1984, Diagenetic mineralogy and controls on albitization and laumontite formation in Paleogene arkoses, Santa Ynez Mountains, California, *in* McDonald, D.A., and Surdam, R.C., eds., Clastic diagenesis: American Association of Petroleum Geologists Memoir 37, p. 239-276.

Hopson, C.A., and Frano, C.J., 1977, Igneous history of the Point Sal ophiolite, southern California, *in* Coleman, R.G., and Irwin, W.P., eds., North American ophiolites: Oregon Department of Geology and Mineral Industries Bulletin 95, p. 161-183.

Hornafius, J.S., 1985, Neogene tectonic rotation of the Santa Ynez Range, western Transverse Ranges, California, suggested by paleomagnetic investigation of the Monterey Formation: Journal of Geophysical Research, v. 90, no. B14, p. 12,503-12,522.

Howell, D.G., and Claypool, G.E., 1977, Reconnaissance petroleum potential of Mesozoic rocks, Coast Ranges, central California, *in* Howell, D.G., Vedder, J.G., and McDougall, K.A., eds., Cretaceous geology of the California Coast Ranges, west of the San Andreas fault: Los Angeles, Calif., Society of Economic Paleontologists and Mineralogists, Pacific Section, Pacific Coast Paleogeography Field Trip Guide 2, p. 85-90.

Howie, J.M., 1991, Time-transgressive evolution of the Pacific-North American transform plate boundary in central California: constraints from crustal structure, chap. 3 *of* Howie, J.M., Seismic studies of crustal structure and tectonic evolution across the central California margin and the Colorado Plateau margin: Stanford, Calif., Stanford University, Ph.D. dissertation, p. 113-165.

Huffman, E.W.D., Jr., 1977, Performance of a new automatic carbon dioxide coulometer: Microchemical Journal, v. 25, p. 567-573.

Hunt, J.M., 1979, Petroleum geochemistry and geology: San Francisco, W.H. Freeman, 617 p.

Hyndman, D.W., 1985, Petrology of igneous and metamorphic rocks (3d ed.): New York, McGraw-Hill, 786 p.

Isaacs, C.M., 1987, Sources and deposition of organic matter in the Monterey Formation, south-central coastal basins of California, *in* Meyer, R.F., ed., Exploration for heavy crude oil and natural bitumen: American Association of Petroleum Geologists Studies in Geology, v. 25, p. 193-205.

———1988, Marine petroleum source rocks and reservoir rocks of the Miocene Monterey Formation, California, U.S.A., *in* Wagner, H.C., Wagner, L.C., Wang, F.F.H., and Wong, F.L., eds., Petroleum resources of China and related subjects: Houston, Tex., Circum-Pacific Council for Energy and Mineral Resources Earth Science Series, v. 10, p. 825-848.

Isaacs, C.M., and Magoon, L.B., 1984, Thermal indicators of organic matter in the Sisquoc and Monterey Formations, Santa Maria basin, California [abs.]: Abstracts, Annual Midyear Meeting, San Jose, Calif., August 10-13, 1984, Society of Economic Paleon-

tologists and Mineralogists, Pacific Section, p. 40.
Isaacs, C.M., and Petersen, N.F., 1987, Petroleum in the Miocene Monterey Formation, California, *in* Hein, J.R., ed., Siliceous sedimentary rock-hosted ores and petroleum: New York, Van Nostrand Reinhold, p. 83-116.
Isaacs, C.M., and Tomson, J.H., 1990, Reconnaissance study of petroleum source-rock characteristics of core samples from the Sisquoc and Monterey Formations in a north-south subsurface transect across the onshore Santa Maria basin and in surface sections along the Santa Barbara-Ventura coast, southern California: U.S. Geological Survey Open-File Report 89-108, 43 p.
Jackson, L.L., Brown, F.W., and Neil, S.T., 1987, Major and minor elements requiring individual determination, classical whole rock analysis, and rapid rock analysis: U.S. Geological Survey Bulletin 1770-G, p. G1-G23.
Johnson, S.Y., and Stanley, R.G., 1994, Sedimentology of the conglomeratic lower member of the Lospe Formation (lower Miocene), Santa Maria basin, California: U.S. Geological Survey Bulletin 1995-D, p. D1-D21.
Kablanow, R.I., III, and Surdam, R.C., 1984, Diagenesis and hydrocarbon generation in the Monterey Formation, Huasna basin, California, *in* Surdam, R.C., ed., A guidebook to the stratigraphic, tectonic, thermal, and diagenetic histories of the Monterey Formation, Pismo and Huasna basins, California: Society of Economic Paleontologists and Mineralogists, Guidebook No. 2, p. 53-68.
Katz, B.J., 1983, Limitations of Rock-Eval pyrolysis for typing organic matter: Organic Geochemistry, v. 4, no. 3/4, p. 195-199.
———ed., 1990, Lacustrine basin exploration—case studies and modern analogs: American Association of Petroleum Geologists Memoir 50, 340 p.
Keller, M.A., 1984, Silica diagenesis and lithostratigraphy of the Miocene Monterey Formation of the northwestern Ventura basin, California, including biostratigraphy, pyrolysis results, chemical analyses, and a preliminary temperature zonation of the opal-CT zone: U.S. Geological Survey Open-File Report 84-368, 79 p.
King, J.D., and Lillis, P.G., 1990, Thermal modeling using biomarkers in the Santa Maria basin, California [abs.]: American Association of Petroleum Geologists Bulletin, v. 74, no. 5, p. 695.
Kleinpell, R.M., 1938, Miocene stratigraphy of California: Tulsa, Okla., American Association of Petroleum Geologists, 450 p.
———1980, The Miocene stratigraphy of California revisited: Tulsa, Okla., American Association of Petroleum Geologists Studies in Geology No. 11, p. 1-53.
Kvenvolden, K.A., Rapp, J.B., Hostettler, F.D., King, J.D., and Claypool, G.E., 1988, Organic geothermometry of petroleum from Escanaba Trough, offshore northern California: Organic Geochemistry, v. 13, nos. 1-3, p. 351-355.
Kvenvolden, K.A., and Simoneit, B.R.T., 1990, Hydrothermally derived petroleum: examples from Guaymas basin, Gulf of California, and Escanaba Trough, northeast Pacific Ocean: American Association of Petroleum Geologists Bulletin, v. 74, no. 3, p. 223-237.
Laughland, M.M., Underwood, M.B., and Wiley, T.J., 1990, Thermal maturity, tectonostratigraphic terranes, and regional tectonic history: an example from the Kandik area, east-central Alaska, *in* Nuccio, V.F., and Barker, C.E., eds., Applications of thermal maturity studies to energy exploration: Denver, Colo., Rocky Mountain Section, Society of Economic Paleontologists and Mineralogists, p. 97-111.
Lewan, M.D., 1985, Evaluation of petroleum generation by hydrous pyrolysis experimentation: Philosophical Transactions, Royal Society of London, series A, v. 315, p. 123-134.
Leythaeuser, Detlev, 1973, Effects of weathering on organic matter in shales: Geochimica et Cosmochimica Acta, v. 37, no. 1, p. 113-120.
Lillis, P.G., and King, J.D., 1991, Controls on the variation of crude oil quality, Santa Maria basin, California [abs.]: American Association of Petroleum Geologists Bulletin, v. 75, no. 2, p. 372.
Luyendyk, B.P., 1991, A model for Neogene crustal rotations, transtension, and transpression in southern California: Geological Society of America Bulletin, v. 103, no. 11, p. 1528-1536.
Macdonald, G.A., 1972, Volcanoes: Englewood Cliffs, N.J., Prentice-Hall, Inc., 510 p.
McCrory, P.A., Ingle, J.C., Jr., Wilson, D.S., and Stanley, R.G., 1995, Neogene geohistory analysis of Santa Maria basin, California, and its relationship to transfer of central California to the Pacific plate: U.S. Geological Survey Bulletin 1995-J, p. J1-J38.
McCulloh, T.H., 1979, Implications for petroleum appraisal, *in* Cook, H.E., ed., Geologic studies of the Point Conception deep stratigraphic test well OCS-CAL 78-164 No. 1, outer continental shelf, southern California, United States: U.S. Geological Survey Open-File Report 79-218, p. 26-42.
McLean, Hugh, 1991, Distribution and juxtaposition of Mesozoic lithotectonic elements in the basement of the Santa Maria basin, California: U.S. Geological Survey Bulletin 1995-B, p. B1-B12.
McLean, Hugh, and Stanley, R.G., 1994, Provenance of sandstone clasts in the lower Miocene Lospe Formation near Point Sal, California: U.S. Geological Survey Bulletin 1995-E, p. E1-E7.
Namson, Jay, and Davis, T.L., 1990, Late Cenozoic fold and thrust belt of the southern Coast Ranges and Santa Maria basin, California: American Association of Petroleum Geologists Bulletin, v. 74, no. 4, p. 467-492.
Niem, A.R., and Niem, W.A., 1985, Oil and gas investigation of the Astoria basin, Clatsop and northernmost Tillamook counties, northwest Oregon: Oregon Department of Geology and Mineral Industries, Oil and Gas Investigation OGI-14, scale 1:100,000, 8 p.
Orr, W.L., 1984, Sulfur and sulfur isotope ratios in Monterey oils of the Santa Maria basin and Santa Barbara Channel area [abs.]: Abstracts, Annual Midyear Meeting, San Jose, Calif., August 10-13, 1984, Society of Economic Paleontologists and Mineralogists, Pacific Section, p. 62.
Perregaard, J., and Schiener, E.J., 1979, Thermal alteration of sedimentary organic matter by a basalt intrusive (Kimmeridgian shales, Milne Land, East Greenland): Chemical Geology, v. 26, p. 331-343.
Peters, K.E., 1986, Guidelines for evaluating petroleum source rock using programmed pyrolysis: American Association of Petroleum Geologists Bulletin, v. 70, no. 3, p. 318-329.
Peters, K.E., Moldowan, J.M., and Sundaraman, P., 1990, Effects of hydrous pyrolysis on biomarker thermal maturity parameters: Monterey phosphatic and siliceous members: Organic Geochemistry, v. 15, no. 3, p. 249-265.
Peters, K.E., Simoneit, B.R.T., Brenner, Shmuel, and Kaplan, I.R., 1978, Vitrinite reflectance-temperature determinations for intruded Cretaceous black shale in the eastern Atlantic, *in* Oltz, D.F., ed., Low temperature metamorphism of kerogen and clay minerals: Los Angeles, Calif., Society of Economic Paleontolo-

gists and Mineralogists, Pacific Section, p. 53-58.
Peters, K.E., Whelan, J.K., Hunt, J.M., and Tarafa, M.E., 1983, Programmed pyrolysis of organic matter from thermally altered Cretaceous black shales: American Association of Petroleum Geologists Bulletin, v. 67, no. 11, p. 2137-2146.
Petersen, N.F., and Hickey, P.J., 1987, California Plio-Miocene oils: evidence of early generation, *in* Meyer, R.F., ed., Exploration for heavy crude oil and natural bitumen: American Association of Petroleum Geologists Studies in Geology, v. 25, p. 351-359.
Platte River Associates, Inc., 1992, BasinMod™, a modular basin modeling system, version 2.95: Available from Platte River Associates, Inc., 2000 West 120th Avenue, Suite 10, Denver, Colo. 80234.
Pollastro, R.M., 1990, Geothermometry from smectite and silica diagenesis in the diatomaceous Monterey and Sisquoc Formations, Santa Maria basin, California [abs.]: American Association of Petroleum Geologists Bulletin, v. 74, no. 5, p. 742.
Powell, T.G., 1986, Petroleum geochemistry and depositional setting of lacustrine source rocks: Marine and Petroleum Geology, v. 3, no. 3, p. 200-219.
Pytte, M.H., 1989, Organic geochemistry of the Miocene Monterey and equivalent formations in five California basins, *in* MacKinnon, T.C., ed., Oil in the California Monterey Formation: American Geophysical Union Field Trip Guidebook T311, p. 11-27.
Redwine, L. E., 1981, Hypothesis combining dilation, natural hydraulic fracturing, and dolomitization to explain petroleum reservoirs in Monterey Shale, Santa Maria area, California, *in* Garrison, R.E., and Douglas, R.O., eds., The Monterey Formation and related siliceous rocks of California: Los Angeles, Calif., Society of Economic Paleontologists and Mineralogists, Pacific Section, p. 221-248.
Robyn, E.S., 1980, A description of the Miocene Tranquillon volcanics and a comparison with the Miocene Obispo tuff: Santa Barbara, Calif., University of California, M.A. thesis, 110 p.
Roehl, P.O., 1981, Dilation brecciation—a proposed mechanism of fracturing, petroleum expulsion, and dolomitization in the Monterey Formation, California, *in* Garrison, R.E., and Douglas, R.O., eds., The Monterey Formation and related siliceous rocks of California: Los Angeles, Calif., Society of Economic Paleontologists and Mineralogists, Pacific Section, p. 285-315.
Schopf, J.M., and Long, W.E., 1966, Coal metamorphism and igneous associations in Antarctica, *in* Given, P.H., ed., Coal science: American Chemical Society, Advances in Chemistry Series, v. 55, p. 156-195.
Simoneit, B.R.T., Brenner, Shmuel, Peters, K.E., and Kaplan, I.R., 1978, Thermal alteration of Cretaceous black shale by basaltic intrusions in the eastern Atlantic: Nature, v. 273, no. 5663, p. 501-504.
———1981, Thermal alteration of Cretaceous black shale by basaltic intrusions in the eastern Atlantic—II: effects on bitumen and kerogen: Geochimica et Cosmochimica Acta, v. 45, p. 1581-1602.
Simoneit, B.R.T., and Kvenvolden, K.A., 1994, Comparison of ^{14}C ages of hydrothermal petroleums: Organic Geochemistry, v. 21, no. 5, p. 525-529.
Stanley, R.G., 1987, Effects of weathering on petroleum-source evaluation of coals from the Suntrana Formation near Healy, Alaska, *in* Hamilton, T.D., and Galloway, J.P., eds., Geologic studies in Alaska by the U.S. Geological Survey during 1986: U.S. Geological Survey Circular 998, p. 99-103.
Stanley, R.G., Johnson, S.Y., Cole, R.B., Mason, M.A., Swisher, C.C., III, Cotton Thornton, M.L., Filewicz, M.V., Vork, D.R., Tuttle, M.L., and Obradovich, J.D., 1992a, Origin of the Santa Maria basin, California [abs.], *in* Carter, L.M.H., ed., USGS Research on Energy Resources—1992 Program and Abstracts, Eighth V.E. McKelvey Forum on Mineral and Energy Resources: U.S. Geological Survey Circular 1074, p. 73.
Stanley, R.G., Johnson, S.Y., Obradovich, J.D., Tuttle, M.L., Cotton Thornton, M.L., Vork, D.R., Filewicz, M.V., Mason, M.A., and Swisher, C.C., III, 1990, Age, facies, and depositional environments of the lower Miocene Lospe Formation, Santa Maria basin, central California [abs.], *in* Carter, L.M.H., ed., USGS Research on Energy Resources—1990 Program and Abstracts, Sixth V.E. McKelvey Forum on Mineral and Energy Resources: U.S. Geological Survey Circular 1060, p. 78-79.
Stanley, R.G., Johnson, S.Y., Tuttle, M.L., Mason, M.A., Swisher, C.C., III, Cotton Thornton, M.L., Vork, D.R., Filewicz, M.V., Cole, R.B., and Obradovich, J.D., 1991, Age, correlation, and origin of the type Lospe Formation (lower Miocene), Santa Maria basin, central California [abs.]: American Association of Petroleum Geologists Bulletin, v. 75, no. 2, p. 382.
Stanley, R.G., Valin, Z.C., and Pawlewicz, M.J., 1992b, Rock-Eval pyrolysis and vitrinite reflectance results from outcrop samples of the Rincon Shale (lower Miocene) collected at the Tajiguas Landfill, Santa Barbara County, California: U.S. Geological Survey Open-File Report 92-571, 27 p.
———1993, Rock-Eval pyrolysis and vitrinite reflectance results from lower Miocene strata in the onshore Santa Maria basin and Santa Barbara coastal area, California [abs.]: American Association of Petroleum Geologists Bulletin, v. 77, no. 4, p. 716-717.
Summer, N.S., and Verosub, K.L., 1992, Diagenesis and organic maturation of sedimentary rocks under volcanic strata, Oregon: American Association of Petroleum Geologists Bulletin, v. 76, no. 8, p. 1190-1199.
Surdam, R.C., and Stanley, K.O., 1984, Diagenesis and migration of hydrocarbons in the Monterey Formation, Pismo syncline, California, *in* Surdam, R.C., ed., A guidebook to the stratigraphic, tectonic, thermal, and diagenetic histories of the Monterey Formation, Pismo and Huasna basin, California: Society of Economic Paleontologists and Mineralogists, Guidebook No. 2, p. 84-94.
Sylvester, A.G., and Darrow, A.C., 1979, Structure and neotectonics of the western Santa Ynez fault system in southern California: Tectonophysics, v. 52, p. 389-405.
Taylor, J.C., 1976, Geologic appraisal of the petroleum potential of offshore southern California: the borderland compared to onshore coastal basins: U.S. Geological Survey Circular 730, 43 p.
Tissot, B.P., and Welte, D.H., 1984, Petroleum formation and occurrence (2d ed.): Berlin, Springer-Verlag, 699 p.
Tolman, C.F., 1927, Biogenesis of hydrocarbons by diatoms: Economic Geology, v. 22, no. 5, p. 454-474.
Turner, D.L., 1970, Potassium-argon dating of Pacific coast Miocene foraminiferal stages, *in* Bandy, O.L., ed., Radiometric dating and paleontologic zonation: Geological Society of America Special Paper 124, p. 91-129.
Vedder, J.G., Howell, D.G., McLean, Hugh, and Wiley, T.J., 1988, Geologic map of Los Machos Hills and Caldwell Mesa quadrangles and part of Tar Spring Ridge quadrangle, California: U.S. Geological Survey Open-File Report 88-253, scale 1:24,000.
Waples, D.W., 1985, Geochemistry in petroleum exploration:

Boston, International Human Resources Development Corporation, 232 p.

Williams, C.F., Galanis, S.P., Jr., Grubb, F.V., and Moses, T.H., Jr., 1994, The thermal regime of Santa Maria province, California: U.S. Geological Survey Bulletin 1995-F, p. F1-F25.

Wissler, S.G., and Dreyer, F.E., 1943, Correlation of the oil fields of the Santa Maria district, *in* Jenkins, O.P., ed., Geologic formations and economic development of the oil and gas fields of California: California Division of Mines Bulletin 118, p. 235-238.

Woodring, W.P., and Bramlette, M.N, 1950, Geology and paleontology of the Santa Maria district, California: U.S. Geological Survey Professional Paper 222, 185 p.

Woodring, W.P., Bramlette, M.N., and Lohman, K.E., 1943, Stratigraphy and paleontology of Santa Maria district, California: American Association of Petroleum Geologists Bulletin, v. 27, no. 10, p. 1335-1360.

Chapter O

Obispo Formation, California: Remobilized Pyroclastic Material

By JEAN-LUC SCHNEIDER and RICHARD V. FISHER

U.S. GEOLOGICAL SURVEY BULLETIN 1995–O

EVOLUTION OF SEDIMENTARY BASINS/ONSHORE OIL AND GAS INVESTIGATIONS—
SANTA MARIA PROVINCE

Edited by Margaret A. Keller

CONTENTS

FIGURES

Obispo Formation, California: Remobilized Pyroclastic Material

By Jean-Luc Schneider[1] *and* Richard V. Fisher[2]

Abstract

The Miocene Obispo Formation, exposed along the south-central coast of California, consists of subaqueously deposited mafic lava flows, rhyodacitic welded tuff, and sedimentary materials composed of reworked rhyodacitic pyroclastic debris (white tuff), some basaltic hyaloclastic debris, epiclastic volcanic beds and background pelagic sediments. The volcaniclastic sedimentary rocks were deposited as pelagic fallout and by sediment gravity flows (debris flows, turbidites) emplaced by easterly moving currents that moved from higher sources into basins with water depths ranging from shallow intertidal to bathyal. There is evidence of abundant water within the depositional environment but no direct evidence that volcanism took place under the water. The volume of the white tuff facies of the Obispo Formation is estimated to be from 250 to 450 km^3, which indicates a caldera source. Sedimentary current-direction indicators in remobilized white tuff facies of the Obispo Formation and flow directions from measurements of the anisotropy of magnetic susceptibility in the welded tuff facies of the Obispo Formation indicate that the source volcano was located westerly, offshore of the present-day coastline. Dikes, flows, and sills are sparsely located throughout the mapped area in the Obispo Formation. The mapped area was perhaps on the flanks of the ancient volcano, but the caldera that produced the abundant white tuff of the Obispo Formation has not been located.

INTRODUCTION

The Obispo Formation (fig. 1), consisting of volcaniclastic rocks and lava flows, exists within a 140- to 200-km northwest-southeast-trending belt of lower middle Miocene volcanic rocks in the Coast Ranges of southern California (Hall, 1981b). This region has been mapped by Hall and colleagues (Hall and Corbato, 1967; Hall, 1973a,b, 1974, 1976, 1978, 1981a; Hall and Prior, 1975; Hall and others, 1979). The formation is dated at 16.5–15.3 Ma (Turner, 1970) and includes a sparse marine fauna indicating a Saucesian to Relizian age (Hall and others, 1966; Lipps, 1967). The cited papers discuss the stratigraphic relationships of the volcanic facies in detail. Here, we mainly focus upon the pyroclastic facies of the Obispo Formation exposed at Twitchell Dam, Nipomo, Shell Beach, and a locality along the frontage road of U.S. Highway 101. We also briefly discuss basaltic lavas and intrusive rocks.

The terminology of volcaniclastic rocks used in this report is from Fisher (1961, 1966). The term "volcaniclastic" is defined to include the entire spectrum of clastic materials composed in part or entirely of volcanic fragments, formed by any particle-forming mechanism (e.g., pyroclastic, hydroclastic, epiclastic, autoclastic), transported by any mechanism, deposited in any physiographic environment, or mixed with any other volcaniclastic type or with any nonvolcanic fragment types in any proportion (Fisher, 1966).

Important types of volcaniclastic particles are pyroclastic, hydroclastic, autoclastic, alloclastic, and epiclastic. *Pyroclasts* form from rapidly expanding magma that loses cohesion and breaks into bits when overburden pressures are exceeded. Magmatic expansion creates pumice that commonly breaks into glass shards from broken vesicles. Phenocrysts are commonly released from the magma with some adhering glass, and explosions may cause breakage and incorporation of lithic fragments from vent walls. *Hydroclasts* form by magma-water interactions that produce chilled glass particles by either explosive or nonexplosive means. Thermal contraction of magma or hot lava in water leads to the formation of shattered angular, poorly vesiculated shards. *Autoclastic* fragments form by mechanical friction of moving lava flows or by gravity crumbling of spines and domes. *Alloclastic* fragments form by disruption of preexisting volcanic rocks by igneous processes beneath the Earth's surface, with or without intrusion of fresh magma. All of the above clastic types

[1]Département des Sciences de la Terre, Laboratoire de Pétrologie, U.R.A.-C.N.R.S. 719, Université des Sciences et Technologies de Lille, 59655 Villeneuve d'Ascq cedex, France.

[2]Department of Geological Sciences, University of California, Santa Barbara, California 93106.

may be reworked by water, wind, or other dispersal agents andthen are termed "reworked pyroclastic," "reworked hydroclastic," etc.

Epiclastic particles are lithic clasts and crystals derived from any type of preexisting rock by weathering and erosion. If the preexisting rocks are volcanic, the epiclasts are considered to be one type of volcaniclastic particle. Pyroclastic and hydroclastic particles reworked by rivers, wind, or other types of transporting agents are not epiclastic because they are not formed by weathering.

Conceptual confusion about the origin of volcaniclastic particles and contemporeneity of deposition is minimized if processes that create the particles (e.g., pyroclastic, hydroclastic, epiclastic) are clearly separated from processes that transport the particles (e.g., wind, running water, ice, volcanic explosion, and gravity transfer by avalanche). Some authors contend that pyroclastic or hydroclastic particles reworked by water or other geomorphic agents can be called epiclastic deposits, but the terms "epiclastic," " pyroclastic," and "hydroclastic" refer to the way that particles are formed, not to how they are transported or deposited. The particles cannot be changed from one particle type to another by merely changing the agent of transportation. The distinction is critical to understanding differences in sedimentation in volcanic and nonvolcanic areas and in determining facies associations. Most nonvolcanic siliciclastic sediments are epiclastic and are, therefore, to varying degrees supply limited depending upon rates of weathering and erosion in the source area. Many volcaniclastic fragments are generated instantaneously and in large volumes, producing unique facies distributions and geometries not encountered in nonvolcanic epiclastic sediments (Fisher and Smith, 1991).

Another nomenclatural problem relevant to this paper concerns pyroclastic flows and ignimbrite. Pyroclastic flows are sediment gravity flows that are hot, gas-particle, density currents that originate from disruption of magma and enter the atmosphere by eruption through vents to become part of the sedimentological domain of the Earth's surface. Clastic components are crystals, glass shards and pumice, and lithic fragments in highly variable proportions depending upon (1) the composition of the magma, (2) the country rock through which the material rises, and (3) the ability of the currents to erode the surface over which they flow. Xenoliths may form the bulk of the lithic fragments.

There are two end-member kinds of deposits (Fisher and Schmincke, 1984, 1994): (1) pyroclastic flow deposits that

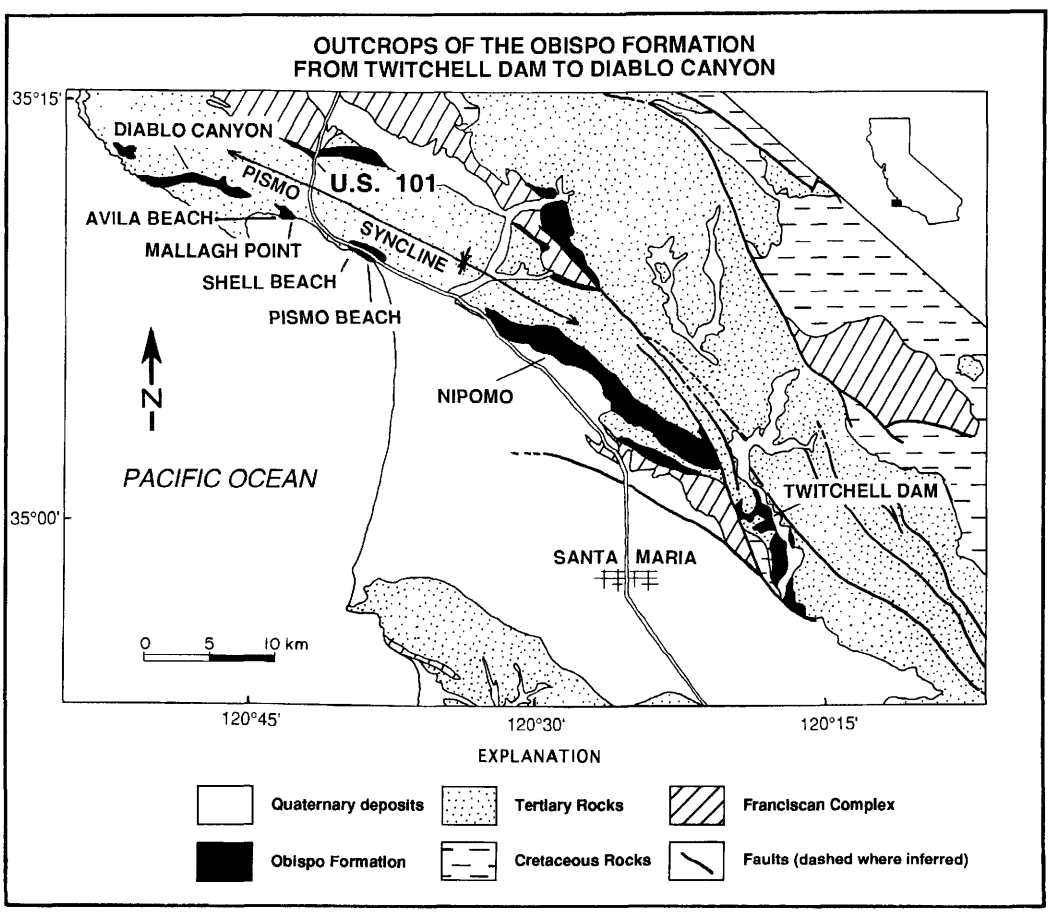

Figure 1. Outcrops of the Obispo Formation from Twitchell Dam to Diablo Canyon.

are relatively thick, poorly sorted, commonly but not invariably containing abundant fine-grained ash in the matrix (<1/16 mm; >4 ϕ), and with crude or no internal bedding; and (2) pyroclastic surge deposits that are relatively thin, better sorted than flow deposits, with or without abundant matrix fines, and well bedded to cross bedded. Surge deposits may occur beneath or on top of pyroclastic flow deposits, or by themselves.

Pyroclastic flow deposits rich in pumice and glass shards are known as ignimbrite. Depending upon emplacement temperature, ignimbrites range from unconsolidated, to cemented by vapor-phase minerals, to welded ignimbrites (welded tuff).

Most known examples of subaqueous pyroclastic flow deposits are marine (Fisher and Schmincke, 1984). Internal textures and structures are used to interpret the origins of these deposits as pyroclastic flows, but in ancient deposits, sedimentological or paleontological evidence is needed from associated sediments to determine unequivocal subaqueous deposition.

ACKNOWLEDGMENTS

This work has been supported by grants to J.L.S. by French Ministère des Affaires Etrangères (bourse "Lavoisier") and by the Leonora Lindsley Memorialship (Institute of International Education, New York City). Many thanks to Michael Fuller and Bob Dunn for assistance during paleomagnetic measurements at the University of California, Santa Barbara. We acknowledge Mrs. Powers, Mr. Dana, Mr. Dowells, and Mr. Cooper for authorizations to visit outcrops in their properties in Nipomo; Pacific Gas and Electric Company (P.G. & E.) for permission to work in the area of the Diablo Canyon nuclear facility; and Mr. Robert Marr for permission to do field work on his property. Thanks also go to Mr. Madonna for permission to do field work on his property near San Luis Obispo. Reviews by Earl Brabb, Donald Peterson, and Wes Hildreth are appreciated. The support and advice of Margaret Keller has been indispensable.

STRATIGRAPHY AND LITHOLOGY

The presence of large volumes of white tuff in the region displayed in figure 1 has long been recognized (Fairbanks, 1904). Bramlette (1946) named these rocks the Obispo Tuff Member of the Monterey Formation. The unit was elevated to formational rank by Hall and others (1966). The Obispo Formation is composed of 400 to 1,300 m of white tuff (an estimated 25 to 50 percent of the formation), mafic lava flows and related hyaloclastites (pillow breccias and hyaloclastic turbidites), and epiclastic volcanic shales and sandstones of turbidite origin (Hall and Corbato, 1967; Ernst and Hall, 1974; Fisher, 1977; Ross, 1987).

The white tuff of the Obispo Formation, the main focus of this chapter, occurs in two main facies—one massive, the other bedded. Sedimentological evidence suggests that both facies were emplaced as pyroclastic materials that were remobilized after emplacement and before consolidation. The tuff consists of well-defined bubble wall shards and pumice clasts with a small percentage of pyrogenic crystals (usually less than 5 percent) and some lithic fragments. In the Nipomo area, a welded tuff facies that occurs in a narrow 4-km-long belt is on strike with the nonwelded white tuff facies of the Obispo Formation. Both facies are within the same stratigraphic interval, and their flow directions suggest a common source.

Hall and Corbato (1967) suggested that part of the Obispo Formation may have originated from subaerial eruptions that deposited material in water, a reasonable assumption based on the Obispo Formation's stratigraphic position between two bathyal marine units. Pervasive zeolitization of the white tuff along with other facies data have led Hall and Corbato (1967), Surdam and Hall (1968, 1984), Surdam and others (1970), and Fisher (1977) to propose that the Obispo Formation was deposited and altered subaqueously. A meager molluscan fauna, locally present in volcaniclastic sandstones (probably coarse-grained tuff reworked by wave base), suggests deposition of this facies in water depths from "intertidal to 50 m; not

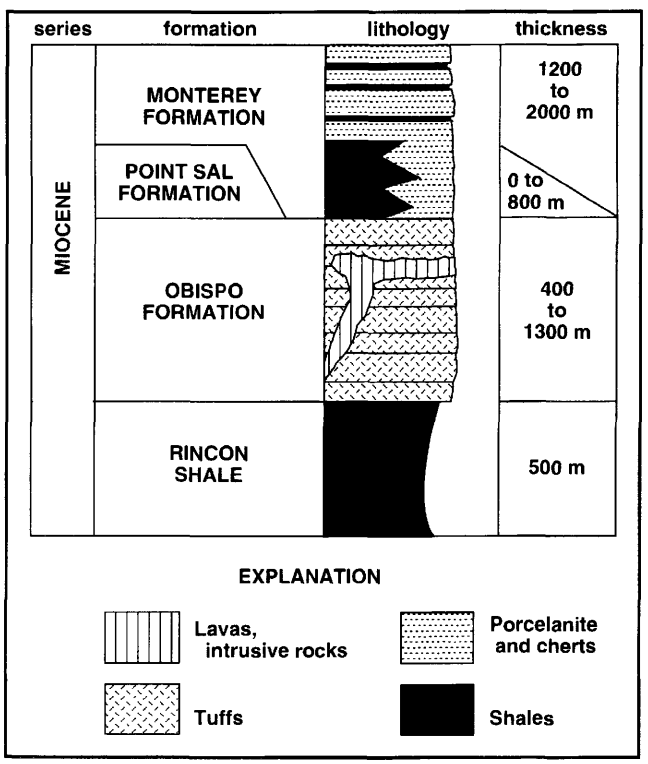

Figure 2. Highly generalized Oligocene and Miocene lithostratigraphy of the Coast Ranges of west-central California. Thicknesses of the Monterey Formation and the Rincon Shale are variable, and locally the Point Sal Formation interfingers with the Obispo Formation (Hall and Corbato, 1967). In some locations, the Obispo Formation rests unconformably on basement rocks of the Franciscan Complex.

deeper than 150 m" (Surdam and Hall, 1984). Mollusks were found about 5 km west of the area shown in figure 3 within volcaniclastic sandstones about 1 m beneath massive white tuff, which is on strike with welded tuff at Nipomo.

The Obispo Formation at most localities is underlain by the Rincon Shale of marine origin (fig. 2). At a few localities, such as north of Nipomo and near the U. S. Highway 101 locality (fig. 1), the Obispo Formation unconformably overlies basement rocks of the Franciscan Complex (Jurassic and Cretaceous age). The absence of Rincon Shale in these localities is probable not because of removal, but because of lack of deposition on basement highs between tectonic basins where Rincon mudrocks accumulated (Tennyson and others, 1991). The Rincon Shale consists mainly of yellow-brown silty claystone (Hall, 1974), with some local tuff beds, and contains Saucesian lower bathyal foraminifera and CN2–CN1c nannofossils (Tennyson and others, 1991). According to Natland (1957) and Oltz and Suchsland (1975), foraminifers of early Zemorrian age in the Nipomo area indicate that the Rincon Shale was deposited in 1,240-m to 2,200-m water depths. Such depths from these reports seem excessive considering that mollusks beneath the welded tuff are from much shallower depths. We do not know, however, the locations of the reported forams from the Rincon Shale.

The Obispo Formation is overlain with apparent conformity by the Miocene marine rocks of the Monterey and Point Sal Formations. The Monterey Formation of middle to late Miocene (Luisian to late Mohnian) age lies with apparent conformity, though perhaps in regional discontinuity, upon the Point Sal and Obispo Formations (Hall and Corbato, 1967). The Monterey Formation consists mainly of chert or laminated porcelaneous siltstone and shale deposited in a bathyal marine environment in 180 m to about 450 m of water (Hall and Corbato, 1967). The Point Sal Formation consists of siltstone and porcelaneous shale, and locally it interfingers with the Obispo Formation.

VOLCANICLASTIC FACIES

Volcaniclastic rocks of the Obispo Formation consist of primary and reworked pyroclastic rocks, volcanic epiclastic rocks, and some hyaloclastites. Specific rock types are welded tuff; reworked (remobilized) pyroclastic rocks (thick massive tuff, tuff breccia, and bedded tuff); fallout tuff; reworked hyaloclastite; and epiclastic volcanic conglomerates, sandstones, and shales. The epiclastic volcanic rocks are not described herein.

We discuss three facies of tuff: welded tuff, massive white tuff, and bedded white tuff. These facies provide information on transport and source directions.

WELDED TUFF

Rhyodacitic welded tuff crops out along a narrow belt in the Nipomo area (fig. 3), forming a prominent exposure continuous for 4 km. The relationship between the welded tuff and the white tuff facies in the Twitchell Dam area is poorly known, and we consider them to be separate facies within the Obispo Formation.

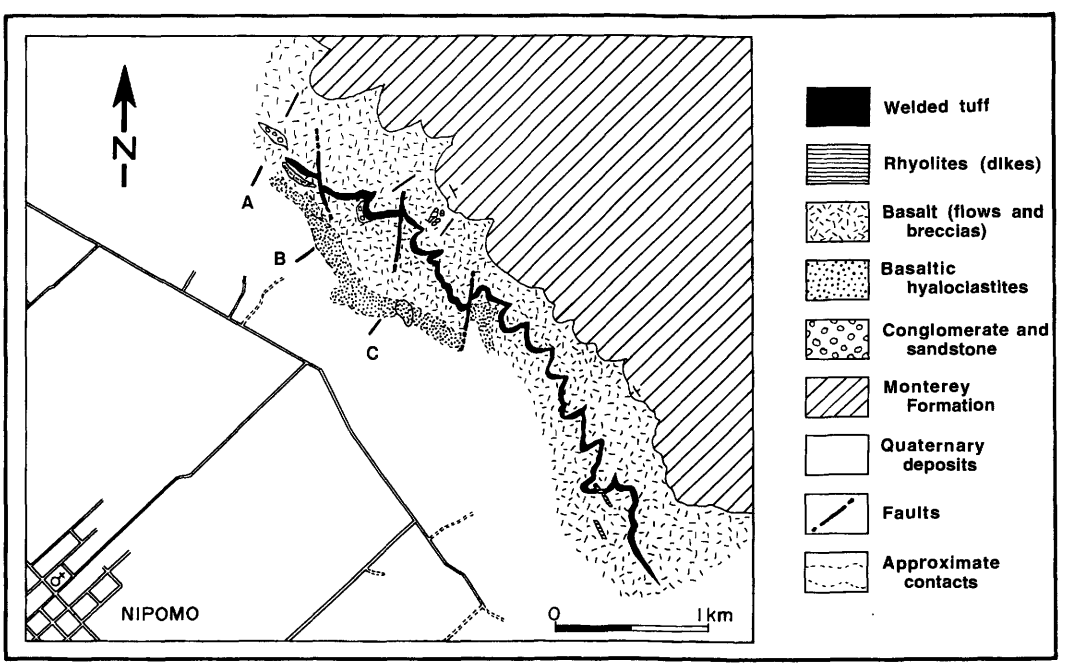

Figure 3. Outcrop map of the Obispo Formation in the Nipomo area. Labels A, B and C show locations of schematic sections shown in figure 4. Mapping done by the authors.

In places, the welded tuff shows columnar joints. The welded tuff ranges in thickness between 5 and 10 m, decreasing to the east and west ends. It lies within a thick complex of sedimentary rocks, breccias, and lava flows (fig. 4). This complex lies between bathyal marine rocks of the Rincon Shale and the Monterey Formation and therefore was most likely deposited subaqueously (Fisher, 1977). We focus particular attention on evidence bearing on the transport direction of the pyroclastic flow that yielded the welded tuff and on its emplacement temperature.

The lithologic features of the tuff are summarized in figure 5. Once-glassy vitrophyre that lies at the base of the welded tuff is now thoroughly devitrified, although we refer to it as "vitrophyre" herein. The vitrophyre is crystal rich with aphyric lithics and includes some spherulites caused by recrystallization of the volcanic glass. Scattered vesicles range in diameter from 1 to 9 cm (fig. 6A). Some vesicles are filled with chalcedony (lithophysae), and some are unfilled. The lithophysae are rounded or irregular in shape. Angular reentrants in the irregular lithophysae are oriented toward the center of the vesicle. This structure is similar to the vesicles described by Bonnischen and others (1989, p. 170).

The vitrophyre contains abundant euhedral plagioclase feldspar and K-feldspar that are commonly fragmented, as well as embayed quartz crystals and broken chips of quartz. The groundmass is composed of glass shards and pumice. This vitroclastic matrix displays welding structures such as sintered glass shards and fluidal welding texture molded around crystals (fig. 6*B*). The welded glass shards define a fluidal foliation within the rock. Fractures within the vitrophyre are filled with chalcedony, clay minerals, and minor calcite.

The deformed shard and fiamme structures in the welded tuff of the Obispo Formation can be traced into areas of nonwelded tuff containing abundant undeformed shards. Such welding is not caused by diagenetic alteration of subaqueous lava flows as described by Allen (1988, 1990), who showed

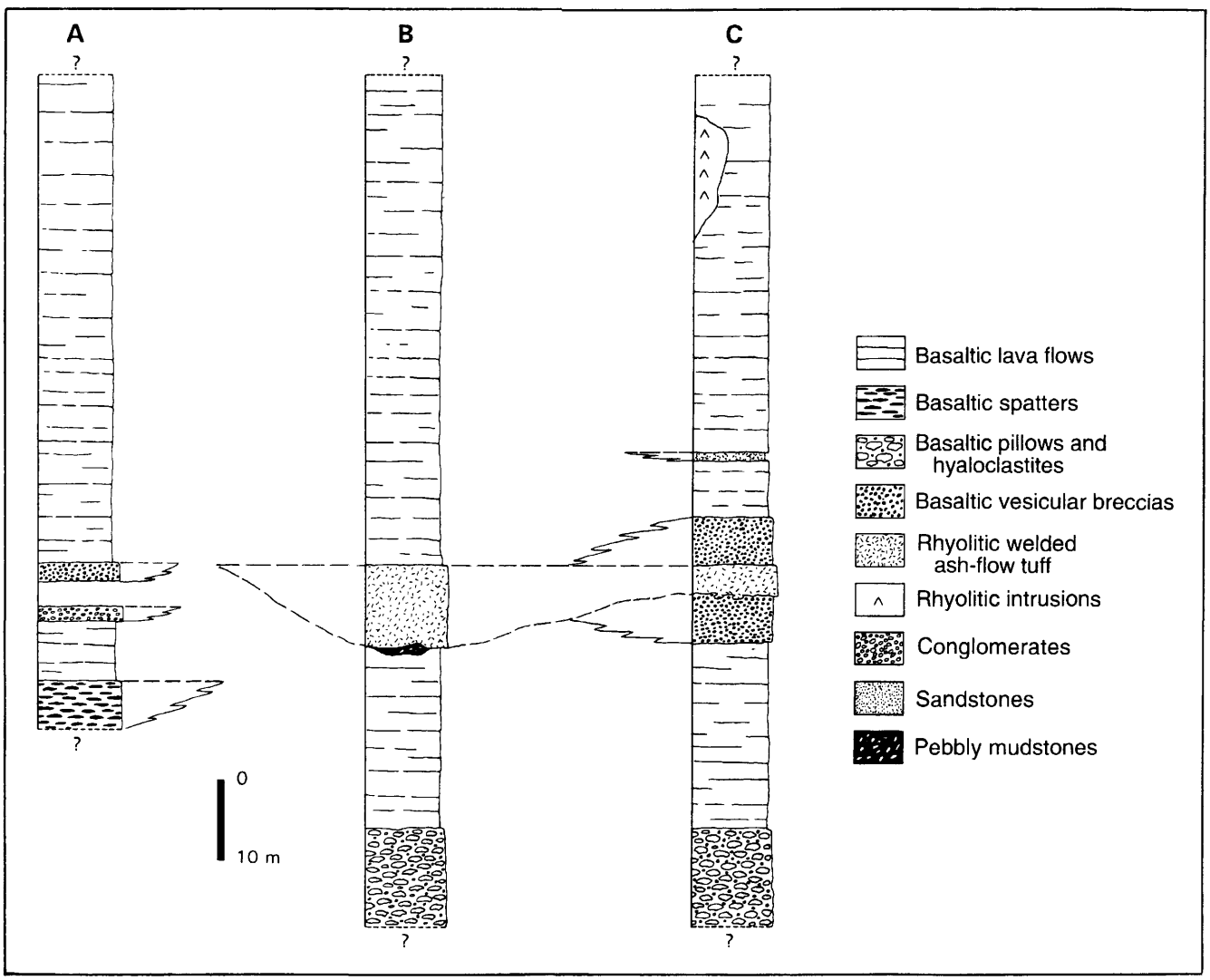

Figure 4. Schematic sections of the Obispo Formation in the Nipomo area. Location of sections A, B and C are shown in figure 3.

that some lava flows can mimic fiamme and welding textures owing to the combined effects of devitrification, perlitic fracture, tectonic shearing, and hydrothermal alteration. Branney and Sparks (1990) described pumice fragments and glass shards that gradually became flattened and aligned owing to overburden pressures and clay alteration, thereby mimicking structures developed by welding at high temperatures. In the Nipomo section, however, shards do not have optic anisotropy, and pumice fiamme are mostly recrystallized as thin high-temperature intergrowths of quartz and feldspar.

The contact at the base of the vitrophyre is irregular but not highly erosive. The underlying sedimentary rocks are deformed in places by pod-shaped masses of the welded tuff. These structures match pod-shaped load casts described by Howells and others (1985) at the base of Ordovician subaqueous welded ash-flow tuff in Wales.

The vitrophyre at Nipomo grades upward within a few centimeters into welded tuff that displays abundant highly elongated fiamme (fig. 6C) with internal foliation corresponding to elongate vesicles of the collapsed pumice. The fiamme range in length from millimeters to 8 cm. The brushlike or frayed ends are similar to the welded fiamme described by Ross and Smith (1961) and Branney and Sparks (1990). The fiamme are pancake shaped in the plane of stratification and emphasize the foliation. Lithic clasts of vitrophyre, dolerite, and granitoid fragments compose about 10 percent of the tuff. Some of the fiamme are molded around rigid lithic clasts.

The top of the ash-flow tuff section is weathered reddish. The fiamme at the top are less flattened than below.

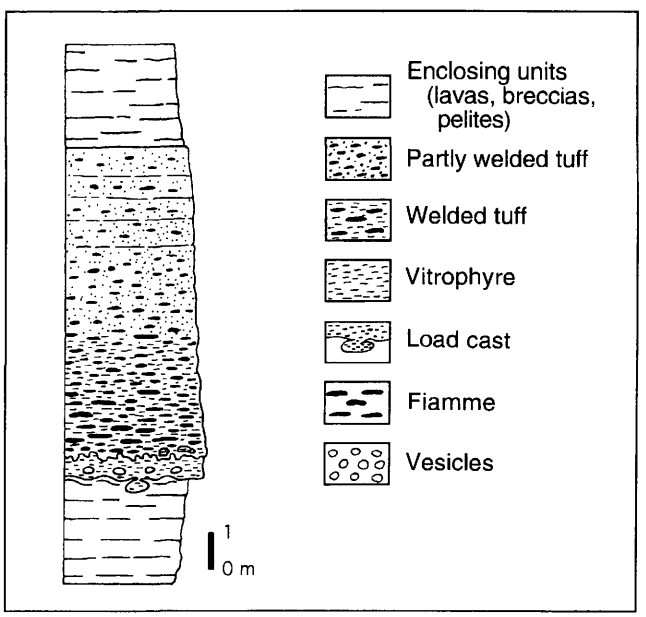

Figure 5. Idealized section of the rhyodacitic welded tuff facies of the Obispo Formation in the Nipomo area. Outcrop distribution shown in figure 3.

Thermoremanent Magnetism

The vitrophyric base and the molded and deformed shards within the welded tuff in the Nipomo section provide strong evidence of welding. Thermal demagnetization studies of some samples from the Nipomo welded tuff also indicate high-temperature emplacement.

Thermal demagnetization curves of two samples are shown in figure 7. Sample A is from the base of the section within the vitrophyre. Sample B is reddish tuff from the top of the welded tuff section. The demagnetization curves (plots of magnetic moment J/J_0 versus temperature; fig. 7) indicate thermoremanent magnetization of the samples. The curve of sample A shows a blockage temperature around 500–550°C. The curve of sample B displays the same characteristics as the curve of sample A except that the blockage temperature is a little cooler (around 450°C). This pattern confirms that temperature was great enough to cause welding of the tuff during emplacement and is consistent with the welding structures determined by petrographic analysis. The techniques used and interpretations that are made are comparable to those obtained on subaerial pyroclastic deposits in Japan (Aramaki and Akimoto, 1957) and Sardinia (Edel, 1979) and for subaqueous ash-flow deposits by Yamazaki and others (1973).

Anisotropy of Magnetic Susceptibility

The determination of an anisotropy of magnetic susceptibility (AMS) has been successfully applied to pyroclastic deposits, especially ignimbrite, to reconstruct source area and flow directions (Ellwood, 1982; Froggatt and Lamarche, 1989; McDonald and Palmer, 1990; Seaman and others, 1991; Fisher and others, 1993). AMS measurements were made from 17 sites of the welded tuff at Nipomo using a Kappabridge instrument. Ellipsoids of anisotropy were obtained with measurements in 15 different orientations of each core.

AMS results indicate that there are two lineations in the Nipomo area. One is NNW.–SSE. and appears to be of tectonic origin. This lineation is parallel to the orientation of the welded tuff exposure (fig. 8) and to faults in the region (fig. 1). The second and dominant lineation, NE.–SW. (N. 20°–35°), could correspond to the flow direction of the pyroclastic flow, but the sense cannot be determined in the Nipomo area because of the absence of other fabric criteria. Columnar jointing causes a third lineation (fig. 8, site 3),a possible perturbation that needs to be considered during AMS studies in welded tuffs and does not pertain to flow directions of the tuff.

White Silicic Tuff Deposits

Tuff, referred to here as the white silicic tuff, constitutes 25 to 50 percent of the volume of the Obispo Formation. It consists of white to blue-gray, ash-sized tuff and lapilli tuff of mainly rhyodacitic composition. It is divided into a massive facies and a bedded facies.

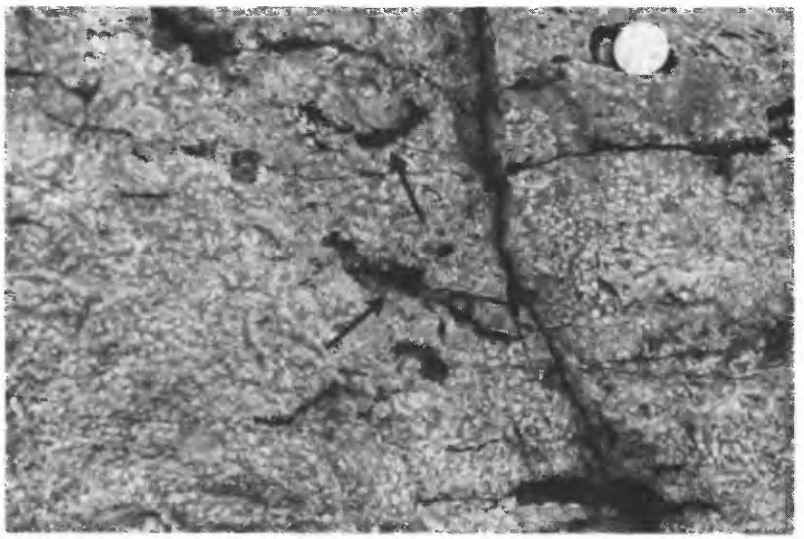

A

Figure 6. Welded tuff facies of the Obispo Formation in the Nipomo area. *A*, Vesiculation of the vitrophyre at the base of the welded tuff sequence [note the angular shape of the vesicles (arrows); coin (2.1 cm) for scale]. *B*, Photomicrograph of the welded tuff showing sintered shards and fluidal textures that mold a glomerophyric plagioclase cluster (scale bar is 0.5 mm; plane-polarized light). *C*, Welded ignimbrite with fiamme molded around a lithic clast (arrow); scale bar is 1 cm.

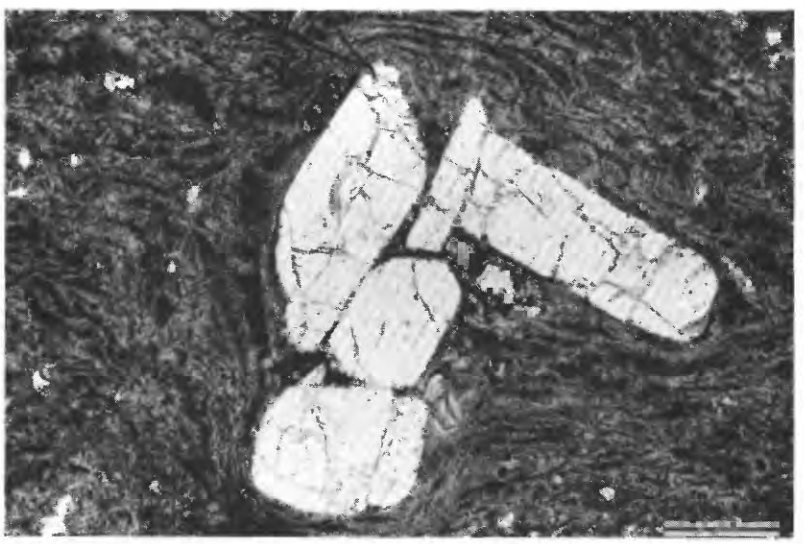

B

Figure 6. Continued

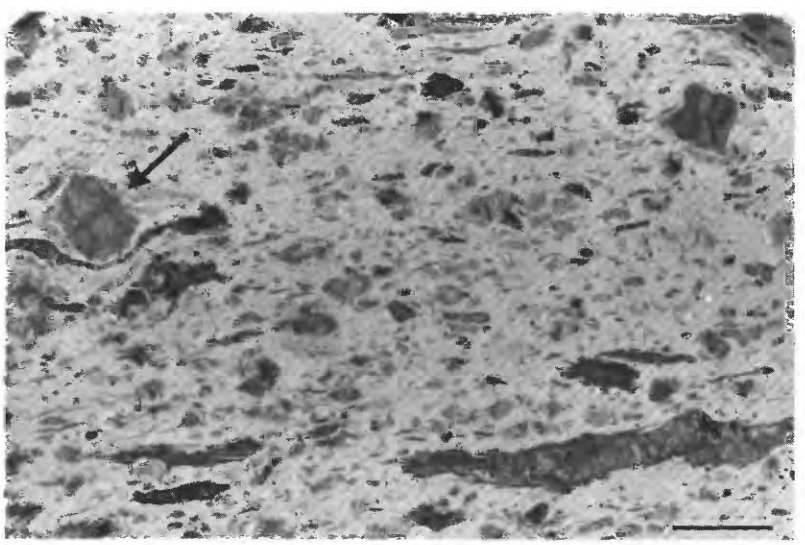

C

Figure 6. Continued

The white silicic tuff is generally fine grained but ranges from very fine grained ash tuff to lapilli tuff. Pumice and bubble wall shards (fig. 9) are commonly zeolitized, with thin rims of acicular heulandite, clinoptilolite, and mordenite (Surdam and Hall, 1984), but bubble-wall shards are unaltered in a few places. Rhyolitic composition is indicated by phenocrysts and fragments of embayed quartz (as much as 10 percent in some layers), plagioclase, and minor potassic feldspar. Pyrogenic minerals are generally rare within the white silicic tuff, and in some instances they are completely lacking. There are some lithic fragments of devitrified glass or vitric tuff in the white tuff. The matrix is commonly argillized and may contain diagenetic calcite or, less commonly, dolomite crystals. The presence of abundant pumice and bubble-wall shards indicates a pyroclastic origin for most particles that make up the white silicic tuff, but sedimentary structures discussed below indicate that the materials have been remobilized as sediment gravity flows, such as turbidity currents and mass flows.

Massive White Tuff Facies

Thick, massive to poorly bedded, white zeolitic tuff deposits are well represented along the coast at Pismo Beach and Shell Beach (fig. 10). They are part of a 950-m sequence in this area (as mapped by Hall, 1973a). This coastal area is on the south limb of the Pismo syncline and occupies the same stratigraphic position as Obispo Formation rocks located 7 to 8 km to the north and northwest on the northern limb of the syncline at the U.S. Highway 101 locality (fig. 1).

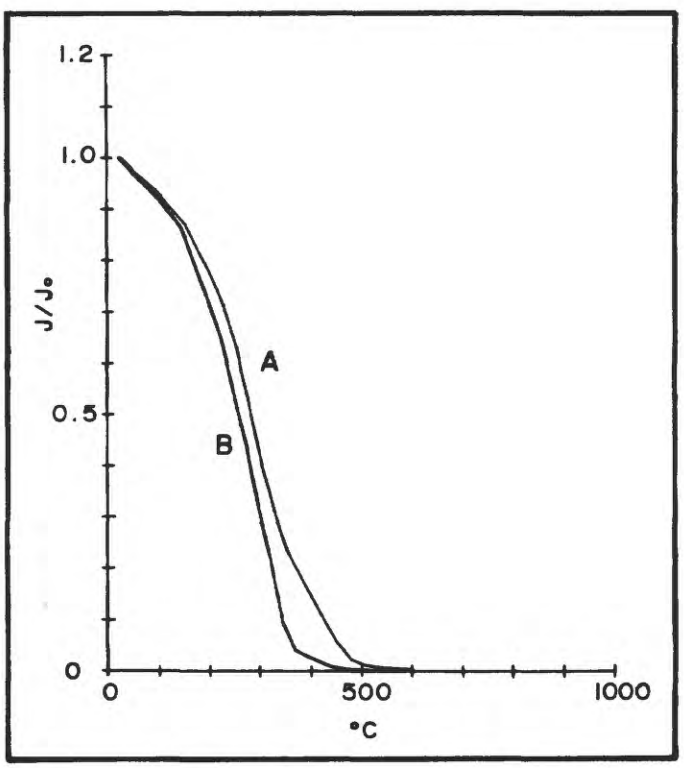

Figure 7. Thermal demagnetization curves of two samples of the rhyodacitic welded tuff. J/J_o = magnetic moment. Sample A (base of section): $J/J_o = 5.46\times10^{-4}$ G cm³/g; sample B (top of section): $J/J_o = 3.99\times10^{-5}$ G cm³/g.

At Shell Beach, massive white tuff crops out beneath and again at the top of a sequence of volcaniclastic siltstone, claystone, and silicified tuff mostly emplaced by turbidity currents. The bedded volcaniclastic turbidite sequence is 59 m thick (fig. 10). The massive white tuff beneath the turbidite sequence extends below sea level, and its base is not exposed. Its exposed part above water measures 5+ m thick. This lower unit is nearly structureless white tuff and lapilli tuff with a few large (1–3 m and less) matrix-supported shale slabs and irregular-shaped, coarse-grained pods of lapilli tuff and tuff breccia. Its upper contact displays flame structures and injection dikes of white tuff extending into the overlying volcaniclastic turbidite units. These features are interpreted to be produced by the deposition and loading of the overlying beds into soft, water-saturated white tuff. Lack of bedding together with matrix-supported large fragments and soft-sediment deformation features (flames and clastic dikes indicating water-saturated materials), suggest that the lower massive white tuff unit was deposited as a debris flow of remobilized pyroclastic material in a subaqueous environment.

The 59-m-thick bedded unit above the lower massive white tuff consists of numerous graded beds of fine-grained volcaniclastic siltstones and a few thin, normally graded hyaloclastic sandstone units with unaltered and altered sideromelane glass shards. Grading is typical of turbidites. There are also a few thin, massive beds with inversely graded bases interpreted to be thin debris flow units. As suggested by the turbiditic bedded stratigraphic sequence that includes turbidites of hyaloclastite composition, deposition occurred during a quiescent volcanic period during which local, explosive basaltic eruptions took place in a subaqueous environment (Ross, 1987). There are no lava flows within this section; consequently, the relationship between basalt flows seen in the Nipomo area, several kilometers to the east, and the formation of hyaloclastites is unknown.

Above the bedded turbidite and debris flow sequence is another unit of massive white tuff totaling 16+ m thick. The upper massive tuff unit has no distinct textural discontinuities except for a few diffuse lenticular bands of matrix-supported lithic fragments (fig. 11). Lack of sharp, distinct bedding planes suggests that the thick tuff bed is a single depositional unit. The base of the tuff is lithic rich and contains large pelitic rip-up clasts (fig. 12*A*, *B*) derived from shale units within the underlying bedded turbidite sequence. Imbrication of fragments suggests that the white tuff unit was emplaced as it moved from left to right (southwest to northeast).

The pelitic units and rip-up pelitic clasts are devoid of fossils. In places within the massive tuff, there are discontinuous packets of tuff bed sequences, up to 2 m long and 1 m or

more thick, that appear to have been picked up and carried during emplacement of the massive tuff. The packets are essentially large-scale clasts within which there is a coherent stratigraphy of thin-bedded, graded turbidite beds deposited prior to the disruption and inclusion of the packets within the massive white tuff. As indicated by sedimentary structures, some beds within the packets are symmetrically graded—reverse at the base reverting to normal grading at the top (reverse to normal grading; Fisher and Schmincke, 1984). Similar graded bedding is displayed by beds within the sequence of bedded tuffs at Twitchell Dam described in a later section.

Several kinds of deformation structures are exhibited beneath or within the base of the upper white tuff at Shell Beach. These include tangential deformation structures with small normal gliding planes (fig. 13*A*) and asymmetric folds (slumping; fig. 13*B*). In places, sedimentary rocks beneath the white tuff are brecciated (fig. 13*C*). Mixing and intrusion of the massive white tuff into underlying units are illustrated by pelitic mega rip-up clasts (fig. 13D), curled shavings of shale (fig. 13*E*) and bundles of pelitic layers swept up into, and deformed by emplacement of, the massive white tuff (fig. 13*F*).

Stereonet projections of deformation structures in the rocks beneath the white tuff are shown in figure 13*G*. Stereonet projections of deformation structures in the pelitic rip-up clasts are shown in figure 13*H*. At one locality, the contact of one massive unit above another shows soft-sediment deformation patterns (fig. 14). Another locality exhibits a clastic dike near the underlying layer (fig. 15). These features are interpreted as being caused by abnormal hydrostatic pressure resulting from mass flow emplacement or slumping of clastic material upon water-saturated materials (Lehner, 1991). At Pismo Beach, there are units showing similar soft-sediment deformation features.

Deformation structures at Shell Beach and Pismo Beach indicate that the sediments were water-saturated and soft or were beginning to be lithified but still plastic. Rip-up fragments within the massive white tuff were very likely derived

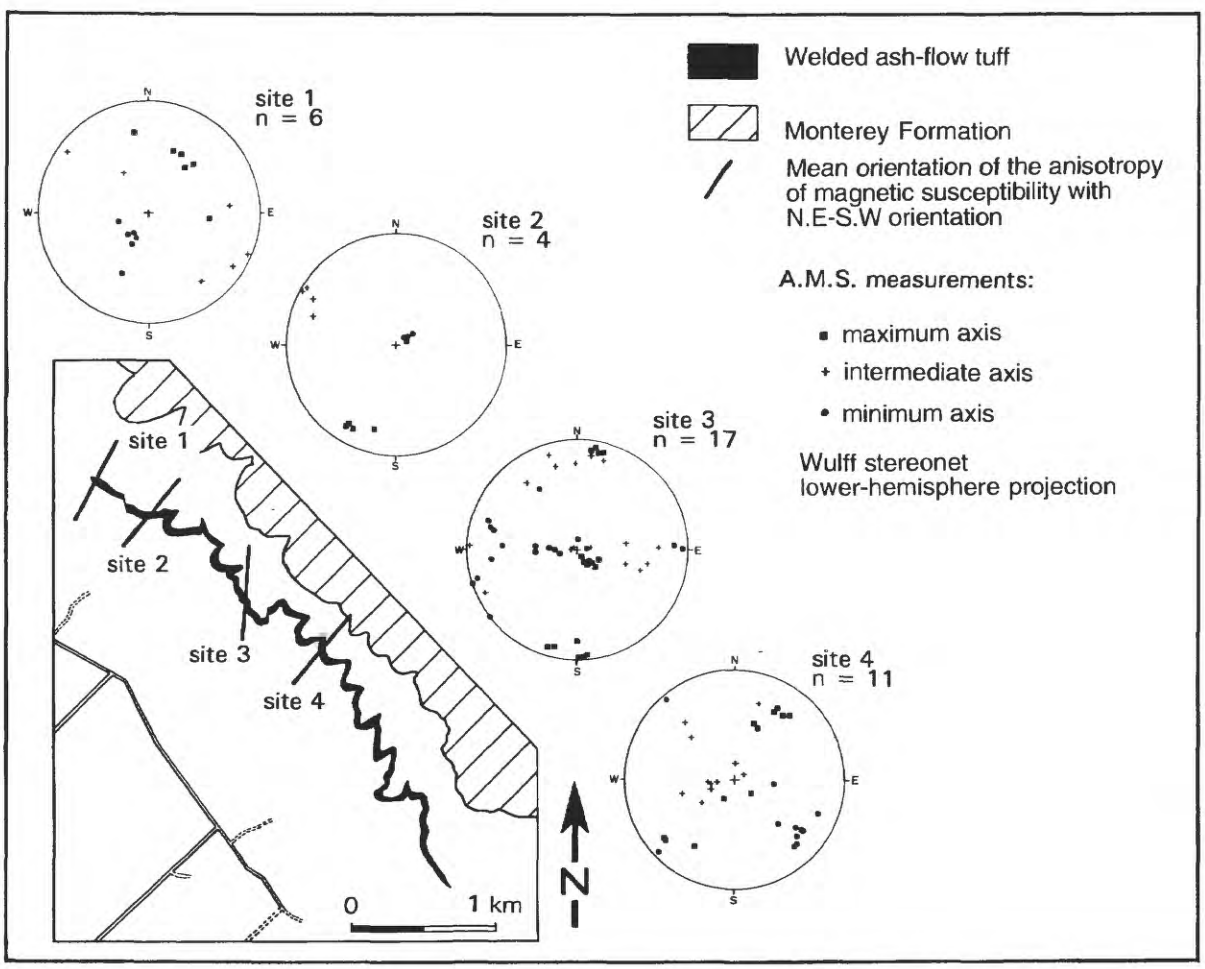

Figure 8. Orientation of the anisotropy of magnetic susceptibility in the welded ignimbrite near Nipomo. The mean direction is SW.–NE. and is consistent with the orientation of a postulated volcanic ridge that could have been a source for some of the volcanic rocks of the Obispo Formation.

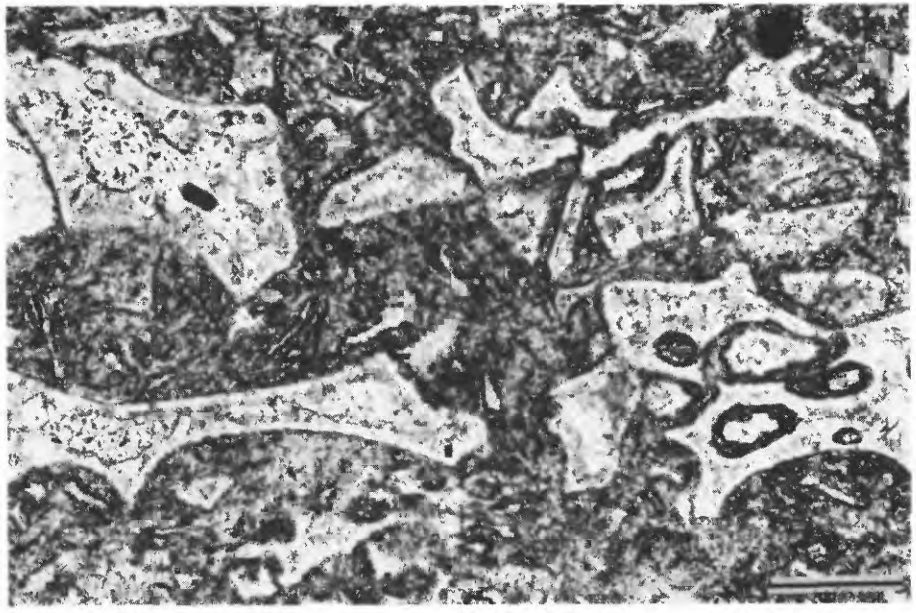

Figure 9. Photomicrograph of a typical zeolitized white tuff with remnant shard structures in the Obispo Formation (from Pismo Beach area). Scale bar is 0.5 mm.

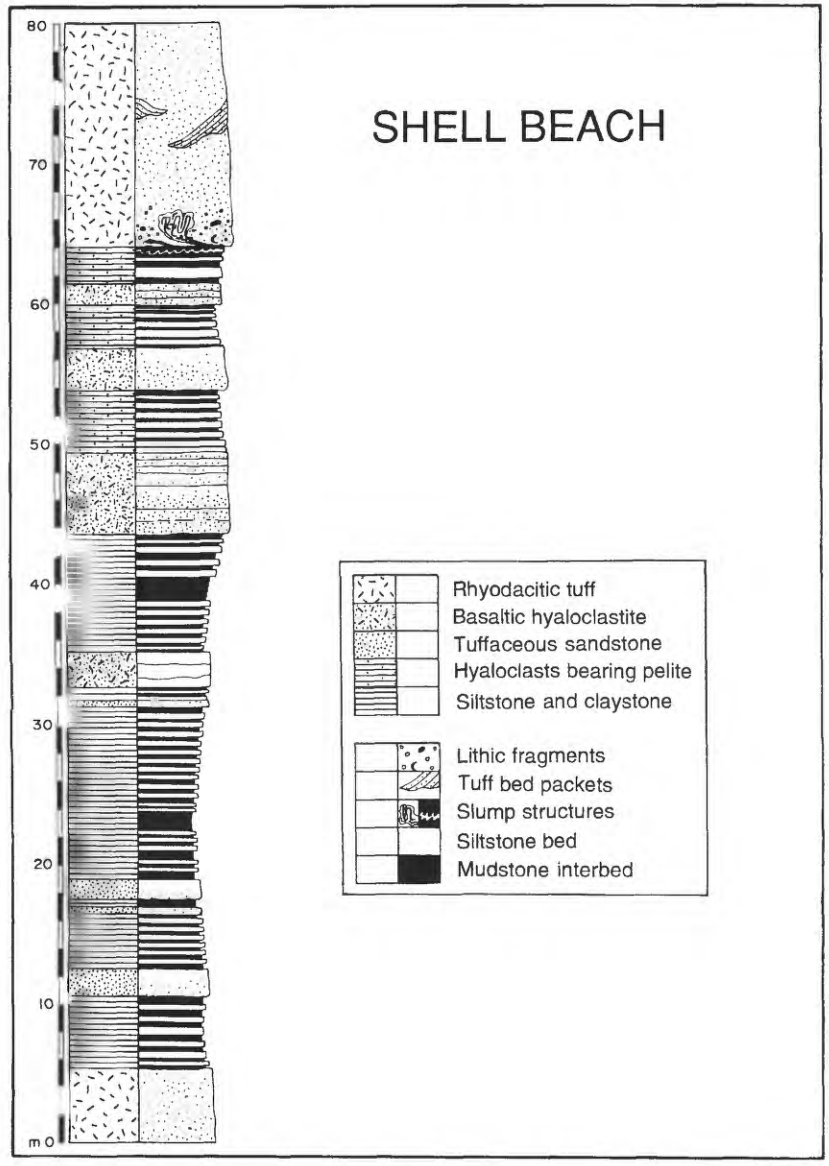

Figure 10. Measured section of the Obispo Formation at Shell Beach (modified from Ross, 1987).

from bedded sediments invaded by the mass flow of pyroclastic material during transport and emplacement of the massive white tuff. Some sedimentary layers have been injected along bedding planes (fig. 13*D*); the missing ends of the beds were carried away within the massive white tuff as it was being emplaced. The contact in some places is marked by ripped-up pelitic chips (fig. 13*E*). Also, beds have been uplifted, rumpled, and folded within the massive white tuff (fig. 13*F*). Stereographic projections suggest a northeasterly direction of movement (fig. 13*G*) as indicated mainly by the direction of bending of a mega rip-up clast shown in figure 13*E* and by uplift directions of invaded bedding planes (fig. 13*H*). Small faults reveal shearing toward the ENE. (fig. 13*G*). The small-fold geometry suggests west, south, and east directions of movement with a large dispersion of the fold axes, but it is likely that the large dispersion is due to the water-saturated character of the sediments during deformation.

Deformation structures at Shell Beach and Pismo Beach are very similar to the structures described in subaqueous pyroclastic flow deposits in Japan (Kano and others, 1988).

Bedded White Tuff Facies

The bedded white tuff facies is well exposed along a frontage road adjacent to U.S. Highway 101 (locality U.S. 101) and in the Twitchell Dam area (fig. 1).

The Obispo Formation at U.S. 101 is on the northern limb of the Pismo syncline, north and northwest of Shell Beach. The depositional sequences were deposited within the same stratigraphic interval (Hall, 1973a). The Shell Beach sequence is coarser grained and thicker than the U. S. 101 sequence, and therefore it is considered to be more proximal.

The U.S. 101 sequence (fig. 16) is about 85 m thick (45 m is unexposed). We divide the sequence into five depositional units, each consisting of several beds. The sequence conformably overlies dark brown to gray silty claystones of the Rincon Shale and is conformably overlain by light-gray shales of the Monterey Formation. The rocks are well- to poorly bedded, crystal-poor, coarse- to fine-grained tuff and lapilli tuff.

Within each of the five units of the sequence, beds at their base are coarse grained and become finer upward. Unit 1 (8.5 m) at the base of the sequence consists of six bedding units that are coarser grained than beds in the rest of the sequence. The lowermost bed is massive, contains shale rip-up clasts from the underlying Rincon Shale, and is inversely graded over a thickness of 20 cm at its base. Each unit in turn begins with a coarser grained bed than at its top, and each of the beds within the units are graded from coarse- to fine-grained at the top. Thus, individual beds within the units are graded from coarser to finer grained upward, each of the five units are graded from coarser to finer grained upward, and overall the entire sequence becomes finer grained upward. Because of the systematic grading, each of the five units is interpreted

Figure 11. Crudely layered white tuff facies of the Obispo Formation at Shell Beach showing subtle bands of lithic-rich zones. Hammer for scale rests on a lithic-rich band in the center of the photograph.

A

Figure 12. Shell Beach. *A*, Photograph of large rip-up clasts of pelitic shale (dark fragments) in white tuff of the Obispo Formation. The 6-m-thick white tuff unit is massive and moved from left to right (southwest to northeast). Elongate shale slab in center is 1 m long. B, Closer view of mixing zone of shale and massive white pumice-bearing tuff of the Obispo Formation. Bent shale clast in center is 40 cm long.

B

Figure 12. Continued

to have been emplaced by a single depositional event. The grading and bedding of the U. S. 101 sequence is therefore considered to be doubly graded, similar to described subaqueous pyroclastic flow deposits in the Tokiwa Formation, Japan (Fiske and Matsuda, 1964).

The Obispo Formation at Twitchell Dam conformably overlies the Rincon Shale (fig. 17). The upper contact is not exposed in this area.

An idealized depositional unit derived from close observation of the measured section exposed on the road to the dam is shown in figure 18 (Fisher, 1977). Depositional units grade upward from coarse to fine grained. The coarse-grained base includes centimeter-scale pumice clasts and is symmetrically graded—reverse at the base reverting to normal grading at the top (reverse to normal grading; Fisher and Schmincke, 1984). Similar graded bedding is displayed by beds in depositional

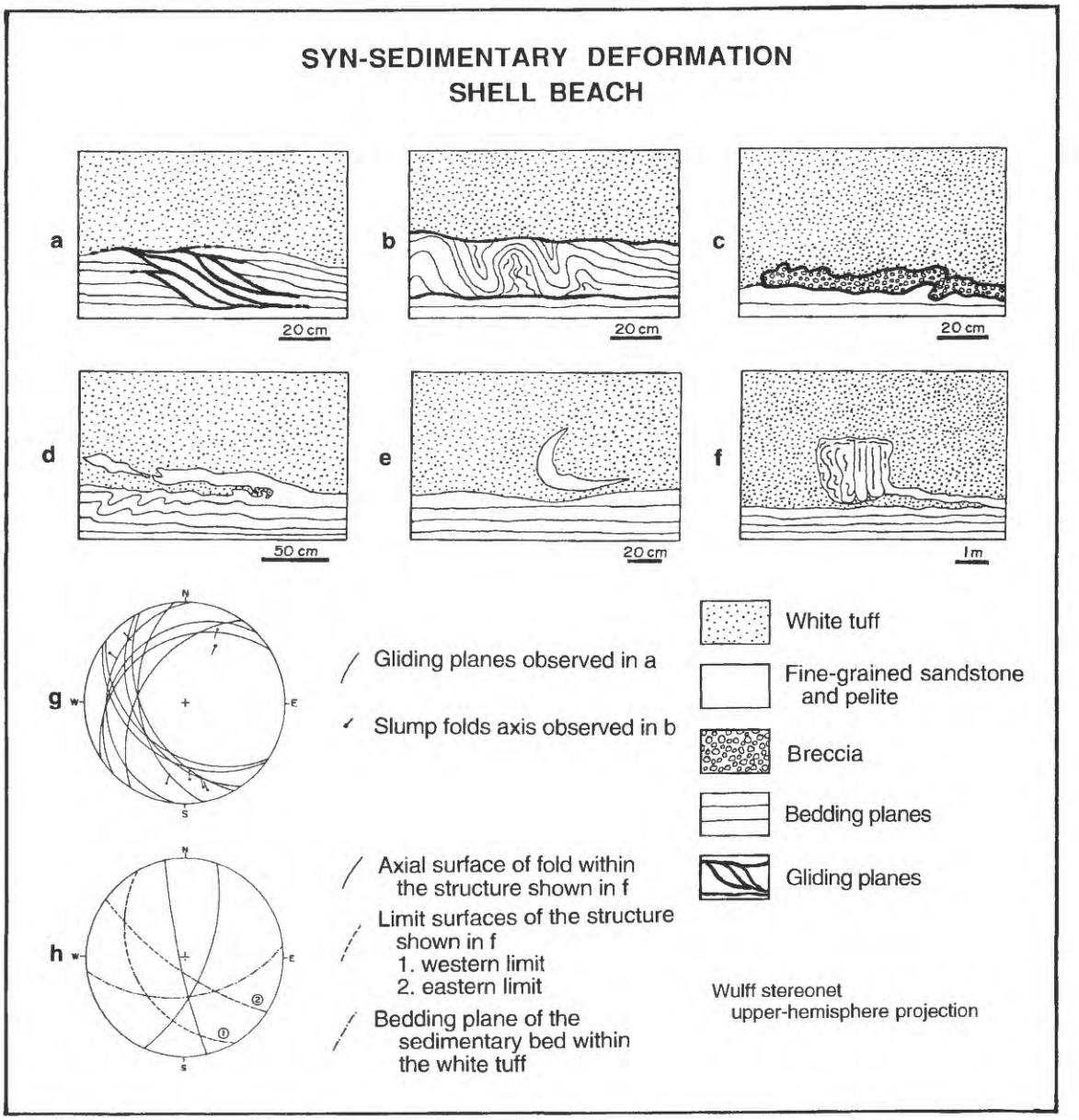

Figure 13. Syn-sedimentary deformation structures at the base of the massive white tuff facies of the Obispo Formation at Shell Beach. *A*, Normal gliding planes in the sediments below the base of the white tuff. *B*, Asymmetric folds in the sediments below the base of the white tuff (probably caused by slumping). *C*, Brecciated sediments below the base of the white tuff. *D*, Pelitic mega rip-up clast within the white tuff. *E*, Curled pelitic rip-up clast at the base of the white tuff. *F*, Pelitic layer swept up and deformed within the white tuff. *G*, Stereographic diagram of the geometric characteristics of the deformation structures in the sediments below the white tuff. *H*, Stereographic diagram of the geometric characteristics of the deformed structures of the pelitic rip-up clasts included in the white tuff. Note the dispersion of the two fold-axis planes within the rip-up clasts.

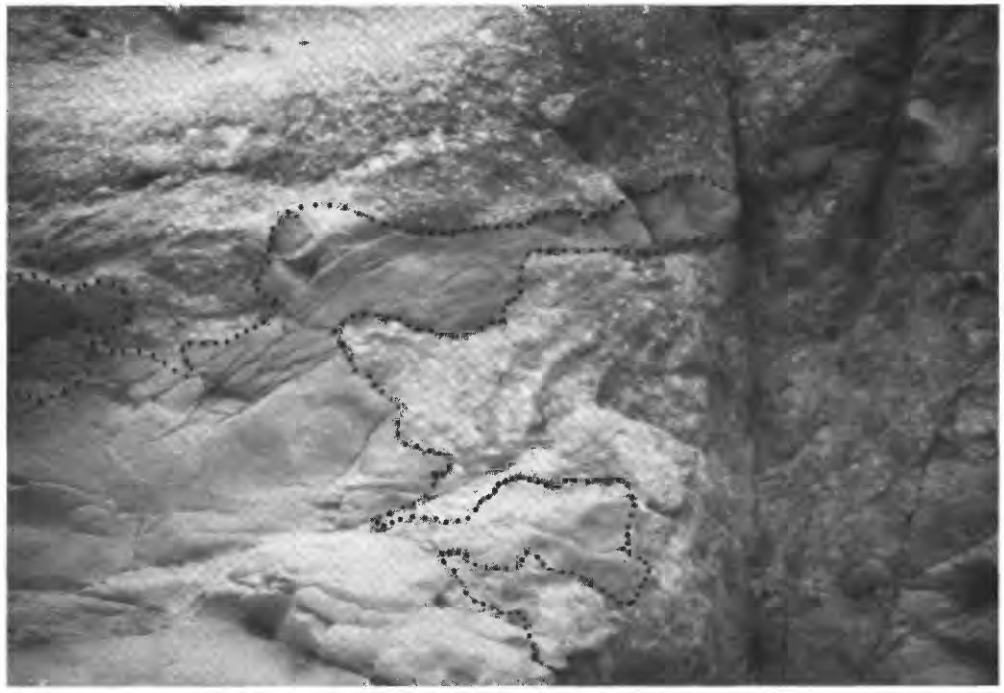

Figure 14. Interfingering of fine- and coarse-grained pumice-bearing tuff of the Obispo Formation at Pismo Beach cliff about 2.5 km southeast of the Shell Beach section. The rounded flames and intermingled contact (outlined with dots) indicates that coarse-grained tuff moved across a surface of fine-grained, water-saturated sediment. Pull-out pattern from left to right (west to east in photograph) suggests movement in that direction consistent with southwest to northeast flow directions indicated in the Shell Beach area. Elongate flamelike protrusion in center of photograph is about 30 cm long.

Figure 15. Clastic dike within the base of a white tuff layer at Shell Beach. Hammer is for scale.

packets that are incorporated within the massive white tuff at Shell Beach. Basal contacts of the depositional units are erosive in places or exhibit load casts into the underlying deposits. Within a single depositional unit, but above the graded tuff, is fine-grained ash tuff that has laminar bedding or current ripples with tangential foreset laminations. The top layer of the idealized sequence is very fine grained, laminated and commonly bioturbated tuff (fig. 18). Many burrows are branched parallel to the bedding. The very fine grained upper tuff includes clasts of isolated megascopic shards and small pumice lapilli.

On bedding surfaces at the top of depositional sequences are current indicators such as parting lamination, flute casts, and impact structures. Impact structures are similar to flute casts but display small fractures surrounding their peripheries. Current markers indicate a flow direction toward the ENE. (fig. 17). These directions are consistent with the flowage directions recognized at Shell Beach (fig. 13).

Most of the Twitchell Dam section consists of well-bedded white tuff and lapilli tuff, but at 60 m above the base (top of the measurable sequence) are two massive tuff breccia units. The lower unit, about 4 m thick, is a brown, coarse-grained, normally graded breccia with 5- to 40-cm-long clasts of angular microcrystalline tuff within the lower meter of the unit, and abundant small angular shale fragments. Above the lower graded part is coarse-grained tuff with pumice lapilli to 5 mm across. A lens of green, thinly bedded, medium-grained tuff lies between the lower breccia and the breccia overlying it. The upper breccia unit, about 6 m thick, has a 10-cm inversely graded zone at its base, becoming normally graded above the

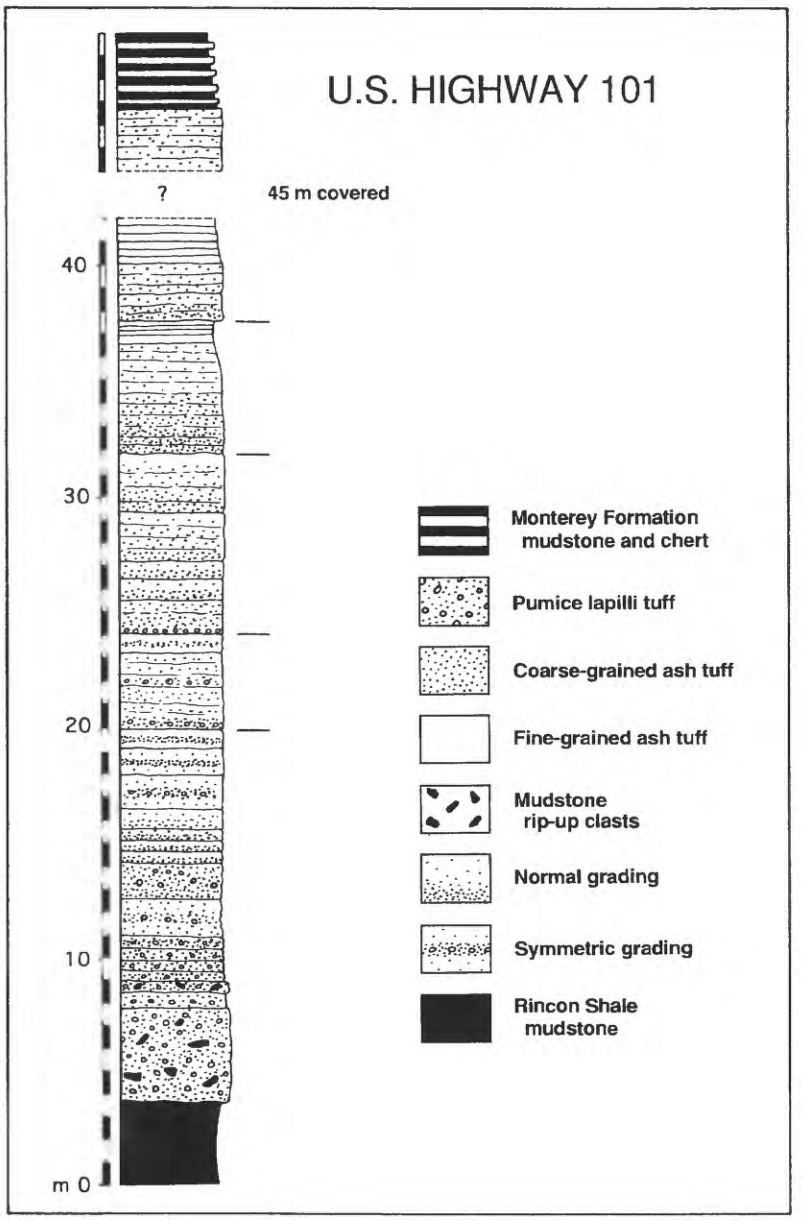

Figure 16. Stratigraphic section from the U.S. Highway 101 section (locality U.S. 101), located about 5 km south of San Luis Obispo along a frontage road on the west side of the highway where the Obispo Formation north of the Pismo Syncline crosses the highway (see fig. 1).

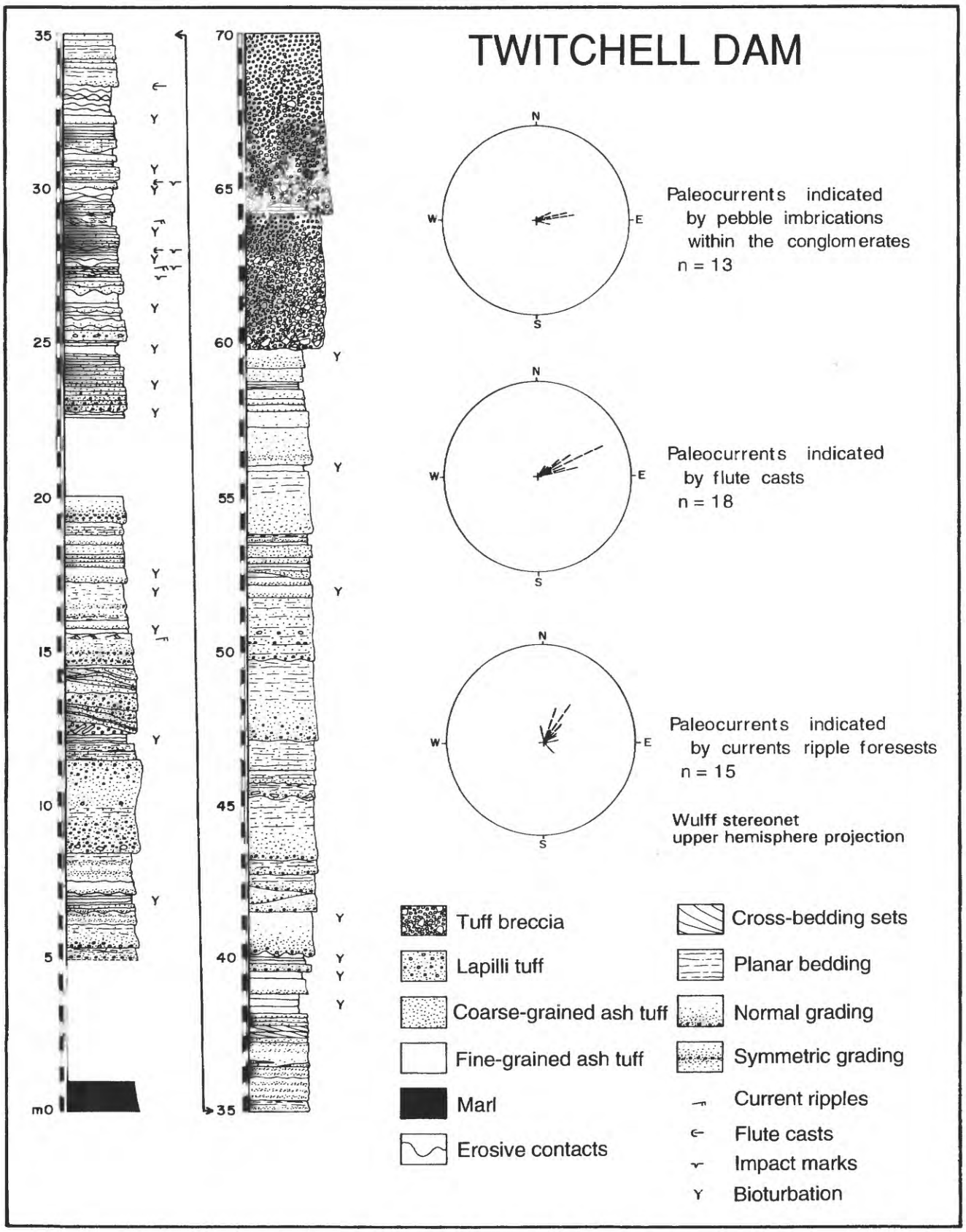

Figure 17. Stratigraphic section of the bedded white tuff facies of the Obispo Formation in the Twitchell Dam area with results of paleocurrent measurements.

base. The upper breccia is composed of angular to subrounded clasts of light-brown tuff, dark-brown diabase, black shale, and light-gray microcrystalline tuff. The clasts are 2–10 cm in longest dimension and are matrix supported. The matrix is brown, coarse-grained tuff.

LAVA AND INTRUSIVE FACIES

Basalt is the most abundant lava type in the Obispo Formation (Hall and Corbato, 1967), but in the study region, basalt crops out mainly in the Nipomo area (fig. 3).

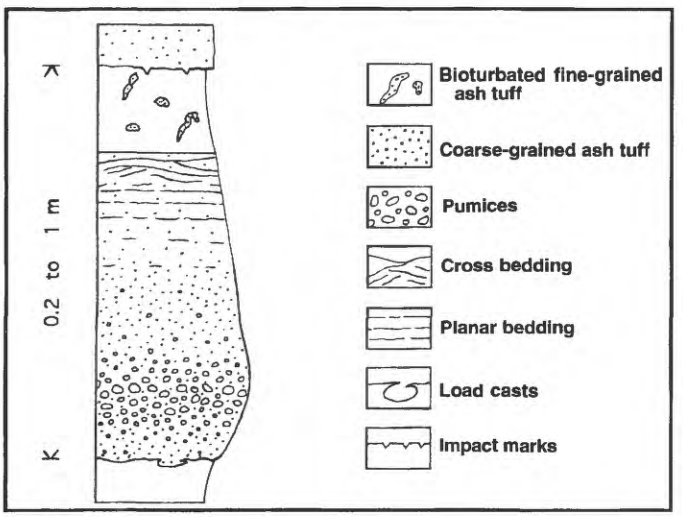

Figure 18. Idealized section of a single tuff turbidite emplacement unit of the Obispo Formation tuff deposits in the Twitchell Dam area.

Basalts examined near Nipomo are highly vesicular. Vesicles range from 2 mm to 4 cm in diameter and are commonly filled by silica or clay minerals. Plagioclase crystals are common as microlites but rare as phenocrysts. Olivine, commonly altered to iddingsite, comprises 10 percent of the rock and is associated with less common pyroxene and magnetite.

Evidence of subaqueous emplacement of basaltic lavas is shown by pillow basalts at the base of the Obispo Formation in the Nipomo area (fig. 19). Pillows display massive microlitic cores surrounded by altered glassy rinds. The vitreous clastic matrix between pillows was likely produced by quenching and spalling of pillow rinds.

Unusual basaltic spatter deposits within the studied area are found only within the Nipomo area as small lens-shaped outcrops on a scale of decimeters. The spatter is an accumulation of basaltic scoria with fragments molded onto one another. The vesicles are collapsed, indicating that the material was emplaced at temperatures high enough to allow plastic deformation. Some of the scoria breccias consist of angular clasts up to 10 cm that are not molded onto each other. The spatter deposits indicate lava fountaining and, therefore, close proximity to a vent. The scoria breccias are interpreted as lower temperature lateral equivalents of the spatter deposits.

Basaltic and silicic dikes intrude rocks in the Nipomo, Pismo Beach, and Diablo Canyon areas. Along the shore in the Pismo Beach area, basaltic dikes that intrude white tuff are oriented N. 40° E. The basaltic intrusives have intergranular textures in which scarce subeuhedral clinopyroxene lies between euhedral plagioclase laths. Sparse olivine is also present. The plagioclase is commonly saussuritized and associated with secondary analcime, calcite, chlorite, and iron oxide.

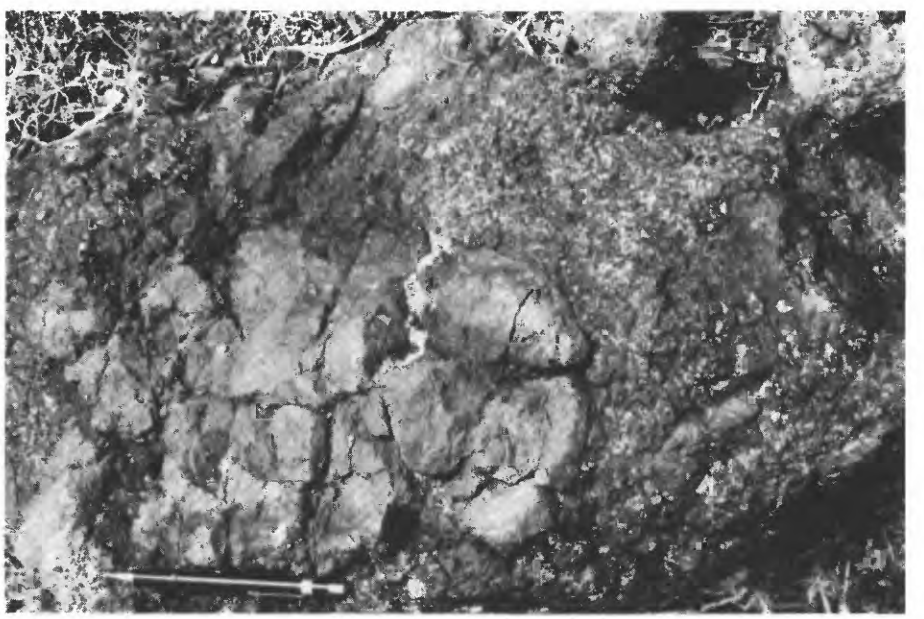

Figure 19. Basaltic pillow in hyaloclastite matrix. Nipomo area. Pen is for scale.

Figure 20. Peperite at the mouth of Diablo Canyon. Shale fragments are in intrusive felsite.

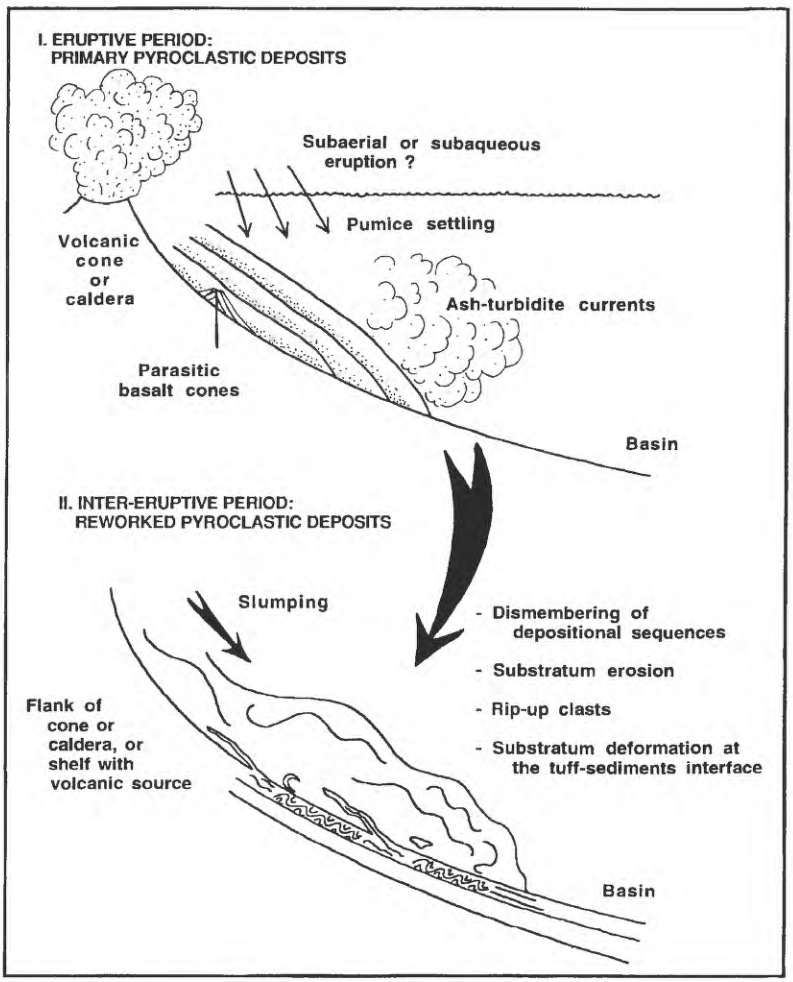

Figure 21. Models for development of white tuff in the proximal areas during eruptive and intereruptive periods.

Small-volume silicic intrusive bodies commonly form dikes oblique to the general strike of stratification in the Nipomo area (fig. 3). These dikes are composed of dacite and rhyolite vitrophyre with a perlitic groundmass. The groundmass is locally flow banded and cut by chalcedony veinlets in a few places. Some vitrophyre contains a relatively high proportion of phenocrysts (as much as 20 percent) of plagioclase and minor amounts of embayed quartz. Primary microstructures are commonly obscured in the vitrophyre because of devitrification.

At the mouth of Diablo Canyon (fig.1), diabase and felsite intrude shales. Many of the intrusions are intimately mixed with sediment and were designated as "good examples of tuff intrusions" by Hall (1973b). The sedimentary units, however, commonly show soft-sediment deformation adjacent to the intrusive bodies, whereas the intrusive bodies contain rounded blebs, blocks, and shreds of shale and sandstone indicative of peperite (Fisher and Schmincke, 1984) (fig. 20).

CONCLUSIONS

The Obispo Formation trends northwestward in a 60-km by 15-km belt. It is composed of 25 to 50 percent rhyodacitic pyroclastic material (the white tuff). We estimate that the total volume of the bedded and massive white tuff to be 250–450 km3. The white tuff consists of bubble-wall shards, pumice clasts, and minor amounts of crystals and lithic fragments. Large volumes of silicic tuff are commonly produced by large Plinian eruptions that are associated with the formation of large calderas and pyroclastic flows (Smith, 1979; Lipman, 1984), but as yet, a vent for the white tuff facies of the Obispo Formation has not been located.

The white tuff was deposited mostly as remobilized mass flows (massive white tuff facies) and turbidity currents (bedded white tuff facies) in marine water (fig. 21). Three possibilities of the origin of the mass flow and turbidite deposits of white silicic ash are that they (1) originated from eruptions beneath sea level, (2) originated from subaerial pyroclastic flows that entered the sea from land, or (3) originated on the subaqueous flanks of a large silicic volcano from accumulations of ash, lapilli, and blocks (pyroclastic flows or fallout ash) that later became remobilized as large submarine slumps, mass flow, and turbidity current transformations. Flow transformations are discussed by Fisher (1983).

Primary and remobilized flow-emplaced materials form the bulk of the white tuff of the Obispo Formation. The evidence is as follows: (1) Primary welded tuff rests on sedimentary rocks emplaced under shallow-marine conditions not far beneath the welded tuff in the Nipomo area. (2) Graded bedding typical of turbidites suggests that sedimentary structures within the bedded white tuff deposits are mainly of turbidity current origin, a conclusion that indicates a remobilized origin for many of the tuff beds.

Bathyal marine sedimentary formations largely of nonvolcanic composition overlie and underlie the Obispo Formation, and soft-sediment deformation structures within bedded white tuff units of the Obispo Formation suggest underwater emplacement. It is not known, however, if the eruptions that gave rise to the massive and bedded white tuff facies occurred in subaqueous or subaerial environments. Underwater eruptions that produce widespread abundant silicic pyroclastic materials in the geologic record are difficult to prove (Fisher and Schmincke, 1984), but pyroclastic flows are known to have entered the sea following subaerial eruptions; an example is the 1902 Mt. Pelée, Martinique, eruption (Lacroix, 1904). More recently, it has been shown that pyroclastic flows entered the sea during the great 1883 eruption of Krakatau, Indonesia (Verbeek, 1884; Simkin and Fiske, 1983), to cause a large destructive tsunami (Self and Rampino, 1981; Sigurdsson and others, 1991). It has also been recently shown that hot gaseous pyroclastic surges transformed to water-saturated debris flows (Scott, 1988) during which interstitial gas of the pyroclastic surges was replaced by interstitial water. Thermoremanent magnetization studies demonstrate that hot pyroclastic flow deposits (~ 500°C) have been emplaced in subaqueous environments (Kato and others, 1971; Yamazaki and others, 1973).

The transformation of hot pyroclastic flows (a mixture of gases and fragments) directly to subaqueous water-saturated mass flows and turbidity currents (a mixture of water and gases) as they move from land into water is possible but difficult to prove by examination of deposits. The process by which interstitial gas is replaced by interstitial water remains to be investigated.

AMS and sedimentological current indicators show that the transport of pyroclastic material within the Obispo Formation was from southwest to northeast—from the present-day offshore region toward the present-day coastal area in the areas investigated (Twitchell Dam, Nipomo, Pismo Beach–Shell Beach, U.S. 101 section, and Diablo Canyon region).

The fact that the remobilized white tuff extends for many tens of kilometers in a northwest-southeast direction (fig. 1) leads us to conclude that it was redistributed from the original source along the shelf area or shoreline of the volcano and on the floor of the adjacent sea. The massive white silicic tuff with crude bedding and large rip-up clasts in the Shell Beach location was emplaced with considerable momentum, indicating high potential energy (elevation) at the source. Areas of bedded white tuff, such as the U.S. 101 and Twitchell Dam sections, with many turbidite units illustrate a more basinward facies farther from the source area.

The distribution of intrusive igneous rocks on both sides of the Pismo syncline indicates that there were local volcanic sources—perhaps vents upon the flanks of a large silicic volcano. However, the vent that produced the voluminous white tuffs of the Obispo Formation (presumably on a major rupture zone) has not been located. The location of the intrusive bod-

ies were thought by Surdam and Hall (1984) to lie along the axis of a postulated leaky transform fault.

The large volume of silicic pyroclastic material argues circumstantially for a very large discharge eruption of caldera origin; the elongate distribution pattern suggests longshore redistribution of the pyroclastic debris. It is possible that some of the tuff of the Obispo Formation (such as the welded ignimbrite of Nipomo) had a volcanitectonic origin similar to Permian calcalkaline rocks of northern Vosges, France, where silicic eruptions that produced ignimbrites erupted from extensional fissures without caldera formation (Schneider and others, 1994). However, the large volume of the white tuff of the Obispo requires collapse and caldera formation (Smith, 1979; Lipman, 1984). Basaltic volcanism, exemplified by basaltic hyaloclastic turbidites at Shell Beach between thick bodies of massive white tuff, and basaltic and andesitic lava flows elsewhere (Hall and Corbato, 1967) suggest that mafic vents may have erupted on the flank of a larger silicic volcano.

REFERENCES CITED

Allen, R.D., 1988, False pyroclastic textures in altered silicic lavas with implications for volcanic-associated mineralisation: Economic Geology, v. 83, p. 1424-1446.

———1990, Subaqueous welding, or alteration, diagenetic compaction and tectonic dissolution [abs.]: International Volcanological Congress, Mainz, Abstracts Volume.

Aramaki, S., and Akimoto, S.I., 1957, Temperature estimation of pyroclastic deposits by natural remanent magnetism: American Journal of Science, v. 225, p. 619-627.

Bonnischen, B., Christiansen, R.L., Morgan, L.A., Moye, F.J, Hackett, W.R., Leeman, W.P., Honjo, N., Jenks, M.D., and Godchaux, M., 1989, Silicic volcanic rocks in the Snake River Plain–Yellowstone Plateau province, in Chapin, C.E., and Zideck, J., eds., Field excursions to volcanic terranes in the western United States, v. 2: Cascades and Intermountain West: New Mexico Bureau of Mines and Mineral Resources, Memoir 47, p. 135-182.

Bramlette, M.N., 1946, The Monterey Formation of California and the origin of its siliceous rocks: U.S. Geological Survey Professional Paper 212, 57 p.

Branney, M.J., and Sparks, R.S.J., 1990, Fiamme formed by diagenesis and burial-compaction in soils and subaqueous sediments: Journal of the Geological Society of London, v. 147, p. 919-922.

Edel, J.B., 1979, Paleomagnetic study of the Tertiary volcanics of Sardinia: Journal of Geophysics, v. 45, p. 259-280.

Ellwood, B.B., 1982, Estimates of flow direction for calc-alkaline welded tuffs and paleomagnetic data reliability from anisotropy of magnetic susceptibility measurements: central San Juan Mountains, southwest Colorado: Earth and Planetary Science Letters, v. 59, p. 303-314.

Ernst, W.G., and Hall, C.A., Jr., 1974, Geology and petrology of the Cambria Felsite, a new Oligocene formation, west-central California Coast Ranges: Geological Society of America Bulletin, v. 85, p. 523-532.

Fairbanks, H.W., 1904, Geological Survey Atlas, San Luis Folio: U.S. Geological Survey Folio 101, p. 4-5.

Fisher, R.V., 1961, Proposed classification of volcaniclastic sediments and rocks: Geological Society of America Bulletin, v. 72, p. 1409-1414.

———1966, Rocks composed of volcanic fragments and their classification: Earth Science Reviews, v. 1, p. 287-298.

———1977, Geologic guide to subaqueous volcanic rocks in the Nipomo, Pismo Beach and Avila Beach areas: The Geological Society of America Penrose Conference on the Geology of Subaqueous Volcanic Rocks, November 30, 1977, 29 p.

———1983, Flow transformations in sediment gravity flows: Geology, v. 11,p. 273-274.

Fisher, R.V., and Schmincke, H.U., 1984, Pyroclastic rocks: Berlin, Springer-Verlag, 472 p.

———1994, Volcaniclastic sediment transport and deposition, in Pye, K., ed., Sediment transport and depositional processes: Blackwell Scientific Publications, p. 351-388.

Fisher, R.V., and Smith, G.A., 1991, Volcanism, tectonics and sedimentation, *in* Fisher, R.V., and Smith, G.A., eds., Sedimentation in volcanic settings: Society of Economic Paleontologists and Mineralogists, Special Publication, no. 45, p. 1-5.

Fisher, R.V., Orsi, G., Ort. M., and Heiken, G., 1993, Mobility of a large-volume pyroclastic flow—emplacement of the Campanian ignimbrite, Italy: Journal of Volcanology and Geothermal Research, v. 56, p. 205-220.

Fiske, R., and Matsuda, T., 1964, Submarine equivalents of ash-flows in the Tokiwa Formation, Japan: American Journal of Science, v. 262, p. 76-106.

Froggatt, P.C., and Lamarche, G., 1989, Determination of flow direction and vent positions in Whakamaru ignimbrite using anisotropy of magnetic susceptibility [abs.]: New Mexico Bureau of Mines and Mineral Resources, Bulletin 131, IAVCEI General Assembly, "Continental Magmatism," Abstracts, p. 99.

Hall, C.A., Jr., 1973a Geology of the Arroyo Grande 15-minute quadrangle, San Luis Obispo County, California: California Division of Mines and Geology, Map Sheet 24, scale 1:48,000.

———1973b, Geologic map of the Morro Bay South and Port San Luis quadrangles, San Luis Obispo County, California: U.S. Geological Survey Miscellaneous Field Studies Map MF-511, scale 1:24,000.

———1974, Geologic map of the Cambria region, San Luis Obispo County, California: U.S. Geological Survey Miscellaneous Field Studies Map MF-599, scale 1:24,000.

———1976, Geologic map of the San Simeon–Piedras Blancas region, San Luis Obispo County, California: U.S. Geological Survey Miscellaneous Field Studies Map MF-784, scale 1:24,000.

———1978, Santa Maria and Tepusquet Canyon quadrangles, geologic map of Twitchell Dam and parts of Santa Barbara County, California: U.S. Geological Survey, Miscellaneous Field Studies Map MF-933, scale 1:24,000.

———1981a, Map of Geology along the Little Pine fault, parts of Sisquoc, Foxen Canyon, Zaca Lake, Los Olivos, and Figueroa Mountain quadrangles, Santa Barbara County, California. U.S. Geological Survey Miscellaneous Field Studies Map MF-1285, scale 1:24,000.

———1981b, San Luis Obispo transform fault and middle Miocene rotation of the Western Transverse Ranges, California: Journal of Geophysical Research, v. 86, p. 1015-1031.

Hall, C.A., Jr., Ernst, W.G., Prior, S.W., and Wiese, J.H., 1979, Geologic map of the San Luis Obispo–San Simeon region, California: U.S. Geological Survey Miscellaneous Investigation Series Map

I-1097, scale 1:48,000.
Hall, C.A., Jr., and Corbato, C.E., 1967, Stratigraphy and structure of Mesozoic and Cenozoic rocks, Nipomo quadrangle, southern Coast Ranges, California: Geological Society of America Bulletin, v. 78, p. 559-582.
Hall, C.A., Jr., and Prior, S.W., 1975, Geologic map of the Cayucos–San Luis Obispo region, San Luis Obispo County, California: U.S. Geological Survey, Miscellaneous Field Studies Map MF-686, scale 1:24,000.
Hall, C.A., Jr., Turner, D.L., and Surdam, R.C., 1966, Potassium-argon age of the Obispo Formation with Pecten lompocensis Arnold, southern Coast Ranges, California: Geological Society of America Bulletin, v. 77, p. 443-446.
Howells, M.F., Campbell, S.D.G., and Reedman, A.J., 1985, Isolated pods of subaqueous welded ash-flow tuff: a distal facies of the Capel Curig Volcanic Formation (Ordovician), North Wales: Geological Magazine, v. 122, p. 175-180.
Kano, K., Nakano, S., and Mimura, K., 1988, Deformation structures in shale bed indicate flow direction of overlying Miocene subaqueous pyroclastic flow: Bulletin of Volcanology, v. 50, p. 380-385.
Kato, I., Murai, I., Yamazaki, T. and Abe, M., 1971, Subaqueous pyroclastic flow deposits in the upper Donzurubo Formation, Nijo-san district, Osaka, Japan: Journal of the Geological Society of Japan, v. 77, p. 193-206.
Lacroix, A., 1904, La Montagne Pelée et ses eruptions: Paris, Masson et Cie, 662 p.
Lehner, B.L., 1991, Neptunian dykes along a drowned carbonate platform margin: an indication for recurrent extensional tectonic activity?: Terra Nova, v. 3, p. 593-606.
Lipman, P.W., 1984, The roots of ash flow calderas in western North America: windows into the top of granitic batholiths: Journal of Geophysical Research, v. 89, p. 8801-8841.
Lipps, J.H., 1967, Planktonic foraminifera, intercontinental correlation and age of California mid-Cenozoic microfaunal stages: Journal of Paleontology, v. 41, p. 994-999.
McDonald, W.D., and Palmer, H.C., 1990, Flow directions in ash-flow tuffs: a comparison of geological and magnetic susceptibility measurements, Tshirege member (upper Bandelier Tuff), Valles Caldera, New Mexico, U.S.A.: Bulletin of Volcanology, v. 53, p. 45-59.
Natland, M.L., 1957, Paleoecology of west coast Tertiary sediments, *in* Ladd, H.S., ed., Treatise on marine ecology and paleoecology, v. 2: Geological Society of America Memoir 67, p. 543-572.
Oltz, D., and Suchsland, R., eds., 1975, Geologic field guide of the eastern Santa Maria area: Society of Economic Paleontologists and Mineralogists Annual Fall Field Trip, 24 p.
Ross, C.S., and Smith, R.L., 1961, Ash-flow tuffs: their origin, geologic relations and identification: U.S. Geological Survey Professional Paper 366, 77 p.
Ross, K.A., 1987, Sedimentological interpretation of a mafic sequence of the Obispo Formation at Shell Beach, California: M.A. thesis, Santa Barbara, Calif., University of California, 143 p.
Schneider, J.L., Edel, J.B., and Montigny, R., 1994, Structural control on the volcanic facies geometry: Permian rhyodacitic volcanism of northern Vosges (France). A facies and paleomagnetic approach [abs.]: International Association of Sedimentologists, Ischia, 1994, Abstracts Volume, p. 378-379.
Scott, K.M., 1988, Origins, behavior, and sedimentology of lahars and lahar-runout flows in the Toutle–Cowlitz River system: U.S. Geological Survey Professional Paper 1447-A, 74 p.
Seaman, S.J., McIntosh, W.C., Geissman, J.W., Williams, M.L., and Elston, W.E., 1991, Magnetic fabric of the Bloodgood Canyon and Shelley Peak Tuffs, southwestern New Mexico: implications for emplacement and alteration processes: Bulletin of Volcanology, v. 53, p. 460-476.
Self, S., and Rampino, M., 1981, The 1883 eruption of Krakatau: Nature, v. 292, p. 699-704.
Sigurdsson, H., Carey, S., and Mandeville, C., 1991, Krakatau: National Geographic Research and Exploration, v. 7, p. 310-327.
Simkin, T., and Fiske, R.S., 1983, Krakatau 1883: The volcanic eruption and its effects: Washington, D.C., Smithsonian Institution Press, 464 p.
Smith, R.L., 1979, Ash-flow magmatism: Geological Society of America Special Paper 180, p. 5-27.
Surdam, R.C., and Hall, C.A., Jr., 1968, Zeolitisation of the Obispo Formation, Coast Ranges of California: Geological Society of America Abstracts with Programs, p. 338.
———1984, Diagenesis of the Miocene Obispo Formation, Coast Ranges, California, *in* Surdam, R.C., ed., A guidebook to the stratigraphic, tectonic, thermal and diagenetic histories of the Monterey Formation, Pismo and Huasna basin, California: Society of Economic Paleontologists and Mineralogists, Guidebook, No. 2, p. 8-20.
Surdam, R.C., Turner, D.L., and Hall, C.A., Jr., 1970, Distribution and genesis of authigenic silicates in the Obispo Formation [abs.]: Geological Society of America Abstracts with Programs, Cordilleran Section, v. 2, no. 2, p. 151-152.
Tennyson, M.E., Keller, M.A., Filewicz, M.V., Thornton, M.L., and Vork, D., 1990, Early Miocene sedimentation and tectonics in western San Luis Obispo County, central California [abs.]: American Association of Petroleum Geologists Bulletin, v. 74, no. 5, p. 777.
Tennyson, M.E., Keller, M.A., Filewicz, M.V., and Thornton, M.L., 1991, Contrasts in early Miocene subsidence history across Oceanic–West Huasna fault system, northern Santa Maria province, California [abs.]: American Association of Petroleum Geologists Bulletin, v. 75, no. 2, p 383.
Turner, D.L., 1970, Potassium-argon dating of Pacific coast Miocene foraminiferal stages, in Bandy O.L., ed., Radioactive dating and paleontologic zonation: Geological Society of America Special Paper 124, p. 91-129.
Verbeek, R.D.M., 1884, The Krakatoa eruption: Nature, v. 30, p. 10-15.
Yamazaki, T., Kato, I., Muroi, I., Abe, M., 1973, Textural analysis and flow mechanism of the Donsurubo subaqueous pyroclastic flow deposits: Bulletin Volcanologique, v. 37, p. 231-244.

☆ U.S. GOVERNMENT PRINTING OFFICE: 1996 - 774-045 / 20061 REGION NO. 8

SELECTED SERIES OF U.S. GEOLOGICAL SURVEY PUBLICATIONS

Periodicals

Earthquakes & Volcanoes (issued bimonthly).
Preliminary Determination of Epicenters (issued monthly).

Technical Books and Reports

Professional Papers are mainly comprehensive scientific reports of wide and lasting interest and importance to professional scientists and engineers. Included are reports on the results of resource studies and of topographic, hydrologic, and geologic investigations. They also include collections of related papers addressing different aspects of a single scientific topic.

Bulletins contain significant data and interpretations that are of lasting scientific interest but are generally more limited in scope or geographic coverage than Professional Papers. They include the results of resource studies and of geologic and topographic investigations; as well as collections of short papers related to a specific topic.

Water-Supply Papers are comprehensive reports that present significant interpretive results of hydrologic investigations of wide interest to professional geologists, hydrologists, and engineers. The series covers investigations in all phases of hydrology, including hydrology, availability of water, quality of water, and use of water.

Circulars present administrative information or important scientific information of wide popular interest in a format designed for distribution at no cost to the public. Information is usually of short-term interest.

Water-Resources Investigations Reports are papers of an interpretive nature made available to the public outside the formal USGS publications series. Copies are reproduced on request unlike formal USGS publications, and they are also available for public inspection at depositories indicated in USGS catalogs.

Open-File Reports include unpublished manuscript reports, maps, and other material that are made available for public consultation at depositories. They are a nonpermanent form of publication that may be cited in other publications as sources of information.

Maps

Geologic Quadrangle Maps are multicolor geologic maps on topographic bases in 7 1/2- or 15-minute quadrangle formats (scales mainly 1:24,000 or 1:62,500) showing bedrock, surficial, or engineering geology. Maps generally include brief texts; some maps include structure and columnar sections only.

Geophysical Investigations Maps are on topographic or planimetric bases at various scales, they show results of surveys using geophysical techniques, such as gravity, magnetic, seismic, or radioactivity, which reflect subsurface structures that are of economic or geologic significance. Many maps include correlations with the geology.

Miscellaneous Investigations Series Maps are on planimetric or topographic bases of regular and irregular areas at various scales; they present a wide variety of format and subject matter. The series also includes 7 1/2-minute quadrangle photogeologic maps on planimetric bases which show geology as interpreted from aerial photographs. The series also includes maps of Mars and the Moon.

Coal Investigations Maps are geologic maps on topographic or planimetric bases at various scales showing bedrock or surficial geology, stratigraphy, and structural relations in certain coal-resource areas.

Oil and Gas Investigations Charts show stratigraphic information for certain oil and gas fields and other areas having petroleum potential.

Miscellaneous Field Studies Maps are multicolor or black-and-white maps on topographic or planimetric bases on quadrangle or irregular areas at various scales. Pre-1971 maps show bedrock geology in relation to specific mining or mineral-deposit problems; post-1971 maps are primarily black-and-white maps on various subjects such as environmental studies or wilderness mineral investigations.

Hydrologic Investigations Atlases are multicolored or black-and-white maps on topographic or planimetric bases presenting a wide range of geohydrologic data of both regular and irregular areas; the principal scale is 1:24,000, and regional studies are at 1:250,000 scale or smaller.

Catalogs

Permanent catalogs, as well as some others, giving comprehensive listings of U.S. Geological Survey publications are available under the conditions indicated below from USGS Map Distribution, Box 25286, Building 810, Denver Federal Center, Denver, CO 80225. (See latest Price and Availability List.)

"Publications of the Geological Survey, 1879-1961" may be purchased by mail and over the counter in paperback book form and as a set microfiche.

"Publications of the Geological Survey, 1962-1970" may be purchased by mail and over the counter in paperback book form and as a set of microfiche.

"Publications of the U.S. Geological Survey, 1971-1981" may be purchased by mail and over the counter in paperback book form (two volumes, publications listing and index) and as a set of microfiche.

Supplements for 1982, 1983, 1984, 1985, 1986, and for subsequent years since the last permanent catalog may be purchased by mail and over the counter in paperback book form.

State catalogs, "List of U.S. Geological Survey Geologic and Water-Supply Reports and Maps For (State)," may be purchased by mail and over the counter in paperback booklet form only.

"Price and Availability List of U.S. Geological Survey Publications," issued annually, is available free of charge in paperback booklet form only.

Selected copies of a monthly catalog "New Publications of the U.S. Geological Survey" is available free of charge by mail or may be obtained over the counter in paperback booklet form only. Those wishing a free subscription to the monthly catalog "New Publications of the U.S. Geological Survey" should write to the U.S. Geological Survey, 582 National Center, Reston, VA 22092.

Note.–Prices of Government publications listed in older catalogs, announcements, and publications may be incorrect. Therefore, the prices charged may differ from the prices in catalogs, announcements, and publications.